MICROENCAPSULATION OF A PALM OIL-BASED ALKYD BY AMINO RESINS FOR SELF-HEALING APPLICATION

NURSHAFIZA BINTI SHAHABUDIN

FACULTY OF SCIENCE
UNIVERSITY OF MALAYA
KUALA LUMPUR

2016

MICROENCAPSULATION OF A PALM OIL-BASED ALKYD BY AMINO RESINS FOR SELF-HEALING APPLICATION

NURSHAFIZA BINTI SHAHABUDIN

THESIS SUBMITTED IN FULFILMENT OF THE REQUIREMENTS FOR THE DEGREE OF DOCTOR OF PHILOSOPHY

FACULTY OF SCIENCE
UNIVERSITY OF MALAYA
KUALA LUMPUR

2016

UNIVERSITY OF MALAYA

ORIGINAL LITERARY WORK DECLARATION

Name of Candidate:	NURSHAFIZA BINTI SHAHABUDIN
Matric No.:	SHC110093
Name of Degree:	Doctoral
Title of Thesis ("this Work"):	MICROENCAPSULATION OF A PALM OIL-BASED ALKYD BY AMINO RESINS FOR SELF-HEALING APPLICATION
Field of Study:	Polymer Chemistry

I do solemnly and sincerely declare that:

(1) I am the sole author/writer of this Work;
(2) This Work is original;
(3) Any use of any work in which copyright exists was done by way of fair dealing and for permitted purposes and any excerpt or extract from or reference to or reproduction of any copyright work has been disclosed expressly and sufficiently and the title of the Work and its authorship have been acknowledged in this Work;
(4) I do not have any actual knowledge nor do I ought reasonably to know that the making of this work constitutes an infringement of any copyright work;
(5) I hereby assign all and every rights in the copyright to this Work to the University of Malaya ("UM"), who henceforth shall be owner of the copyright in this Work and that any reproduction or use in any form or by any means whatsoever is prohibited without the written consent of UM having been first had and obtained;
(6) I am fully aware that if in the course of making this Work I have infringed any copyright whether intentionally or otherwise, I may be subject to legal action or any other action as may be determined by UM.

Candidate's Signature Date: 13/09/2016

Subscribed and solemnly declared before,

Witness's Signature Date: 13/09/2016

Name: PROF. DR. GAN SENG NEON

Designation: Professor, Department of Chemistry, University of Malaya.

ABSTRACT

The failure of many structural polymers usually begins from the micro-cracks formed within the materials. Materials which contain healing agents (in microcapsules) can autonomously repair these cracks to prevent further propagation and failure. When cracks occur and rupture the microcapsules, the healing agent released would solidify through selected mechanism. In this work, a potential healing material was developed using an alkyd from palm kernel oil (PKO). The alkyd was synthesized to have a controlled amount of carboxylic groups (COOH), capable to form crosslinking reaction with the epoxide groups in the epoxy matrix. The alkyd was encapsulated into poly(urea-formaldehyde) (PUF) and poly(melamine-urea-formaldehyde) (PMUF) resins forming the microcapsules, which were embedded into an epoxy matrix. The functional groups of alkyd and shell materials in the microcapsules were confirmed by the appearance of the respective characteristic peaks using attenuated total reflectance-Fourier transform infrared (ATR-FTIR). Differential scanning calorimetry (DSC) analysis of the microcapsules showed a glass transition (T_g) around −12° C due to the alkyd and sharp melting temperature (T_m) at 148°C and 192°C due to the PUF and PMUF shells respectively. Another broad T_m at 0−15°C was attributed to the alkyd core. Thermogravimetric analysis (TGA) revealed that the PUF and PMUF microcapsules were thermally stable up to 250°C and 260°C, respectively. Field emission scanning electron microscopy (FESEM) examination of the broken shell of the microcapsules showed a smooth inner surface and a rough outer surface. The outer surface consisted of layered structures formed by PUF and PMUF nanoparticles. The microcapsules mix readily into the epoxy and were found to disperse well in the matrix as revealed by images in optical microscope and FESEM. Microcapsules of 1−3 wt. % could be incorporated into an epoxy matrix without noticeably affecting the flexural strength and micro-indentation hardness. To demonstrate the plausible healing reaction between the alkyd and the epoxy,

a small amount of the amine hardener was replaced with the alkyd in the epoxy formulation. Curing was carried out at room temperature for 24 h and 100°C for 2 h and the blends hardened readily.

ABSTRAK

Kegagalan struktur kebanyakan polimer biasanya bermula dari retakan mikro yang terbentuk dalam polimer tersebut. Bagi bahan swa-pulih, retakan boleh dibaiki atau perambatan retak boleh dicegah. Apabila retakan berlaku dan mikrokapsul pecah, agen pemulihan akan di keluarkan dan mengeras menggunakan mekanisme yang sesuai. Bahan swa-pulih yang berpotensi telah dibangunkan menggunakan pada alkid daripada minyak isirong sawit. Alkid ini mempunyai jumlah karboksil (COOH) tertentu yang mampu membentuk rangkai silang dengan kumpulan epoksida dalam matriks epoksi. Kumpulan-kumpulan berfungsi alkid dan bahan kulit kapsul telah disahkan oleh kemunculan puncak berciri menggunakan "attenuated total reflectance-Fourier transform infrared" (ATR-FTIR). Analisis "differential scanning calorimetry" (DSC) terhadap mikrokapsul menunjukkan suhu peralihan kaca (T_g) sekitar −12°C, dan suhu lebur yang tajam (T_m) pada 148°C dan 192°C dan satu lagi T_m pada 0−15°C. "Thermogravimetric analysis" (TGA) mendedahkan mikrokapsul poli(uria-formaldehid) (PUF) dan poli(melamin-uria-formaldehid) (PMUF) adalah stabil sehingga 250°C dan 260°C. Pemeriksaan "field emission scanning electron microscopy" (FESEM) terhadap kulit mikrokapsul yang dipecahkan menunjukkan permukaan dalaman yang licin dan permukaan luaran yang kasar, yang terbentuk daripada partikel nano PUF dan PMUF. Mikrokapsul telah dicampurkan ke dalam epoksi dan didapati bersurai dengan baik dalam matriks seperti yang ditunjukkan oleh imej mikroskop optikal dan FESEM. Penambahan 1−3 % mikrokapsul ke dalam matriks epoksi tidak mengubah kekuatan lenturan dan kekerasan mikro (Vickers). Untuk menunjukkan tindak balas swa-pulih di antara alkid dan epoksi, sedikit pengeras amina telah digantikan dengan alkid dalam formulasi epoksi. Campuran alkid dan epoksi telah mengeras apabila di "cure" pada suhu bilik selama 24 j dan hanya 2 j pada suhu 100°C.

ACKNOWLEDGEMENTS

Praise be to Allah, the Most Gracious and the Most Merciful, for given me the opportunity to complete this study.

I would like to express my sincerest gratitude and utmost appreciation to my supervisors: Professor Dr Gan Seng Neon and Professor Dr Rosiyah Yahya for their generous guidance, support and motivation throughout this study. All patience and help during my candidature and the tireless proofreading efforts for published works from both of them are highly appreciated. Special thanks to Professor Gan who had given me this project.

I thank the staff of Chemistry Department for all their support, particularly: Prof. Rauzah Hashim and the FSSA team (especially Dr Malinda, Dr Idayu and Mr Melloney) for their cooperation and generosity with the instruments at their laboratory; Dr Desmond, Dr Noordini and Dr Masmira for their scientific insights; Mr Shukri and Ms Noor Nadila for the help with FESEM and NMR analyses. My appreciation also goes to the Biomaterial research laboratory (BRL) at the Faculty of Dentistry, UM, in particular: Dr Noor Azlin for allowing me to conduct my research at BRL; Mrs Zarina and Mrs Chantiriga for their support with the mechanical testing. I acknowledge the staff of INFRA Analysis Laboratory of Research Management & Innovation, UM, particularly Mr Zulhizan Zakaria for his help with the FESEM analysis of the microcapsules and Mrs Fatimah Zahrah for her support with STA. I also acknowledge the proofreading favor by Prof Jawakhir Mior.

I am also indebted to the former and current members of Prof. Gan's research group. It has been a real pleasure to work with them, especially Sonja who had set the foundation of the encapsulation work at the laboratory and had been a good mentor; Yoke Kum,

Siang Yin and Mei Chan for their guidance with the alkyd synthesis and polymer characterizations; Mrs Rohani A. Bakar for her technical assistance with the GPC and scientific discussions; Pedram, Pejvak and W. Nurhidayah for their help and info-sharing; Hazira, Irma and Mariam for their support in the laboratory. I also thank Prof. Rosiyah's group members in particular Danial for the support with the literature; Farhana and Vidhya for their assistance at the department.

I would like to reserve a special mention to my beloved family who has been the fundamental base for every success and to whom this work is dedicated, especially my parents, Mr Shahabudin and Mrs A'ishah, my sisters and brothers, for their endless support, preserverance and patience throughout my study years. I could not have done this without any of them.

This study was supported by the Ministry of Science, Technology and Innovation, Malaysia (MOSTI) (03-01-03-SF0874) and University of Malaya (PG050-2014A). I also acknowledge the funding of my presentations at conferences: Faculty of Science postgraduate fund, PPP Travel Fund of University of Malaya and IUPAC for MACRO 2014 student support. Finally, I am truly grateful to the Ministry of Higher Education, Malaysia (MOHE) for the MyBrain15−Ph.D scholarship.

TABLE OF CONTENTS

LIST OF FIGURES

LIST OF TABLES

LIST OF ABBREVIATIONS

AlkydFA35	:	Alkyd with acid number of 55 mg KOH/g alkyd
AlkydPKO65	:	Alkyd with 65 % oil length and acid number of 15 mg KOH/g alkyd
DCPD	:	Dicyclopentadiene
DGEBA	:	Diglycidyl ether of Bisphenol-A
DSC	:	Differential scanning calorimeter
EMA	:	Ethylene(maleic anhydride)
FESEM	:	Field-emission scanning electron microscopy
^{1}H-NMR	:	Proton nuclear magnetic resonance
OM	:	Optical microscope
PDES	:	Polydiethoxysiloxane
PDMS	:	Poly(dimethylsiloxane)
PKO	:	Palm kernel oil
PMMA	:	Poly(methyl methacrylate)
PMF	:	Poly(melamine-formaldehyde)
PMUF	:	Poly(melamine-urea-formaldehyde)
PUF	:	Poly(urea-formaldehyde)
SENB	:	Single-edge notched bending
STA	:	Simultaneous thermal analyzer
TDCB	:	Tapered double cantilever beam
T_g	:	Glass transition
TGA	:	Thermogravimetric analysis
T_m	:	Melting temperature
WTDCB	:	Width-tapered double cantilever beam

LIST OF APPENDICES

CHAPTER 1: INTRODUCTION

1.1 Background of Study

The failure of many polymers begins from microcracks formed within the materials (Kessler, 2012). The undetected or inaccessible microcracks made early repair unavailable. The microcracks (**Fig. 1.1**) will then propagate until failure occurs and consequently will result in major losses. Traditional repairs such as welding and patching are limited to visible damages and only applicable when the failure has already occurred or worsened. Furthermore, inspection is needed as these methods are not autonomic nor instantaneous (Hia et al., 2016).

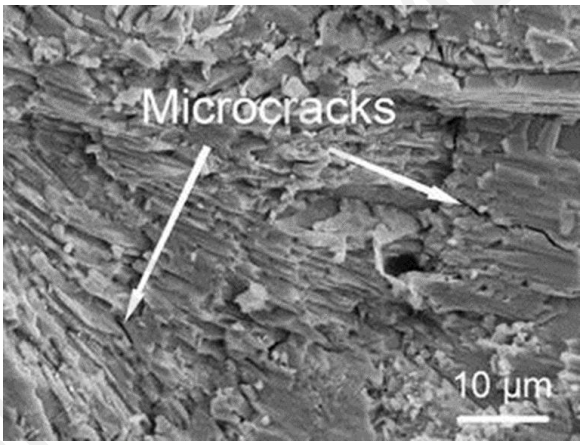

Fig. 1.1: SEM micrograph of fracture surface with microcracks. Adapted from Li et al. (2014)

Therefore, self-healing materials was introduced about 15 years ago (White et al., 2001) to overcome these limitations and intense research has been going on in this field for the past decade. Self-healing or self-repairing in materials in general and polymers in particular, is demonstrated by the ability to regain original properties lost during external damage. Partial recovery of the main functionality of the material also can be considered as a self-healing ability (Zheludkevich, 2009). Self-healing also can be defined as the ability of a material to repair damages autonomously, i.e. without any external intervention. However, the incorporation of self-healing properties in manmade materials

very often cannot perform the healing action without an external trigger, thus according to Ghosh (2009), self-healing can be autonomic or non-autonomic (i.e. needs human intervention). Synthetically mimicking the biological system of wound healing, materials should be able to sense and respond to damage over its lifetime, restoring chemical and physical features without adverse effects (Urban, 2015). **Fig. 1.2** shows the healing mechanism of human skin, where an injury causes a blood vessel wall to break and thus platelets are activated. They can change shape from round to spiny, stick to the broken vessel wall and each other and begin to plug the break. Besides, they also interact with other blood proteins to form fibrin, which forms a net that entraps more platelets and blood cells, producing a clot that plugs the break. This phenomena has inspired material scientists in the last two decades to mimic the natural self-healing of living organisms.

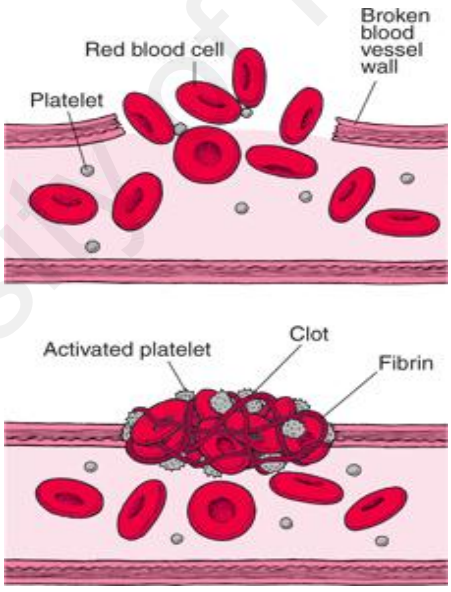

Fig. 1.2: Blood clotting in an injured vessel. Reproduced from MSD manuals consumer version (Moake, 2016) © Merck & Co. Inc

Amongst other methods, self-healing can be achieved particularly via microcapsules-based. In microcapsules-based self-healing, healing agent is loaded into a matrix material using microcapsules. When microcracks occur, the microcapsules will break and release the healing agent to polymerize or cure after reacting with the already embedded catalyst or even with the matrix host itself. This concept is illustrated in **Fig. 1.3**.

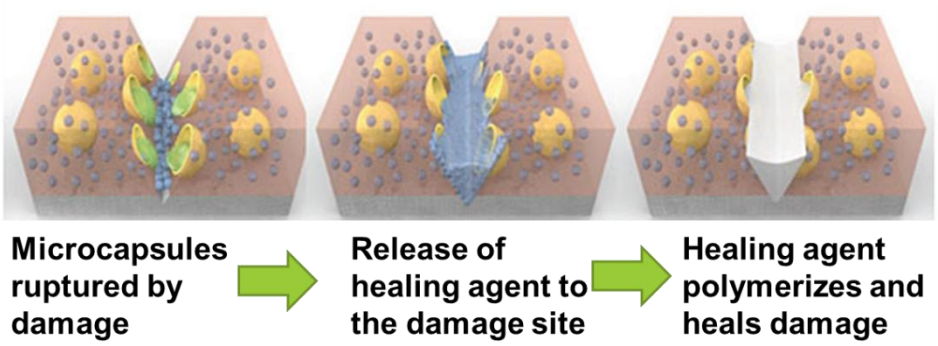

Fig. 1.3: Concept of microcapsules-based self-healing. Adapted from Cho et al., 2009

1.2 Problem Statement

Different healing agents are introduced to function in different polymeric materials, involving selected healing mechanism. In particular, there were many research works on self-healing of epoxy materials. The thermosetting epoxies are useful in a wide variety of applications, which range from aerospace engineering down to coatings, adhesives and microelectronics. This is due to their excellent adhesion, thermal and mechanical properties, superior chemical and corrosion resistance, low shrinkage and good electrical insulation. However, they are inherently brittle rendering them susceptible to damage in the form of micro cracks. Material failure generally begins at the nano-scale, which then develops to the micro- and macro-scales until failure occurs (Takahashi & Ushijima, 2007). Thus, developing self-healing epoxy composites that can repair themselves to fully/partially recover its functionality is an important venture. Likewise, the introduction of self-healing functionality into protective epoxy coating is also a better alternative for long term corrosion protection of metallic structures (Vijayan & AlMaadeed, 2016).

The encapsulated dicyclopentadiene (DCPD) could react with a Grubbs' catalyst in a thermosetting epoxy matrix (White et al., 2001). However, the catalyst could lost its activity upon prolonged exposure to air and moisture. It could interact with diethylenetriamine (DETA) and loss its ability to crosslink DCPD (Jones et al., 2006). It was also inevitably expensive and less robust (Coope et al., 2011), besides having a

tendency to agglomerate and led to delamination within the samples (Kessler et al., 2003). Following that, a number of research had been carried out to encapsulate different healing agents in poly(urea-formaldehyde) (PUF), poly(melamine-formaldehyde) (PMF), poly(melamine-urea-formaldehyde) (PMUF) and poly(methyl methacrylate) (PMMA) shells for self-healing epoxy composites and coatings. The healing agents include organic solvents (Caruso et al., 2007), drying oils (Suryanarayana et al., 2008) and epoxy resin itself as curing agent. Epoxy was encapsulated as it is more thermally stable than DCPD and can be applied to polymer manufactured at low and elevated temperatures (>100°C) (Yuan et al., 2006). To encapsulate the curing agent, particularly amine, which is amphoteric and highly reactive in nature, is challenging and Yuan et al. (2008) have proposed the use of PMF instead of PUF, to encapsulate mercaptan (as hardener instead of amine). Another alternative is to use PMMA as shell material to encapsulate the hardener as suggested by Li et al. (2013b). Some others variant were also recommended such as the use of hollow capsules, where the amine was infiltrated by vacuum to encapsulate the amine inside PUF microcapsules (Jin et al., 2012). Some more recent research suggested a more complex method of using Pickering emulsion to encapsulate the amine in the solid particles (McIlroy et al., 2010; Yi et al., 2015).

In general, the microcapsules containing self-healing materials must be able to withstand the conditions of high temperatures epoxy resins application. Besides, the preferred should be healing agent that is reasonably priced. Thus, the introduction of less expensive and more environmental friendly components would be beneficial. The use of catalyst-free healing agents such as solvents and epoxy resins have been developed in search of cost reduction (Vijayan & AlMaadeed, 2016), but there are still room for improvement.

1.3 A Selected Alkyd as Healing Agent

In this work, an alkyd resin, a bio-based and relatively cheap healing agent derived from renewable palm oil, was proposed as healing agent for epoxy matrix. Alkyds are actually polyesters that were first developed about 87 years ago (Kienle & Ferguson, 1929). They are tough resins typically synthesized from polybasic acid, polyhydric alcohol and vegetable oil (a triglyceride) such as soya, castor, rapeseed and linseed oils or the free fatty acids derived from triglyceride. Alkyds are conventionally used in paints, adhesives, inks and coatings. They have become one of the major synthetic resins in the coating industry. Alkyd can offer an alternative to their petroleum-based counterpart as it is relatively cheaper as it is renewable and also very versatile.

The versatility of alkyd is due to its compatibility with a number of polymers such as nitrocellulose, chlorinated and cyclized rubber and many resins such as phenolic, epoxy, amino, silicone, hydrocarbon and acrylic. Alkyd resins can also be designed to suit a broad range of applications by changing the oil length and modifying the chain stopping agents and the related resins (Hofland, 2012). Moreover, alkyd is high gloss, has good film performance and fast drying property (Nabuurs et al., 1996).

Normally, the drying or curing mechanism of an alkyd is attributed to the air oxidation of the unsaturated alkyd structure. Palm oil and palm kernel oil (PKO) are classified as non-drying oils because of their low level of unsaturation, making their alkyd unable to air dry. However, this lack of unsaturation can be counteracted by adding a certain amounts of carboxylic (–COOH) and hydroxyl (–OH) groups, which could be the reactive sites for other reactions. Here, the reaction of the carboxylic group of alkyd with the epoxide group of epoxy resin is proposed for the self-healing epoxy. Selection of palm oil-based alkyds as potential healing agent was also due to their high thermal stability up to 200°C (Teo et al., 2015), which is suitable for the high temperature process of epoxy curing.

1.4 Research Objectives

Therefore, this study is guided by these three main objectives:

1) Alkyd from palm oil will be synthesized and characterized. Characterization includes its chemical structure and some relevant physical properties.
2) The alkyd will be encapsulated using amino resins, mainly urea-formaldehyde (UF) and melamine-urea-formaldehyde (MUF). Factors affecting the synthesis of the microcapsules be investigated and optimized, i.e. the agitation rates, core/shell weight ratio, the viscosity of the medium and the emulsifier. The microcapsules formed will be characterized using thermal and microscopy analyses. Other relevant characterizations such as chemical structures, size and yield of microcapsules and the core loading will also be determined.
3) The performance of the microcapsules in the epoxy matrix will be evaluated. Effect of the inclusion of microcapsules on the mechanical properties of the epoxy matrix will be investigated. Furthermore, a curing reaction of alkyd with the epoxy will be examined using blending of epoxy/alkyd and the reaction will be studied using FTIR.

CHAPTER 2: LITERATURE REVIEW

2.1 Introduction

This chapter gives a review on the use of microencapsulation in self-healing polymeric materials, particularly in epoxy composites and coatings. The microencapsulation process and related parameters are discussed. The choice of a selected alkyd as healing agent for epoxy matrix will be explained.

2.2 Self-Healing and Its Development

Ancient Roman and Egyptian civilizations may not know about the self-healing mechanism, when they created concrete as construction materials. However, they knew through observations that the construction of a long lasting materials is needed to last their empire. Their constructions of arches, pipes and monuments such as the Pantheon and the pyramids are all evidences of long-lasting materials construction technology (Binder, 2013).

In modern times, the first self-healing material was reported by Malinskii et al. who studied the laminates of aluminum foil-poly(vinyl acetate). They concluded that self-healing occurs at the tip of a crack of an unloaded specimen, which led to an increase of strength during the relaxation time, relative to the strength of an unhealed specimen. This increase of strength (characterized by the value of the relaxation coefficient β) increases with temperature, especially near the glass transition and flow temperatures of the polymer (Malinskii et al., 1969). Several studies of crack healing materials with manual intervention then appeared in 1970s. Wiederhorn and Townsend (1970) reported 80% strength recovery of cracks in soda-lime-silica glass during crack closure, due to highly active surface fracture with dangling bonds and strained Si-O bonds. Inagaki et al. tested similar glass using an indentation method and concluded that the crack healing was more

prevalent in an inert atmosphere, occurring only minimally in air while earlier work by Wiederhorn and Townsend reported a bigger fracture energy when tested using a double-cantilever-cleavage technique in dry nitrogen (Inagaki et al., 1985).

The crack healing behavior in hard elastic polypropylene, styrene-butadiene-styrene (SBS) block copolymers and carbon black filled vulcanized natural rubber was studied. It is concluded that the microvoids could heal instantaneously or slowly, depending on the microstructural damage and molecular rearrangements incurred during the debonding process. The crack healing rate increased with temperature and no healing was observed below effective T_g of active molecular healing component. The second cycle stress response depended on the healing time of the fibers between deformation cycles, as shown in **Fig. 2.1**. At short healing time (t), considerable stress softening was observed but at longer times, the original mechanical properties of the fibers were restored as the crack healed (Wool, 1980).

The studies on crack repairs in polymers used thermal or solvent processes, where the polymer is softened by heating or by using solvents and the cracks weld themselves in several stages (Wang et al., 1994). However, to apply the same treatment to a large composite structure is not practical (Wool, 2001).

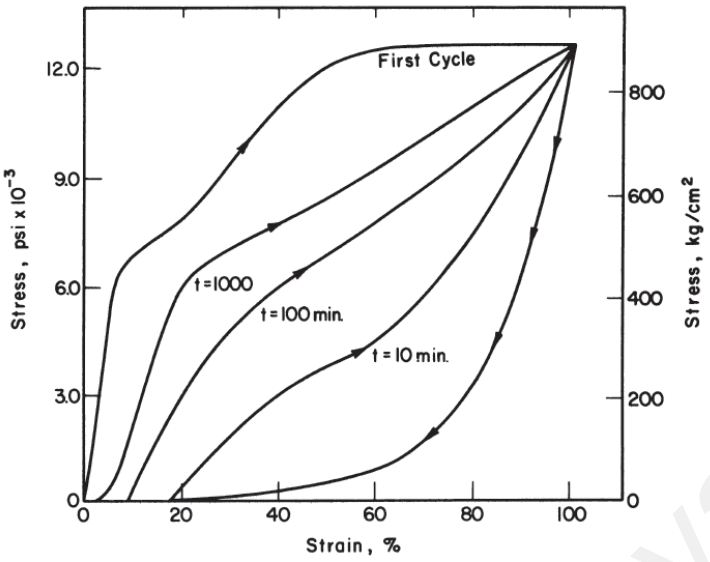

Fig. 2.1: The effect of healing time on the stress-strain behavior of hard elastic polypropylene fibers at room temperature. Reproduced from Wool RP (ed. L.H-Lee) © 1980 Plenum Press

A passive self-repair concept was introduced in the construction field (Dry, 1994), followed by in polymers (Dry, 1996), where in the latter adhesives and crosslinking or air cured polymers/ monomers were investigated. Controlled release of adhesive or crack filler material from a stretched or cracked repair fiber is then used to seal matrix microcracks and re-bond damaged interfaces. Materials that are capable of passive, smart self-repair consist of: 1) an agent of internal deterioration such as dynamic loading, which induces cracking; 2) a stimulus to release the repairing chemical; 3) a fiber; 4) a coating or fiber wall , which can be removed or changed in response to the stimulus; 5) a chemical carried inside the fiber; and 6) a method of hardening the chemical in the matrix in the case of crosslinking polymers or a method of drying the matrix in the case of a monomer (Dry, 1996; Dry & Sottos, 1993).

The previous manual crack repairs leads to the finding of an autonomous self-healing approach using microcapsules. White et al., have demonstrated an approach to use microcapsules containing dicyclopentadiene (DCPD) instead of fibers. The concept is illustrated in **Fig. 2.2**, where microencapsulated healing agent is embedded in a structural

epoxy matrix containing a catalyst (Grubb's) capable of polymerizing DCPD. Microcracks form in the matrix; (a) and rupture the microcapsules to release the healing agent into the crack plane (b). Then, the DCPD comes in contact with the catalyst, which is randomly distributed in the matrix and (c) triggers the polymerization reaction that helps to heal the damage by bonding the crack surfaces (White et al., 2001).

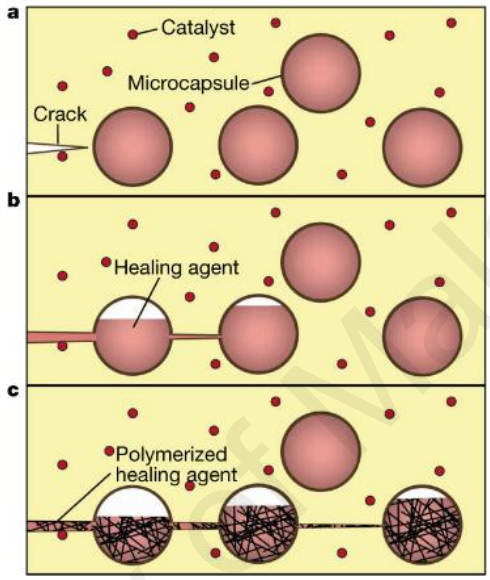

Fig. 2.2: Autonomous self-healing concept introduced by White and co-researchers in 2001. Reproduced from White et al. © 2001 Nature Pub. Group

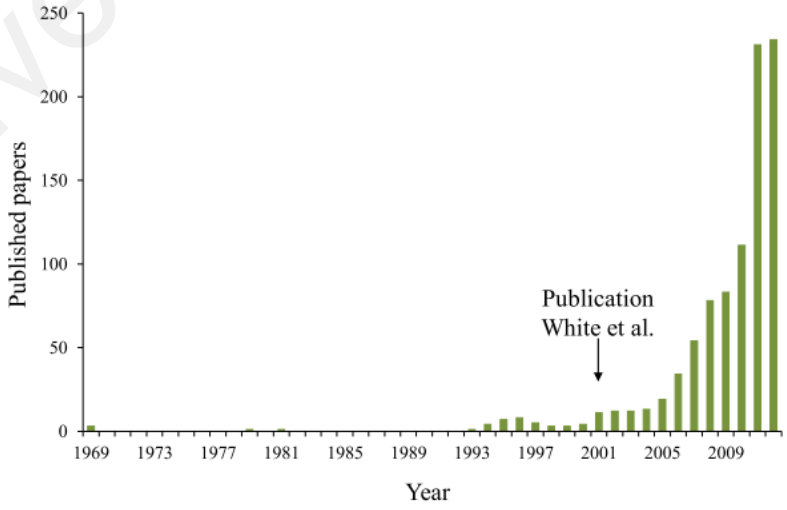

Fig. 2.3: Evolution of the amount of papers published on self-healing materials. Reproduced from Tittelboom and de Belie © 2013 MDPI

Following that work, the research of self-healing materials has expanded drastically (**Fig. 2.3**). Multi-authored books, book chapters and special issues in scholarly periodicals (e.g. *Journal of the Royal Society of Interface, Journal of the Composite Materials*) on self-healing materials are already available. Regular international conferences have been established such as the "*International Conference on Self-Healing Materials*" (Noordwijkaan Zee, Netherlands (2009), Chicago, US (2009), Bath, UK (2011), Durham, UK (2013) and Ghent, Belgium (2015). In 2006, the Dutch government, collaborating with the industry, funded an 8-year and 20 million euro research program on self-healing materials. This program has two main objectives. First is to explore all opportunities to create self-healing behavior in engineering and functional materials; and secondly to employ the new materials to real life applications. This program was the pioneer for the integrated, multi-materials approach in this field (van der Zwaag & Brinkman, 2015).

Malaysia is catching up with the rest of the world in the research on advanced materials. Then et al. reported the optimization of microencapsulation method of DCPD as healing agent for dental materials (Then et al., 2011a), followed by the performance evaluation of the encapsulated healing agent in the dental matrix. They found that the inclusion of up to 5% microcapsules did not adversely affect the mechanical properties of the dental materials (Then et al., 2011b). Other than microcapsules, fibers were also used as an alternative to contain the healing agent in a matrix. Electrospun nanofibrous mats of polyacrylonitrile (PAN) containing epoxy and amine healing solutions were incorporated into an epoxy matrix to impart self-healing functionality. About 75% and 38% recovery of fracture toughness were obtained at 50°C and at room temperature respectively, with a repeated self-healing of six times at room temperature (Vahedi et al., 2015).

In another approach, a vibration analysis was used to study the healing of hybrid epoxy composite with carbon fibers and shape memory alloy (SMA) wires. Alebrahim et al. used the Timoshenko beam model and used various volume fractions of wires in the epoxy. They found that a volume fraction of 2.5% can repair the defected beam as healthy one. It was observed that, using high volume fraction of SMA wires can significantly reduce deflection (Alebrahim et al., 2015).

An interesting work has investigated two local indigenous micro-organisms, *P. mirabilis* and *P. vulgaris*, which were isolated from soil and can produce calcium carbonate. Broken concrete was treated by a medium culture containing micro-organisms. The result showed that cracked concrete could be filled by calcium carbonate after the treatment, although it has affected the strength of concrete (Talaiekhozani et al., 2014). Application of a grounded group decision-making (GGDM) model to find the optimal inoculation method of the bacteria used in biological self-healing concrete has also been developed (Keyvanfar et al., 2014).

In a different approach, encapsulated zeolite in PUF microcapsules were incorporated into an anti-fouling coating. This was to prevent corrosion induced by bacteria in saline environment (Ahdash et al., 2014). The corrosion behavior was investigated through salt spray test and immersion tests in nutrient rich simulated seawater (NRSS) medium with *Pseudomonas aeruginosa* bacteria. The thickness for self-healing coating was between 50 μm to 175 μm. The embedded microcapsules did not affect the adhesion of the coating on steel substrates. The release of the core material after rupturing the microcapsules gave total healing for the crack after 21 days left at room temperature. Both specimens immersed in salt spray chamber and NRSS medium with the bacteria showed excellent anti-corrosion properties (Hamzah & Ahdash, 2016).

In other work, epoxy/mercaptan microcapsules were dispersed into a commercialized two-part epoxy adhesive layer of about 180 um thickness. 12% to 28% recovery of the shear strength were achieved after self-healing depending on the microcapsules content. The self-healing adhesives exhibited recovery of both cohesion and adhesion properties with room temperature healing (Ghazali et al., 2016a). Similar encapsulated healing agents with 1:1 ratio in carbon fiber/epoxy laminates were also tested, giving a 80% recovery of fracture toughness when measured using width-tapered double cantilever beam (WTDCB). It was also observed that the recovery of fracture toughness was directly correlated with the amount of healant covering the fracture plane, with the highest healing efficiency obtained for the laminate with large capsules (Ghazali et al., 2016b).

In intrinsic healing, Sirajudin and co-researchers demonstrated a 92% of tensile strength recovery in their poly(2-hydroxyethylmethacrylate) (HEMA) hydrogel, using 1-cystine as a crosslinker (Sirajuddin et al., 2014). They used the fluorescence by UV light to capture the image of healed gel, to demonstrate the diffusion of the gel. The intermolecular diffusion mechanism was proposed to be responsible for the healing (Sirajuddin & Jamil, 2015). Summary of the other self-healing works in Malaysia are available in Appendix K.

2.3 Epoxy in Industries

Epoxy resin is one of the important class of polymeric materials, characterized by the presence of more than one three-membered ring known as the epoxy, epoxide or oxirane group. By strict definition, epoxy resins refer only to un-crosslinked monomers or oligomers containing epoxy groups. However, in practice, the term epoxy resins is loosely used to include cured epoxy systems (Pham & Marks, 2005). The most commonly used epoxy resins is the diglycidylether of bisphenol-A (DGEBA) and its structure is shown in **Fig. 2.4**. This resin is commercially available under the tradenames such as Epikote

828 or Epon 828 (Hexion), DER (Dow Chemical Company) and Araldite (BASF) to name a few.

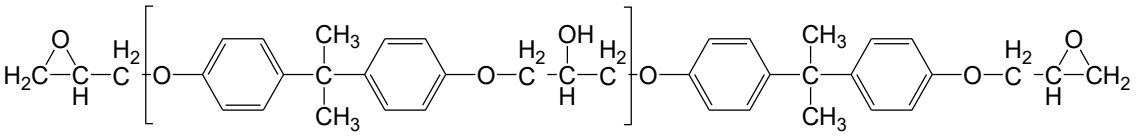

Fig. 2.4: Chemical structure of DGEBA resin

Epoxy resins are also available in other variants with different viscosity and epoxy equivalent. For example, Epikote 240, a relatively lower epoxy resin than Epikote 828, is a blend of a bisphenol A resin (produced from bisphenol A and epichlorohydrin) and a bisphenol F resin (produced from bisphenol F and epichlorohydrin), with added proportion of a mono-epoxidised alcohol as a reactive diluent. The weight of epoxy equivalent of this resin is in the same range as that of Epikote 828. Properties of selected epoxy resins are listed in **Table 2.1**.

Table 2.1: The selected epoxy resins

Epoxy resin	Viscosity at 25°C (Pa.s)	Epoxy group content (mmol/kg)	Epoxy equivalent (g/equivalent)
Epikote 828	12.0 – 14.0	5260 – 5420	184 – 190
Epikote 240	0.7–1.1	5100 – 5400	185 – 196

Source: Hexion Inc. technical datasheet (Hexion.com, 2005, 2007).

Crosslinking agents are used to convert epoxy resins into hard, infusible thermoset networks. These crosslinkers, hardeners or curing agents promote crosslinking or curing of the epoxy. Curing occurs by either homopolymerization initiated by a catalytic curing agent or a polyaddition/ copolymerization reaction with multifunctional curing agent (Ellis, 1993). A wide choice of hardeners are available for cure at room or elevated temperatures. These include amines and derivatives, amides, carboxylic acid functional polyesters, anhydrides, phenol-formaldehyde resins and amino-formaldehyde resins are available as hardeners. However, the most common used curing agents are from the amine

groups. A modified cycloaliphatic amine, Epikure F205 was used as hardener in this study and its properties are listed in **Table 2.2**.

Table 2.2: Characteristics of Epikure F205 curing agent

Epikure F205	Characteristics
Viscosity at 25°C (Pa.s)	0.5 – 0.7
Basic nitrogen content (% M / m)	6.0 – 8.0
Hydrogen equivalent (g/equivalent)	102 – 106
Recommended proportion of Epikote 828 (parts resin per hundreds part resins, p.h.r)	58

Source: Hexion Inc. technical datasheet (Hexion.com, 2006).

Carboxylic acid functional polyesters and anhydrides are the second most important family of curing agents for epoxy resins. The mechanism of the curing reaction involves two stages: (a) addition of carboxyl group to the epoxy functionality and (b) esterification with the secondary hydroxyls on the epoxy backbone (**Fig. 2.5**).

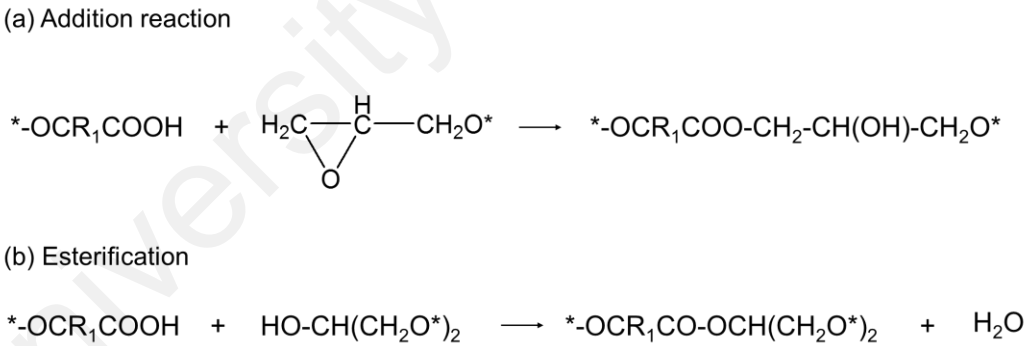

Fig. 2.5: Scheme of curing reaction between epoxy resin and carboxylic acid functional polyester hardener

Although having excellent thermal and chemical resistance, good adhesion and mechanical properties, epoxies are brittle in nature and susceptible to damage induced by mechanical, chemical, thermal, UV-radiationor a combination of these factors. Thus, it can be seen that the development of autonomous self-healing epoxy is a rapidly growing research and certain examples are presented in the next sections.

2.4 Self-Healing Epoxy

Self-healing can be categorized into two major types; first is the intrinsic self-healing (**Fig. 2.6 (a)**), where healing is achieved by the material itself through its chemical nature. The self-repair is achieved through reversibility of bonding of the polymer matrix. It can be accomplished through several approaches, i.e. via thermally reversible reactions, hydrogen bonding, ionomeric arrangementsor molecular diffusion and entanglement.

Second is the extrinsic self-healing, where the healing property is obtained by adding healing agent/s (in/through microcapsules or vasculatures) to the material , which is to be healed. Here, the agent is loaded using pipelines or vascular channels or filled microcapsules as the material itself lacks self-healing mechanism, as illustrated in **Fig. 2.6 (b-c)**. For vascular materials **(b)**, the healing agent is stored in hollow channels or fibers until damage ruptures the vasculature and releases the healing agent. In (micro/nano) capsule-based self-healing materials **(c)**, the healing agent is stored in capsules until they are ruptured by damage or dissolved.

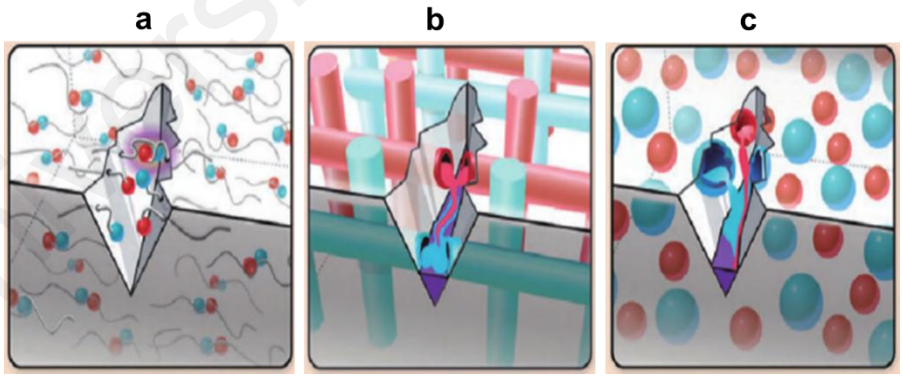

Fig. 2.6: Approaches to self-healing (a) intrinsic (b) vascular-based (c) (micro/nano) capsule-based. Adapted from Blaiszik et al. © 2010 Annual Reviews

2.4.1 Intrinsic Self-Healing Epoxy

As demonstrated by Wudl and his co-researchers, the intrinsic self-healing utilized the reversible reactions of furan-maleimide to produce healing (Chen et al., 2002; Chen et al., 2003; Murphy et al., 2008). The reversible reaction however, is not possible for

thermoset system such as epoxy. The curing reactions of epoxy with hardeners are generally irreversible, thus conventional epoxy can hardly exhibit re-mendable behavior due to lack of the ability of the broken molecules to be recombined. However, two new epoxy with furan and maleimide functionalities later have been introduced. This new group of thermoset was found to possess similar mechanical properties as the commercial epoxy and was also thermally mendable through the reactions of Diels-Alder (DA) and reversed Diels-Alder (rDA) (Tian et al., 2010; Tian et al., 2009). In another approach, Hayes et al. and Pingkarawat et al. have used blends of thermoplastic in epoxy resin to induce intrinsic healing with thermal stimulus of 150°C for a short period (Hayes et al., 2007; Pingkarawat et al., 2015).

2.4.2 Vascular-Based Self-Healing Epoxy

In this type of extrinsic healing, the healing agent is introduced into the vascular network after the network has been integrated in the matrix host. It provides multiple connection points and access to a larger reservoir of healing agents, which increases the reliability of the system (Blaiszik et al., 2010). One of its advantages is the easier refilling of the healing agent. One-dimensional vascular network was introduced by Dry and co-workers, to obtain healing abilities in epoxies with glass pipettes preloaded with cyanoacrylate or a separated two-epoxy system (Dry, 1996; Dry & Sottos, 1993). Toohey and co-workers demonstrated a 3D network of microchannels , which utilized the epoxy-Grubb's catalyst (Toohey et al., 2007) and two-part epoxy chemistries (Toohey et al., 2009), that showed 7 and 16 repeated healing cycles for respective systems.

2.4.3 Microcapsules-Based Self-Healing Epoxy

Although vascular design has allowed multiple healing and is highly reliable, the complexity in designing/manufacturing the networks limits its usage. Thus, the use of microcapsule-based systems has attracted more attention during the last decade. The

advantages of this system include the aesthetic recovery combined with the very fast release of healing agent from the microcapsules (Ullah et al., 2016). Moreover, the microcapsule-based approach are easily integrated in most polymer systems, although their function is locally depleted after a single damage event (Blaiszik et al., 2010). The importance of the microcapsules-based self-healing study was reflected in the number of publications as shown in **Fig. 2.7**.

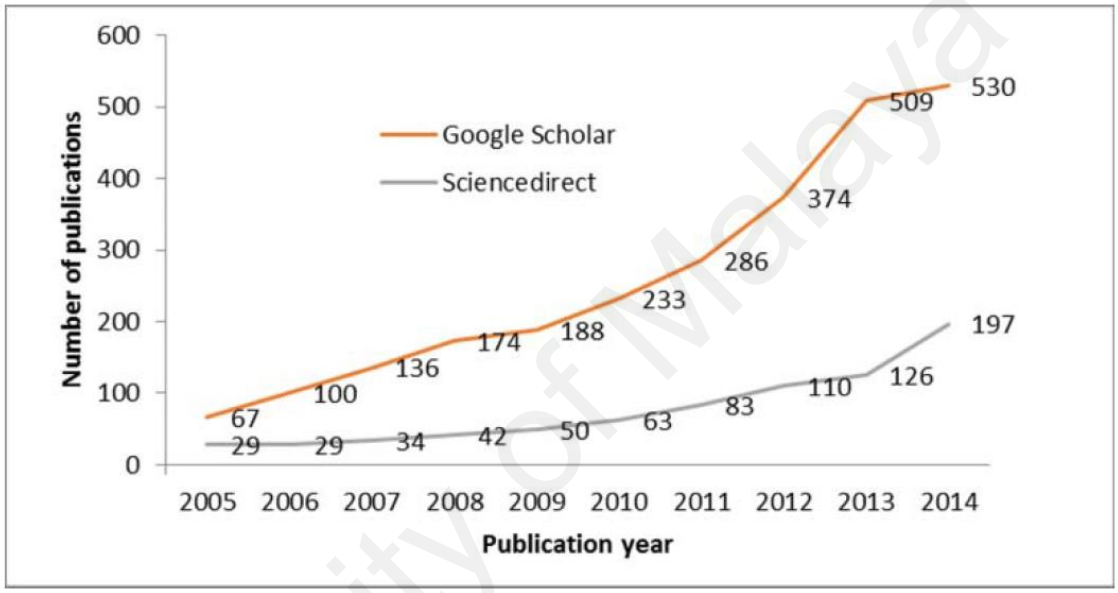

Fig. 2.7: Number of publications per year (2005-2014) shown by Google Scholar and ScienceDirect; keywords "Microcapsules based self-healing materials". Reproduced from Ullah et al. © 2015 Taylor & Francis

The design cycle for microcapsules-based self-healing materials, according to Blaiszik et al., can be divided into 5 steps: the development (encapsulation), integration or incorporation, mechanical characterization, triggering and healing evaluation. The steps are illustrated in **Fig. 2.8 (a).** The first step is to determine the optimal encapsulation method for the healing agent and its curing/healing mechanism. The encapsulation parameters such as solubility, reactivity, viscosity and volatility need to be considered. Next is the integration/ embedment of the microcapsules into the matrix host. The shear forces, induced on the microcapsules during mixing, processing temperature, capsules-matrix reactivity and capsules size may vary. UF, MF/MUF and PU capsules used for

self-healing have shown the ability to withstand processing conditions in common thermoset resins and composites manufacturing. After incorporation of capsules into matrix host, the mechanical properties, triggering mechanism and healing performance can be characterized. Several characteristics of microcapsules such as their bond strength with the matrix, volume fraction and stiffness may affect mechanical properties of the healed materials such fracture toughness, tensile and hardness (Blaiszik et al., 2010).

This work will focus on the development of the encapsulation of the selected healing agent, the integration of the microcapsules into a selected epoxy matrix and the selected mechanical characterization of the epoxy matrix. Only preliminary work of the healing evaluation will be presented.

Several types of microcapsules have been designed for self-healing, which include the microcapsules-catalyst system, dual/ multi-capsules system, microcapsules with latent hardener and phase separation, as shown in **Fig. 2.8 (b).**

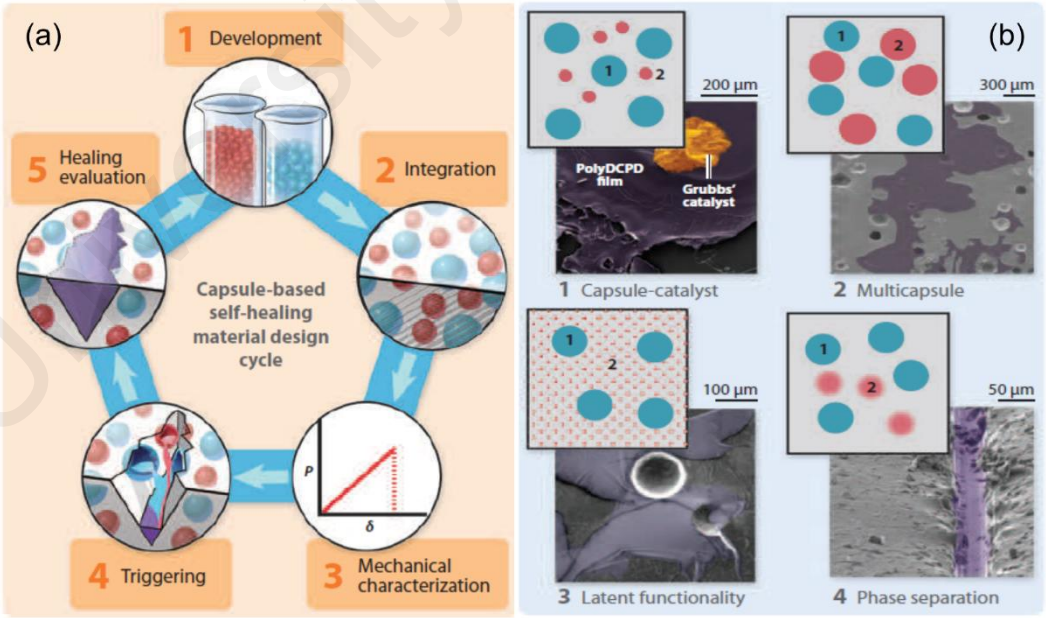

Fig. 2.8: (a) Design cycle of microcapsules-based self-healing material (b) approaches of microcapsules loading into matrix. Reproduced from Blaiszik et al. © 2010 Annual Reviews

Following White et al., approach in using Grubb's catalyst for self-healing (White et al., 2001), subsequently, Jin and co-workers demonstrated a self-healing epoxy adhesive by incorporating a two-part healing system of 15 wt. % micro-encapsulated DCPD and 2.5 wt. % Grubbs' catalyst. The addition of both components to the neat resin epoxy increased the virgin fracture toughness by 26% and a 56% recovery of fracture toughness after 24 h healing at room temperature (Jin et al., 2011). Later, they expanded the self-healing work to a high temperature (110°C for 3 h) cured rubber-toughened epoxy adhesive of ca. 750 mm thickness. *Endo*-DCPD was encapsulated in a more thermally stable, double-walled polyurethane (PU)/UF, which was designed to survive the specific epoxy's harsh curing conditions. Recovery of virgin fracture toughness ranging from 20% to 58% were obtained after assessment with WTDCB test (Jin et al., 2013).

As has been observed, the microcapsules and catalyst self-healing system also has few drawbacks. A poor dispersion of the catalyst and the amine hardener (diethylenetriamine, DETA) destructive attack on the Grubb's catalyst have been reported, which limit the healing efficiency. A new system of encapsulating the catalyst was introduced by Rule et al. The reactivity of the catalyst can be preserved when they were included into the wax microspheres, before being dispersed in the epoxy matrix. A good dispersion of the catalyst was also observed, resulting in efficient healing (maximum 93%) with significantly lower amount of embedded catalyst than the non-wax-encapsulated catalyst (Rule et al., 2005). Although Grubbs' catalyst has a nearly ideal chemical selectivity, its high cost, restricted availability and limited temperature stability preclude its use in high volume, commercial composite and polymeric parts.

An alternative catalyst for DCPD polymerization was introduced, which is cost-effective, widely available and tolerant of moderate temperature excursions. Tungsten(VI) chloride was used as a catalyst precursor for the ring-opening metathesis

polymerization of *exo*-DCPD and have demonstrated an *in situ* healing using 15 wt. % microcapsules with efficiency of approximately 20% (Kamphaus et al., 2008).

Meanwhile, Coope et al. have demonstrated another type of chemistry, which used metal triflates as effective Lewis acid catalyst to initiate DGEBA curing. This catalyst was chosen due to its catalytic activity, relatively low cost and toxicity, high stability and availability (Yadav et al., 2006). The epoxy matrix was embedded with DGEBA, ethyl phenyl acetate microcapsules and scandium(III) triflate catalyst particles as self-healing agents. The achieved healing performances, which were tested using modified tapered double cantilever beam (TDCB) specimen, were comparable to the more expensive and less robust (air and moisture sensitive) Grubbs' catalyst/ DCPD-capsule system (Coope et al., 2011).

In the multi-capsules type of self-healing, a two-part resin system, containing an epoxy resin and its hardener (mercaptan) was introduced whereby the PMF shell was chosen due to its inert properties towards the core. Healing effect was observed at low capsule content, i.e. 43.5% healing efficiency with 1 wt. % capsules and 104.5% healing efficiency with 5 wt. % capsules at 20 °C for 24 h (Yuan et al., 2008). Several years before, a similar approach but using hollow fibers or vascular method was demonstrated by Pang and Bond (2005).

In another approach, a two-component microcapsules system consisting of epoxy and boron trifluoride diethyl etherate ($(C_2H_5)_2O{\cdot}BF_3$) as hardener was introduced for self-healing epoxy composites. Boron trifluoride diethyl etherate has been commercially used as a hardener for low temperature, fast-cure epoxy adhesives. Curing of epoxy by this hardener is by cationic chain polymerization, which is a fast reaction at ambient temperature with low catalyst concentration. A recovery of 80% of impact strength was detected within 30 min at 20°C, at only 5 wt. % epoxy- and 1wt. % of ($(C_2H_5)_2O{\cdot}BF_3$)-

loaded microcapsules. The mechanical properties of the matrix were retained due to the healing effect at low microcapsules content. In addition, stoichiometric ratio between the polymerizable component and its hardener was unnecessary and the healing ability remained unchanged within 5 months. The only drawback of this system was that the high reaction rate of the healing agent resulted in incomplete curing of the epoxy (Xiao et al., 2009).

Jin et al., later introduced a new approach to encapsulate the amine (as epoxy hardener). One microcapsule contained the diluted epoxy resin while another contained the amine. The hardener-containing microcapsules were prepared by vacuum-infiltrating the amine into hollow PUF microcapsules while the epoxy microcapsules were prepared by an *in situ* polymerization method. A 91% recovery of mode-I fracture toughness was obtained in the epoxy matrix with the optimal mass ratio of amine: epoxy microcapsules of 4:6. The aforementioned healing efficiency was achieved with 7 wt. % and 10.5 wt. % of amine and epoxy microcapsules respectively. Moreover, a six month storage stability was demonstrated at ambient conditions (Jin et al., 2012).

Recently, to overcome the challenges in encapsulating the hardener for epoxy resins, a possibility to use PMMA as shell instead of the amino resins was demonstrated. The PMMA microcapsules can withstand 6-12 months storage at room temperature (Li et al., 2013b). They have obtained 43.5% and 84.5% fracture toughness recovery with 5 wt. % and 15 wt. % of microcapsules respectively, at room temperature for 24 h curing (Li et al., 2013a).

In the third approach, microcapsules-latent functionality concept was used where the healing agent is encapsulated or dispersed as particles and the polymerizer is residual reactive functionality in the matrix or an environmental stimulus (Blaiszik et al., 2010). This type of self-healing was first introduced by Yin and colleagues. They used an epoxy

resin as curing agent and distributed a well dispersed latent hardener in a matrix, which is also epoxy-based. As a result, repair of the cracked sites was completed through curing of the released epoxy (Yin et al., 2007). Another example of this system as shown by Caruso et al., utilizes solvents as healing agent. Here, residual amine functionality in an epoxy matrix is used to initiate polymerization with healing agent (Caruso et al., 2007). Other works have incorporated a meltable, thermally polymerizable epoxy microspheres into epoxy composite materials to induce self-healing (Zako & Takano, 1999) and also water-soluble, self-curing epoxy-amine adduct particles in a protective film on a steel substrate (Sauvant-Moynot et al., 2008).

In the fourth approach, a simplified processing method of capsules-catalyst has been suggested by Cho et al. by encapsulating the catalyst and dispersed the healing agent throughout the matrix. Although encapsulated-catalyst healing system was used, the siloxane-based healing agents, i.e. hydroxyl end-functionalized polydimethylsiloxane (HOPDMS) and polydiethoxysiloxane (PDES) mixture were not encapsulated. Owing to their low solubility, the siloxane-based polymers and the encapsulated butyltin di-laurate catalyst mixture were directly blended with the vinyl ester prepolymer, forming a distribution of stable phase-separated droplets and protected catalyst (**Fig. 2.9**). No reactions took place between the HOPDMS and PDES prior to exposure to the catalyst. The authors claimed a stable healing chemistry in humid or wet environments and a stable system for elevated temperature (important for higher thermoset-curing system). The siloxane-based are also widely available and comparatively low in cost (Cho et al., 2006).

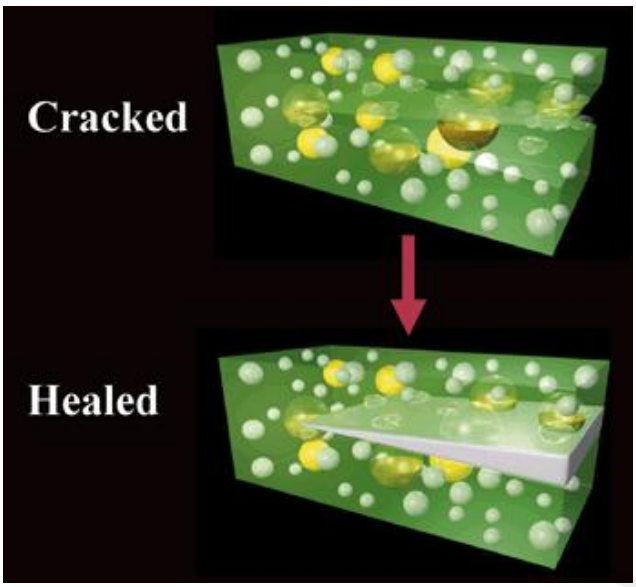

Fig. 2.9: Polydimethylsiloxane (PDMS)-based self-healing is achieved through the tin-catalyzed polycondensation of phase-separated droplets. Reproduced from Cho et al. ©2006 Wiley-VCH

2.4.4 Self-Healing Epoxy Coating

Another attractive application of self-healing is in the epoxy coating. A self-healing epoxy coating system was first introduced by Toohey and co-workers when they included microvascular networks into an epoxy coating. The networks bring the healing agent when cracks occur, thus healed the cracks (Toohey et al., 2007). A concept of self-healing using a drying oil was introduced in low molecular epoxy coating diluted with solvents. Cracks in a paint film were healed when linseed oil was released from microcapsules ruptured under simulated mechanical action. The linseed oil healed area was found to prevent corrosion of the substrate (Suryanarayana et al., 2008).

The encapsulated linseed oil along with solvents and dispersing agent were added to the epoxy coating. Two types of coatings were compared; one was filled with talc as fillers and the other was filled with microcapsules. At the same amount of filler, the latter formed fewer and smaller cracks. The enhanced impact resistance of the microcapsules-filled coating might be due to higher elasticity of microcapsule polymeric material compared to hard inorganic filler particles (i.e. plasticizer effect). The addition of

microcapsules to the epoxy binder matrix did not compromise coating performance, based on preliminary salt spray exposure of coatings (Nesterova et al., 2012).

The possibilities of sonication to produce nanocapsules containing linseed oil as healing agent in epoxy coating was examined by Boura et al. The sonication was to produce smaller size of capsules. The nanocapsules made less trouble for coating/substrate bonding, created higher healing performance for the coating matrix and had better wet adhesion and corrosion resistivity than the micro ones. The healing ability however, weakened the dry adhesion strength, which can be compensated by lowering the size of the microcapsules using the ultrasonic energy (Boura et al., 2012). Tung oil was also encapsulated to impart self-healing ability in epoxy paint films. Scratching were healed efficiently with satisfactory anti-corrosive properties (Samadzadeh et al., 2011).

Encapsulated Grubbs' catalyst and DCPD in silica coated micron and sub-micron size capsules had been demonstrated by Jackson and co-researchers. The silica served as a protective and functional layer to the microcapsules and particles. This silica coat significantly improved dispersion of the capsules and catalyst particles in the epoxy (up to 20 wt. %). The coated capsules and catalyst particles were successfully incorporated into the epoxy without significant loss of healing agent. It also enabled the capsules and particles to be dispersed at high concentrations with little loss of reactivity (Jackson et al., 2011).

Cho et al. extended their concept of phase separated self-healing concept to an anti-corrosion epoxy coating. They demonstrated a dramatic corrosion reduction of metal protected by the coating, as shown in **Fig. 2.10**. The optical images show the condition after 120 h of immersion in salt water. **Fig. 2.10 (a)** shows the control sample which consisted the epoxy vinyl ester matrix and adhesion promoter and **(b)** the self-healing coating, consisting of the matrix, adhesion promoter, microencapsulated catalyst and

phase-separated PDMS healing agent. The SEM images of the scribed region of (c) the control coating and (d) the self-healing coating after healing were also shown (Cho et al., 2009).

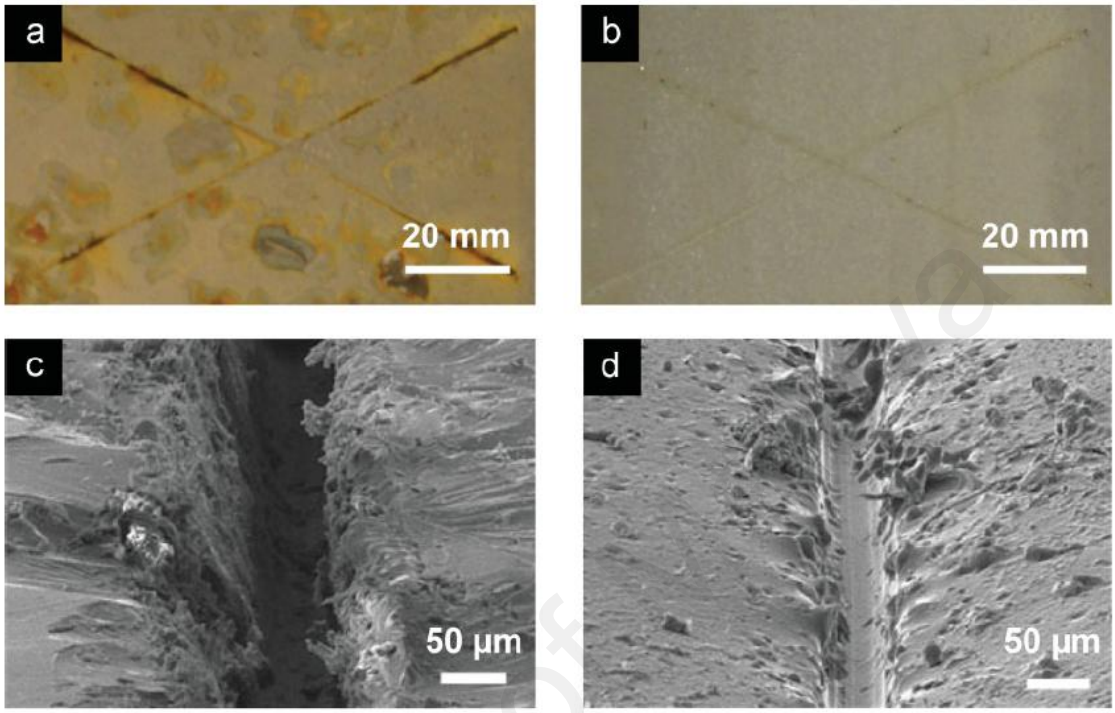

Fig. 2.10: (a,b) Optical images after 120 h immersion in salt water of (a) control sample (b) self-healing coating; (c,d) SEM images of the scribed region of (c) the control coating (d) the self-healing coating after healing. Reproduced from Cho et al. © 2009 Wiley-VCH

2.5 Alkyd as Potential Healing Agent

Alkyds are mostly used for surface coatings such as in paints, enamels, lacquers and varnishes, in which the resins function as binders, forming a tough continuous film that adheres to the coated object. Other uses include as ink binders, caulks, adhesives and plasticizers (Jones, 2012). As it is versatile, it can be tailored to have functionalities such as carboxyl and hydroxyl, which are used in crosslinking reactions with other resins.

2.5.1 Epoxy/Alkyd Reaction

The interaction between alkyd and epoxy resins normally exists in the form of blending. Epoxy and alkyd are normally blended in order to improve properties of

individual resin, usually for coating application. Blending can be physical or chemical combination making use of each resin's superior properties. Several works have studied the blending of alkyds and epoxies, their characteristics and performance in coatings. Coatings with better drying time, hardness, flexibility and gloss amongst others, were reported by blending a nahar seed oil-based alkyd with epoxy (Dutta et al., 2006). A palm oil-based alkyd have also been used to blend with epoxy, also meant for coating applications (Issam et al., 2011; Ong et al., 2015). Assanvo et al. used a *Ricinodendron heudelotii* oil-based alkyd blended with epoxy resin to improve the performance of potential coatings (Assanvo et al., 2015). All these works showed good compatibility of the blending and have improved the coating properties. In different application, a *Jatropha curcas* oil-based alkyd/epoxy blends was used as bio-reinforced composites and been reinforced with expanded graphite (Gogoi et al., 2014).

Palm oil-based alkyds were also found to be compatible with epoxidized natural rubber (ENR) and formed some crosslinking, which could modify the properties of rubber compounds (Khong & Gan, 2013; Lee et al., 2011). Moreover, the crosslinking reaction between carboxylic acid functional polyesters with epoxy resins is used for the epoxy cure as has been detailed earlier (Section 2.3). As alkyd is versatile and can be synthesized with a certain amount of carboxylic acid, the reaction of crosslinking between these two resins is being proposed in this work as a healing reaction in an epoxy matrix.

2.5.2 Palm Kernel Oil as Source of Fatty Acids and the Polyol

Palm oil is extracted from palm tree, a versatile plant oil compared to other vegetable oils (Basiron, 2007) and has become an important raw material in the world's oil and fat (Kongsager & Reenberg, 2012). Oil palm in Malaysia is a century old and was introduced as an ornamental in 1871. The oil palm was commercially exploited as an oil crop from 1911, when the first palm plantation was established (Basiron & Weng, 2004). Malaysia

is the second largest producer and the largest exporter of the world palm oil. Until 2005, palm oil has accounted for 11% of the world's production of oils and fats and 26% of export trade of oils and fats (Sime Darby, 2011).

Palm fruit contains an outer mesocarp, which produces palm oil and the hard, inside layer kernel that gives palm kernel oil (PKO). These two oils are different in their fatty acid composition, while PKO is similar to coconut oil in terms of fatty acids composition. The PKO is also called the lauric oil due to its high content of lauric acid. Palm kernel production is about 10% of the quantity of palm oil produced (Basiron, 2007). While palm oil is used mainly for food, PKO goes mainly into the oleochemical industry for making soaps, detergents and toiletry products. PKO was used as a source of fatty acid in this work, to synthesize the alkyd. PKO has low unsaturation or double bonds, as reflected in their Iodine value (Wijs) of ~18. It is yellow in color, semi-solid at room temperature and is refined physically for edible and inedible purposes.

2.5.3 Alkyd Synthesis

Alkyds are polyesters that can be obtained by the polycondensation of three monomers; polyols, dicarboxylic acids or anhydrides and natural fatty acids or triglycerides. They can be made directly from oils (monoglyceride process) or from the fatty acids; and either with or without solvents (fusion). These two have respective advantages, for instance, solvent cook gives better temperature and viscosity control while fusion cook requires simpler preparation and less expensive to operate (Patton, 1962).

In monoglycerides process, the oil is first reacted with sufficient glycerol to give the total desired glycerol content. Phthalic anhydride (PA) is one of the most commonly used anhydride in alkyd cook. Since it is not soluble in the oil, but is soluble in the glycerol, transesterification of oil with glycerol must be carried out as a separate step before the

PA is added; otherwise, glyceryl phthalate gel particles would form early in the process (Wicks, 2002). This two-stage procedure is often called the monoglyceride process. Here, the insoluble polyol and glycerides phases are converted into a single monoglyceride phase. Although the process is called the monoglyceride process, the transesterification reaction actually results in a mixture of unreacted glycerol, monoglycerides, diglycerides and unconverted drying oil. The composition depends on the ratio of glycerol to oil and on catalyst, time and temperature (Wicks, 2002). The transesterification runs at 230–250°C in the presence of a catalyst, such as calcium hydroxide and lithium hydroxide. The completion of reaction is measured by the change of acidity of the reacted PA and the extent of reaction can be calculated by measuring the acid number of the alkyd produced.

In the other method, fatty acids are used instead of oils, hence the name, fatty acid process. Here, the synthesis can be performed in a single step with reduced time in the reactor. Any polyol, polyol blends, fatty acid or fatty acid blends can produce alkyd, with greater freedom in formulation and improved performance properties (Patton, 1962). However, the cost of separating fatty acids from the reaction mixture increases the cost of the alkyd (Wicks, 2002). Other drawbacks include the corrosive nature of fatty acids, which necessitates the use of corrosion resistant equipment and the susceptibility of this type of alkyd to discoloration during storage (Patton, 1962).

2.6 Microencapsulation for Self-Healing

Microencapsulation is the process of coating small solid particles, liquid droplets or gas bubbles with a thin film of coating or shell materials. Microcapsule is used to describe particles with diameters between 1 and 1000 μm (Thies, 2005). Microcapsules consist of a core-shell structure where the active substance is surrounded by a membrane (reservoir system) and the particles range from ca. 1-1000 μm in diameters (Lamprecht & Bodmeier,

2010). The shell or wall material of the microcapsules and the process of encapsulation are selected according to the physical properties of the core and the intended application.

There are many reasons certain materials are encapsulated. The microcapsules are used to increase the storage life of a volatile compound. Core substance can also be protected from the effects of UV rays, moisture and oxygen using microcapsules. Besides, chemical reaction between two active species can be prevented by physical separation using microencapsulation. Microcapsules are also able to preserve a substance in a finely divided state so the substance can be released as required. Encapsulation of liquid can effectively convert the liquid to a fine powder solid form, while preserving the reactivity of the liquid core. By doing this, it can improve the ease in the handling of the liquid reactants.

Since around 1950s (Green & Schleicher, 1957), microencapsulation technology has widely been used in various fields including imaging applications, toners for electrophotography and thermo-sensitive printing paper. Carbonless copy paper was the first large scale commercial application of microcapsules (Konishi et al., 1974). Microencapsulation is currently widely applied in the pharmaceutical industry to mask the taste and odor of the drugs and also for drug delivery. Microcapsules are used in biomedical and biological applications, food ingredients or additives and pesticides and agrochemicals. They have also been used to encapsulate fragrances, catalysts, edible and inedible oils and self-healing agent.

Microcapsules containing self-healing agents are embedded into polymeric materials during its manufacturing stage. In the case of a crack, these microcapsules are ruptured and the agent is poured into cracks and solidifies when reacted with the catalyst or the matrix itself. Liquid active agents including monomers, dyes, catalysts and hardeners are encapsulated to suit the chemistry of the intended matrix and applications. These active

agents behave like internal glue that seal the polymeric matrix from inside the system. Some materials that have been developed to have self-healing capabilities include ionomers, concrete, elastomers, ceramics, metals and alloys and polymeric materials.

There are several important factors to be considered in designing a microcapsules-based self-healing system. These include the healing agent must be inert to the polymer shell and the microcapsules should be compatible with the host matrix. The monomer/ healing agent should has low volatility and low viscosity to promote capillary flow to cracks. The characteristics of each factor are summarized in **Table 2.3**.

Table 2.3: Important factors for construction of microcapsule-based self-healing system

Parameters	Influencing factors
Microcapsule	Healing agent must be inert to the polymer shell Longer shelf life of the capsules Compatibility with the dispersion polymer medium Weak shell wall to enhance rupture Proximity to catalyst Strong interfacial attraction between polymer matrix and capsule shell wall to promote shell rupture
Monomer	Low viscosity monomer to flow to the crack upon capillary action Less volatility to allow sufficient time for polymerization/curing
Polymerization/curing mechanism	Should be fast Stress relaxation and no cure induced shrinkage Ideally room temperature polymerization
Catalyst	Dissolve in monomer No agglomeration with matrix polymer
Healing	Must be fast Multiple
Monomer	Low viscosity monomer to flow to the crack upon capillary action Less volatility to allow sufficient time for polymerization/curing

Source: Ghosh (2009).

2.6.1 Amino Resins

Amino resins are thermosetting plastic materials that are produced by the reaction between amino group (NH bearing compounds such as aniline, guanamines, urea, melamines, thiourea, ethylene urea and sulfonamide) and formaldehyde. The two most popular amino resins are urea-formaldehyde (UF) and melamine-formaldehyde (MF). The structures of UF and MF resins are shown in **Fig. 2.11**. Amino resins are also used as curing agents for epoxy resins: first, through the etherification process with loss of water or alcohol; second through the addition reaction of *N*-methylol groups to the epoxy functionality (Ellis, 1993).

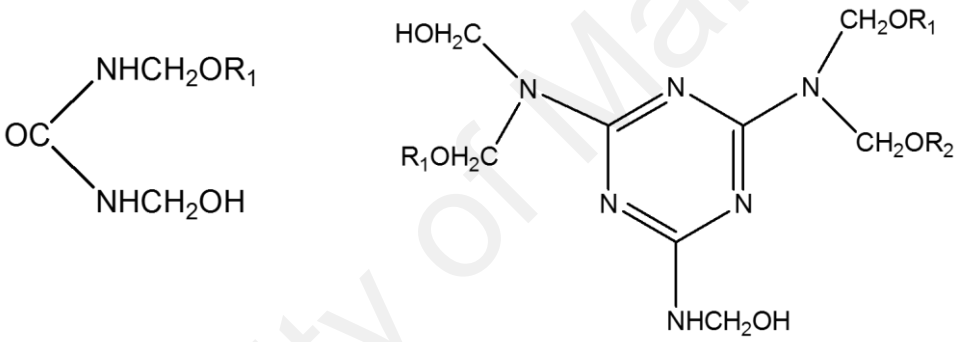

UF resin MF resin

R_1 = *n*-C_4H_9, *iso*-C_4H_9, C_2H_5, CH_3; R_2 = another MF resin

Fig. 2.11: Chemical structures of UF and MF resins

In addition to their light color, both UF and MF resins exhibit enhanced water and heat resistance. The major producer of MF resins is American Cyanamid Company, having begun the first commercial manufacture in the U.S. in 1939. Other manufacturers include Fiberite Corp., Ciba-Geigy Corp. and Allied Corp (Ibeh, 1998). These resins are widely used in industries as adhesives, impregnating resins, molding materials, strengtheners for building materials, flame retardant coatings, foamed resins for many purposes, grinding wheels, ion-exchange resins, sewage flocculants and microcapsule production. However, the woodworking industry shown the largest usage of amino resins,

for examples as resin glues in the particle board, plywood and furniture industries (Diem et al., 2010).

2.6.2 Urea-Formaldehyde Resin (UF) and Melamine-Modified UF (MUF) Resin as Shell of Microcapsules

As mentioned earlier, urea-formaldehyde (UF) resins are widely used in adhesives, particleboard, molded objects and in specialized applications such as in the fabrication of natural fiber reinforced polymers (Singha & Thakur, 2008). UF has also been used in the preparation of microcapsules due to several reasons. It can be crosslinked to form the shells that protect the healing agents. Nanoparticles of UF would deposit on the shell, to form a rough surface that aids in the adhesion of the microcapsules with the polymer matrix (Murphy & Wudl, 2010; Nesterova et al., 2011). During the preparation, a low molecular weight pre-polymer is formed from the condensation of urea and formaldehyde at the initial stage. Subsequently, the pre-polymer becomes attached onto the surface of the dispersed core material and polymerizes to form the shell (Brown et al., 2003).

Liu and co-researchers have reported the modification of poly(urea formaldehyde) (PUF) resin by mixing urea with melamine-formaldehyde pre-polymer forming poly(melamine-urea-formaldehyde) (PMUF) for encapsulating 5-ethylidene-2-norbornene (ENB) and its crosslinking agent (Liu et al., 2009). Microcapsules with PMUF shell are more robust and easier to handle than those with PUF shell. Tong and colleagues have replaced up to 12 wt. % of urea with melamine in the formulation, to encapsulate an epoxy resin. They reported that the PMUF microcapsules exhibited better resistance against solvent, acid and alkali (Tong et al., 2010). Other researchers had replaced 1%–5% of urea with a commercially available melamine resin, Cymel 303®, as shell materials for microcapsules containing DCPD. The microcapsules were strong enough to withstand the mixing with a viscous restorative dental resin (Then et al.,

2011b). Nesterova and co-researchers have prepared microcapsules of epoxy resins, DCPD, linseed oil and alkylglycidyl ether using both PUF and PMUF resins. They had also reported that PMUF shells were more stable and produced higher yield (Nesterova et al., 2011).

2.6.3 Encapsulation Technique for Self-Healing

There are many techniques of microencapsulation that includes *in situ* polymerization (Brown et al., 2003), miniemulsion (Tiarks et al., 2001), coacervation (Kruif et al., 2004), internal-phase separation (Jiang et al., 2007) and layer-by-layer assembly (Ai et al., 2003). Nevertheless, most of the microcapsules used for self-healing materials are prepared by *in situ* and interfacial polymerization in an oil-in-water (o/w) emulsion. Samadzadeh and co-researchers have discussed several methods to synthesize the microcapsules such as interfacial polymerization, coacervation, *in situ* polymerization, extrusion and sol–gel methods. Among these various methods, *in situ* polymerization was found to be the easiest and best process for encapsulation, because it does not require high level technology (Samadzadeh et al., 2010).

The microcapsules were synthesized via *in situ* polymerization to form the shell. First, a water-immiscible liquid (or solid core material) was dispersed in an aqueous phase that contains urea, melamine, water-soluble urea–formaldehyde condensate or water-soluble urea–melamine condensate. In most cases, the aqueous phase also contains a modifier that enhances shell formation. Shell formation occurs once formaldehyde is added and the aqueous phase is acidified, e.g., pH 2–4.5. The system is heated for several hours at 40–60°C. This technology is unique because the polymerization occurs in the aqueous phase, thus producing a condensation oligomers that deposits on the surface of the dispersed core particles and continue to polymerize to produce a water-insoluble, cross-

linked polymer shell. The process has already been commercialized and produces a range of commercial capsules (Thies, 2005).

2.6.4 Process Parameters

There are several process parameters affecting the formation and the size of the microcapsules. The factors are discussed as follows.

2.6.4.1 Core and shell weight ratio

The core/shell weight ratio was calculated based on the weight of core over the weight of the total raw materials forming the shell. Brown and his colleague have used a 6.2/1 ratio in the UF- *in situ* polymerization (Brown et al., 2003). This ratio has been adopted by a number of other researchers (Noh & Lee, 2013; Then et al., 2011a; Tong et al., 2010). Blaiszik et al. however, increased the ratio to 6.45/1 to get the intended microcapsules, which were spherical and well-formed. Initially by using the ratio by Brown et al., they got microcapsules with a thick layer of porous UF on the surface, which caused agglomerations in solution (Blaiszik et al., 2009).

The diameters of microcapsules have been found to increase with the enhancement of weight ratio of core–shell material. Keeping the other processing parameters constant, an increase in the core/shell weight ratio increases the size of core droplet in emulsion. Consequently, the core material and the size of microcapsules increase and the shell wall thickness may decrease. However, excess core materials cause poor dispersion, promoting aggregation of core droplets, resulting in lower yield of microcapsule and fragility of microcapsules due to the thinner shell wall (Yuan et al., 2006).

2.6.4.2 Concentration and types of emulsifiers

The concentration of emulsifiers has a crucial role during the *in situ* polymerization, too low, the droplets will tend to agglomerate into bigger sizes while an increase in

concentration will maintain the sizes of the droplets (Guo & Zhao, 2008; Tiarks et al., 2001). Sodium dodecyl benzene sulfonate (SDBS) is one of the surfactant used in the production of microcapsules by *in situ* polymerization (Yuan et al., 2006), while sodium dodecyl sulfate (SDS), gum Arabic and gelatin are normally used in coacervation method (Guo & Zhao, 2008; Song et al., 2007). Poly(vinyl alcohol) (PVA) is also used in PUF encapsulation (Yin et al., 2007; Suryanarayana et al. 2008). However, the polyelectrolyte species are most commonly used emulsifiers in the production of PUF microcapsules, such as ethylene maleic anhydride (EMA) copolymer, methylvinyl ether maleic anhydride copolymer and styrene maleic anhydride copolymer (Salaün et al., 2009).

The use of surfactant lowers the interfacial tension between the two phases (oil and water phase) and prevents the regrouping of the particles formed. The adsorption at the interface between water and air reduces the surface tension (Salaün et al., 2009). When the concentration of stabilizer is increased, finer emulsion is produced. Consequently, the size of microcapsules will be reduced and their size distribution will be narrowed down (Yuan et al., 2006; Zhu et al., 2013). However, an increase in nanoparticles formation will also occur, which will caused problem during filtration (Nesterova et al., 2012). In a separate study, Fan and Zhou (2010) have also observed pH variation as they increased the concentration of EMA.

The effect of different concentrations of emulsifiers has been studied by Ting et al. At low concentration, agglomeration of microcapsules occurred. The microcapsules were also had irregular shapes and unevenly distributed. An increase of concentration to 3 wt. % improved the size distribution, but if in excess, the microcapsules appeared very small with uneven distribution (Ting et al., 2010). Overall, the concentration of emulsifier or surfactant must be optimized to get the desired size and a good yield.

2.6.4.3 Viscosity of organic and aqueous phases

The successful production of microcapsules is greatly affected by the method of encapsulation. It is difficult to generalize on the relative importance of individual aspects of the encapsulation, however, the viscosity of the organic phase (alkyd/ oils/ others) and viscosity of the aqueous phase have been shown to be significant (Jyothi et al., 2010; Thies, 2005). The viscosity of the aqueous phase of microencapsulation can be controlled or adjusted by the use of emulsifier or viscosity adjuster.

Meanwhile, the viscosity of the organic phase differs according to the core content used. Commonly encapsulated materials such as inks, fragrances and pesticides are liquids with low viscosity. According to Ghosh (2009), the monomers for self-healing materials should have low viscosity in order to flow into the microcracks, once the microcapsules are ruptured. For this purpose, encapsulated healing agents are mostly liquid or resin, which has low viscosity, such as DCPD, solvents, oils and amine. Although commonly available as high molecular weight resin with medium to high viscosity, epoxy resins can be diluted with either reactive or non-reactive diluents, prior to encapsulation. For example, DGEBA resin was diluted with reactive diluent 1-butyl glycidyl ether (BGE) with 0.2 wt. ratio of BGE/DGEBA (Yuan et al., 2006). In another work, 40 g of E-51 (bisphenol-A epoxy resin) was diluted with 800 mL sodium polyacrylate prior to encapsulation to produce self-healing epoxy composites (Yin et al., 2007).

An un-diluted epoxy resin, diglycidyl tetrahydro-o- phthalate (DTHP), with 0.36 Pa·s viscosity, was encapsulated for self-healing epoxy (Yuan et al., 2008). In further work, they studied the effect of using epoxy resins with different viscosities (with similar epoxide value) on the healing efficiency. EPON 828, Epoxy 731 and Epoxy 711 resins with viscosity values of 12.5 Pa·s, 0.85 Pa·s and 0.53 Pa·s respectively, were used without

any dilution. The lowest viscosity epoxy resin (Epoxy 711) achieved the highest mixing efficiency (83.4%), as compared with Epoxy 731 (79.3%) and EPON 828 (63.7%). They concluded that, amongst other factors, the healing reaction would be favored when the encapsulated epoxy prepolymer has rather low viscosity (Yuan et al., 2009).

Blaiszik et al. screened a number of solvents to be used as diluent for epoxy resins (EPON 828 and EPON 862) and recommended solvents ideally should have dielectric constant (ε) between 5 and 38. The selection is based on 3 parameters: dielectric constant (ε), boiling point and flash point. The solvents chosen for their study were chlorobenzene and the less toxic and have low flammability phenylacetate (PA) and ethyl phenylacetate (EPA). The combination of 60 mL of epoxy-15 pph EPA was concluded as best combination for solvent-promoted self-healing epoxy (Blaiszik et al., 2009).

Using different core content, PDMS resin was used as healing agent (S31 and S35). Due to their high molecular weight and thus higher viscosity, S31 and S35 were added with 30 wt. % and 53 wt. % xylenes respectively, prior to encapsulation. Yet, the addition of solvent was set to a minimum in order to maximize the quantity of healing agent delivered. These microcapsules with solvents were compared with microcapsules containing only PDMS resin as control. The control showed best microcapsules production with good shape, free flowing and little debris. On the other hand, microcapsules containing S31 and S35 were less uniform in shape with more debris and had a tendency to cluster, which required sieving. The inclusion of solvent also lowered their thermal stability. In terms of healing efficiency, S35 showed highest healing efficiency at certain loading limit and the efficiency decreased when the content loading exceeded 0.3 mg/cm^2. This observation was explained; as the molecular weight of PDMS resin increases, the strength of the polymerized PDMS also increases. However, there is a trade-off when using a high molecular weight PDMS, which increases the viscosity of

the core therefore requiring solvent. The use of solvents degrades capsule quality and thermal stability (Mangun et al., 2010).

In a separate study, Nesterova et al. encapsulated different healing agents for epoxy coating, which include linseed oil, 5-ethylidene-2-norbornene (ENB), DGEBA diluted with BGE and DCPD. They concluded that microcapsule stability is core material-dependent and low stability was observed in microcapsules formed with more viscous agents. They explained this was possibly due to the higher elasticity of more viscous compounds, which can put more stress on the shell material during handling of the capsules (Nesterova et al., 2011).

Overall, viscosity of the core content is an important parameter for encapsulation of healing agents although a low viscosity core is preferred for self-healing application. The encapsulation process is unique depending on the core used and the process needs to be optimized accordingly. Viscosity of the core can be modified with certain diluents. However, the inclusion of diluents may or may not has an impact on the encapsulation of the healing efficiency, as the literature suggests the encapsulation process is exclusive for a selected core.

2.6.4.4 Agitation rate

According to Cosco and co-workers, the agitation rate has a great influence on the epoxy microcapsules. As the stirring rate is reduced, the epoxy/water interfacial surface is lowered. Thus, the reaction between urea and formaldehyde will occur mostly in the aqueous phase instead on the interfacial surface. This will result in lots of aggregates, which consequently will reduce the encapsulation capability (Cosco et al., 2007). A high agitation rate can produce smaller core droplets and subsequently smaller microcapsules. However, too high rate leads to frequent collisions that cause the deposition of PUF and core content on the stirrer and reactor's wall, giving low yield (Brown et al., 2003). The

increase in collisions of the droplets also leads to agglomeration of the microcapsules, which also will reduce the yield (Chen et al., 2015). Brown et al., in their study also has established a correlation between average diameter and agitation rate, which is linear in log-log scale (Brown et al., 2003).

2.7 Assessment of Healing Performance

The objective of self-healing is to recover lost or deteriorated function due to damage in a material system. The damage modes in polymers and polymer composites causing loss of function vary depending on the external stimuli such as impact, fatigue, fracture, puncture and corrosion. **Fig. 2.12** summarizes the damage modes normally found in polymeric materials and composites (Blaiszik et al., 2010).

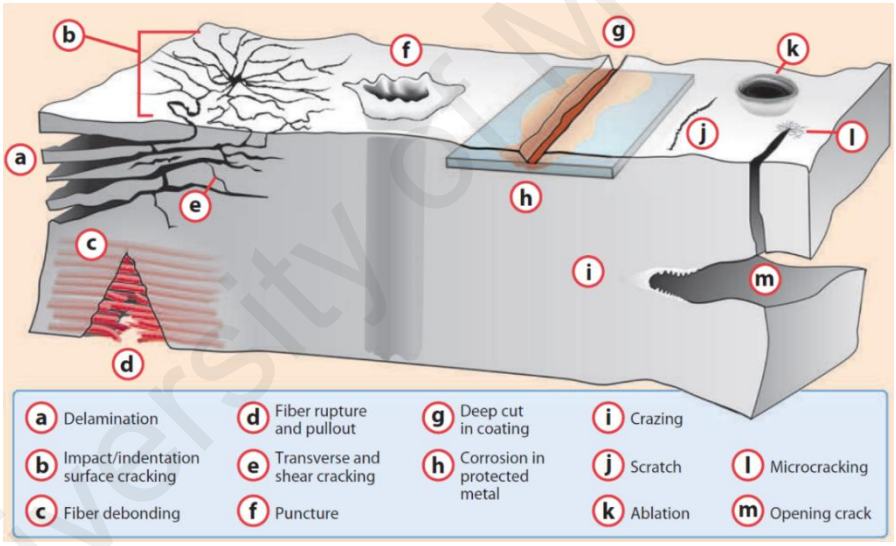

Fig. 2.12: Damage modes in polymer composites. Reproduced from Blaiszik et al. © 2010 Annual Reviews

To quantify healing, researchers have proposed multiple definitions of healing efficiencies and many techniques have been employed to verify healing, quantitatively and qualitatively. For a proper comparison of various healing systems in independent studies, an urgent need arises for more standardized test configurations and data handling procedures, such as defined in ASTM or ISO standards. As the self-healing field is at the stage of development, to date, there is no such standard just yet. However, such standards

are expected in the near future due the fast growing commercial interest in developing self-healing materials (Bose et al., 2013). Some of the healing assessments available in the literature are briefly reviewed in this section.

2.7.1 Recovery of Mechanical Properties

Crack healing in thermoplastic polymers were quantified by comparing the fracture toughness of the virgin material to the fracture toughness measured after crack closure and healing (Wool and Connor, 1981; Jud et al., 1981). Based on these studies, White et al. later defined an efficiency of healing as the ratio of the fracture toughness (K_{IC}) of healed and virgin materials, where η is the healing efficiency (Eqn. 2.1).

$$\eta = K_{IC} \text{ healed} / K_{IC} \text{ virgin} \qquad \textbf{Eqn. 2.1}$$

They used the TDCB specimen, introduced by Mostovoy et al., to undergo the fracture test (mode I). In fracture toughness mode I, a method originally developed for adhesives, tensile force is applied normal to the crack plane. TDCB geometry was chosen because using this, the crack growth can be controlled to be across the center of a brittle epoxy sample (White et al., 2001). Therefore, the fracture toughness measured depends only on the applied load and is independent of the crack length (Mostovoy & Ripling, 1966).

Later, the assessments of healing through the recovery of fracture properties become quite common in epoxy composites (Brown et al., 2002; Brown et al., 2004; Kamphaus et al., 2008; Rule et al., 2005; Rule et al., 2007). The highest healing measure for epoxy composite using this measurement was observed by Caruso et al. with 82−100% recovery using the solvent and solvent with epoxy resin healing approach (Caruso et al., 2008; Caruso et al., 2007). Yuan and his co-researchers also quantified healing based on fracture properties and obtained a 104% recovery based of the fracture toughness tested with

similar method (Yuan et al., 2008). A slightly different, mode I single-edge notched bending (SENB) method was also used to quantify healing based on fracture toughness recovery. A maximum 111% of healing was obtained (Yin et al., 2007).

Tensile testing has also been used widely to determine the relations of stress–strain of polymers, using rectangular or dog-bone geometries. For self-healing studies, tensile experiments can be performed on the fractured and healed samples. However, challenges arise in order to have proper alignment of the healed samples and surface roughness. However, it can still be considered suitable for systems above a threshold rigidity and the problems can be slightly overcomed by using samples with smaller cross-sectional area and smaller gage (Bose et al, 2013).

The lap shear test can be used to measure tensile adhesion for self-healing systems as demonstrated by Keller et al., in their siloxane-based self-healing elastomer. **Fig. 2.13** shows a PDMS tear specimens and testing used by Keller and co-workers (Keller et al., 2007). Yuan and his co-workers complemented their fracture test by determining the adhesion of the epoxy composite using the lap shear test to quantify healing (Yuan et al., 2008) . The advantageous of this test include a controlled re-arrangement of the fractured surfaces and its reproducibility of clamping conditions (Bose et al., 2013).

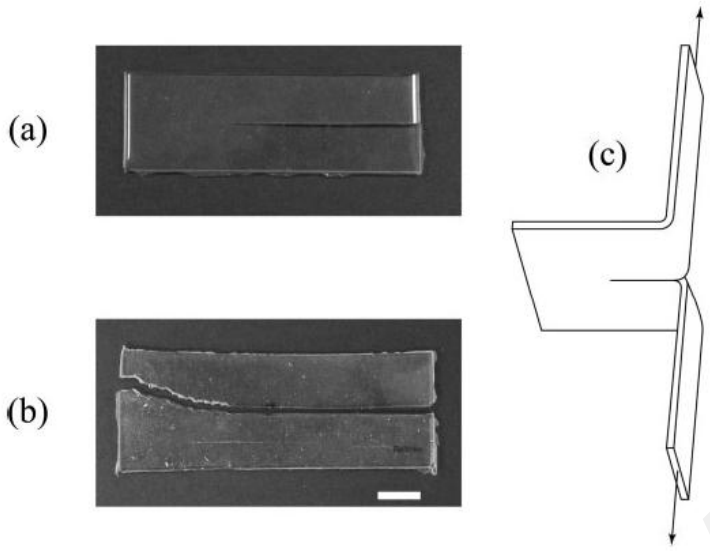

Fig. 2.13: A specimen prepared (a) before testing (b) after tear testing. (c) A schematic representation of a tear specimen during lap shear test. Scale bar = 10 mm. From Keller et al. © Wiley-VCH

2.7.2 Qualitative Assessment

Analyses such as FTIR, NMR or Raman spectroscopies can be used to monitor the progress of healing at a molecular level, where certain bonds appear or disappear in the course of self-healing (Peterson et al., 2009). This analysis can be qualitative as well as quantitative. FTIR was used to quantitatively estimate the extent of conversion of cyanate ester group in their self-healing system, consisting cyanate ester and poly(phenylene oxide) resins (Yuan et al., 2014). Meanwhile, NMR can also be used to confirm the core content of the ruptured microcapsules, where the adhesion between the two glass slides was confirmed due to the presence of the poly(glycidyl methacrylate) (PGMA) (Zhu et al., 2013).

Visualization techniques can also be used in accessing healing while optical microscopy is used to observe change in healed coating. A wide range of magnifications and the relative ease of operation are the main advantages of conventional optical microscopy to monitor damage located at the surface of the sample. However, resolution will be a limitation for optical microscopy. For example, the small (remaining) crack

openings and hair-line cracks, will be difficult to be measured with some accuracy (Bose et al., 2013). The scanning electron microscope (SEM) could offers a much higher resolution than optical microscopes. The acceleration voltage determines the resolution of the SEM. An example of FESEM usage was demonstrated by Cho et al., as depicted in **Fig. 2.14**. In a nutshell, the information from optical microscopy is generally qualitative and need to be complemented by other qualitative or quantitative methods.

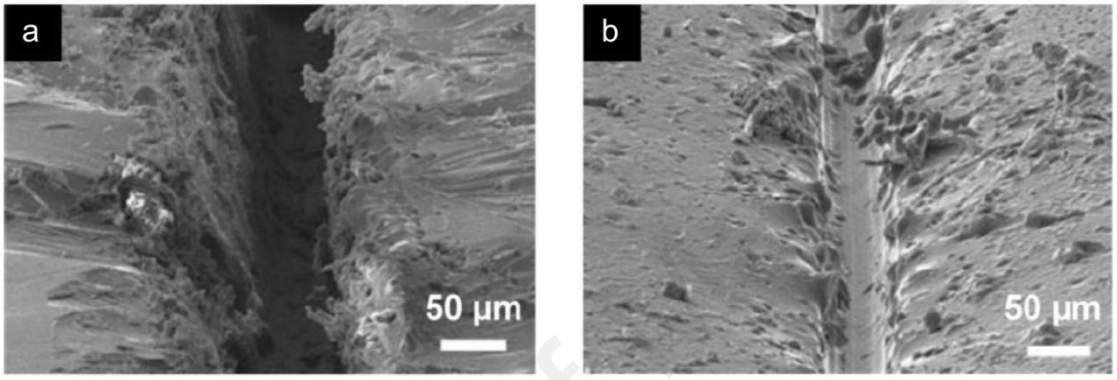

Fig. 2.14: SEM micrographs of the scribed region: (a) control coating (b) the healed coating

2.7.3 Recovery of Corrosion Protection

The performance of linseed oil as a healing agent was evaluated by exposing specimens coated with paint, containing filled microcapsules to salt spray. After 72 h of exposure, specimens with paint-containing microcapsules were found to be corrosion-free at the scribed lines, unlike the control panels, which have corroded after 48 h of exposure. The linseed oils were released from the ruptured microcapsules, filled the crack and formed a film by oxidative polymerization with atmospheric oxygen. This has prevented the admission of moisture and oxygen and therefore inhibited the corrosion (Suryanarayana et al., 2008).

Cho et al. examined multicomponent PDMS-based healing systems in epoxy and vinyl ester coatings on steel. In both phase-separated version and PU capsules-based systems, PDMS, a catalyst and an adhesion promoter were distributed in the matrix so that the

components would combine and cross-link within scratch damage. The electrical conduction measurements of the healed sample (from the phase-separated system) showed a significant reduction of conductance compared to the controls, which confirmed the healing (Cho et al., 2009).

2.8 Mechanical Testing of the Modified and Unmodified of Polymeric Materials and Composites

Mechanical properties evaluation of the self-healing materials were performed to determine the effects of inclusion of healing materials to the original unmodified properties. A list of testings can be done for instance, flexural, tensile, impact and hardness. The hypothesis is that the addition of microcapsules with healing agents up to certain limit will not compromise the mechanical properties of the polymeric materials and composites.

2.8.1 Micro-Indentation Hardness (Microhardness)

The hardness of a material is defined as its resistance to penetration by another body. Hardness is a very complex quantity that depends on Young's modulus, yield stress and stress hardening. There is no general definition of hardness applicable to all materials, neither does a universally applicable testing method. All methods measure the hardness of surfaces and not of the interior of the specimen (Elias & Mülhaupt, 2015).

Micro-indentation hardness (or microhardness) testing is widely used to study fine scale changes in hardness. The applied load and the resulting indent size are small relative to bulk tests, but the same hardness number is obtained. In general, the Vickers indenter is better suited for determining bulk (average) properties, as Vickers hardness is not altered by the choice of the test force, from 25 to 1000 gf. This is because the indent geometry is constant as a function of indent depth (ASTM E384). In the Vickers test, the

load is applied without impact, forcing the indenter into the test piece. The indenter is held in place for 10 or 15 seconds. After the load is removed, the two impression diagonals are measured and averaged. The Vickers hardness (HV) is calculated using:

$$HV = \frac{1854.4\ L}{d^2} \qquad \textbf{Eqn. 2.2}$$

where the load L is in gf and the average diagonal d is in μm. This produces hardness number units of $gf/\mu m^2$ although practically the numbers are reported without the units. An example of a well formed Vickers micro-indentation is exhibited in **Fig. 2.15**.

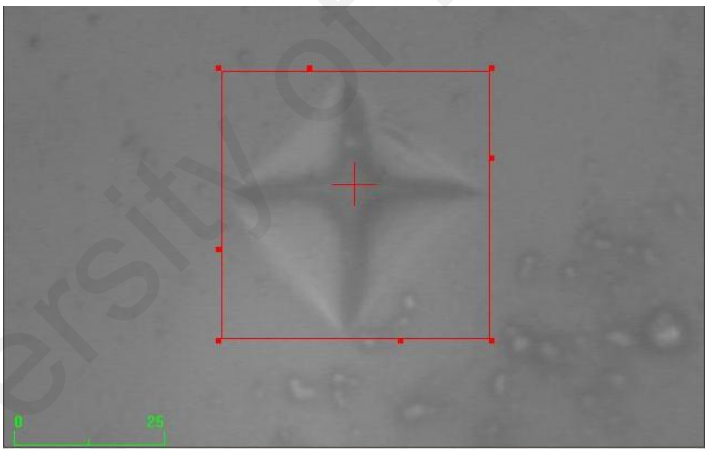

Fig. 2.15: Vickers indentation on the experimental sample of (scale is in μm)

2.8.2 Flexural Strength

To determine the strength of bulk epoxy materials is complicated due to their complex failure mechanisms. In general, the strength of an epoxy resin is determined by the presence and interactions of defects (e.g., voids and microcracks), the generation of the tensile stresses at these defects and the stress gradient along the fracture path. Flexural testing is considered an appropriate measure of the strength because it combines elements of compression, tension and shear, which more closely mimics in vivo stresses than either

compression or tension testing alone (Fard et al., 2014). Flexural strength (σ) is defined by maximum flexural stress sustained by the test specimen during a bending test (ASTM). It is calculated according to Eqn. 2.3;

$$\sigma = 3\ F\ l\ /\ 2\ b\ h_2 \qquad \textbf{Eqn. 2.3}$$

where σ is the maximum stress (Pa); F is the applied force or maximum load (N); *l* is the distance between the supports (mm); *b* is the width of the specimen (mm); *h* is the height or depth of the specimen (mm). The setup of the 3-point bend test is shown in **Fig. 2.16**. The maximum force needed to fracture the sample is normally used to characterize the strength of the material (**Fig. 2.17**). A strong material reveals high flexural strength values whereas low values indicate a weak material (Then, 2011).

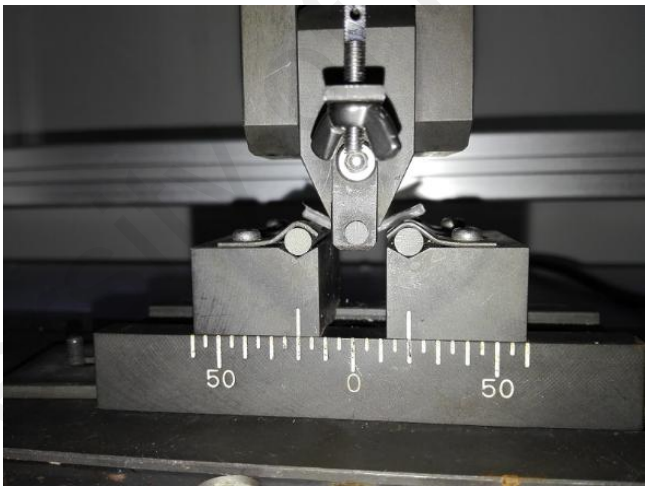

Fig. 2.16: Set up of the three-point-bend test using universal testing machine

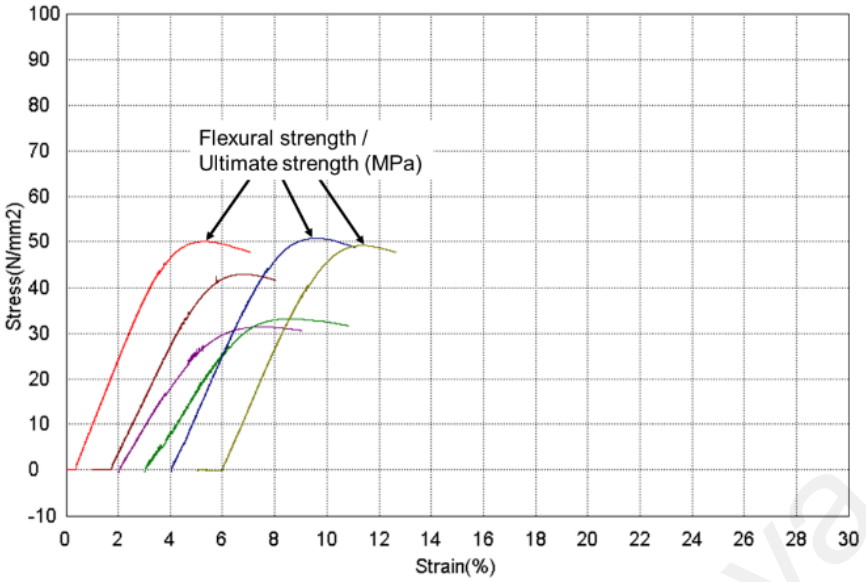

Fig. 2.17: Stress-strain curve of experimental epoxy samples

2.9 Concluding Remarks

This chapter has included a review on several key topics related to the study. The historical development of self-healing materials, the categories, healing assessment and related mechanical testing have been reviewed particularly for epoxy materials. Techniques of encapsulation and the process parameters and the background of alkyd as potential healing agent was explained.

CHAPTER 3: EXPERIMENTAL

3.1 Synthesis and Characterization of Palm Oil-Based Alkyd as Core Material of Microcapsules

A formulated alkyd was prepared using palm kernel oil (PKO) as the source of fatty acids in the alcoholysis and esterification processes. The alkyd was characterized accordingly as described in the ensuing sub-sections.

3.1.1 Palm Kernel Oil (PKO)

A Malaysian refined, bleached and deodorized (RBD) PKO was used as a source of fatty acids to prepare the alkyd as the core content. It is light yellow in colour and is refined physically to produce a very light colored oil used for both edible and inedible purposes. PKO exists as semi-solid at room temperature and is one of the non-drying oil with more than 80% unsaturated fatty acids. The fatty acid composition of PKO is tabulated in **Table 3.1**. Note that the fatty acid compositions of PKO slightly differs according to the region of their production. For instance, the amount of fatty acids of PKO from Thailand (Benjapornkulaphong et al., 2009) and Nigeria (Olaniyi et al., 2014) are different from that of the Malaysian PKO.

Table 3.1: Fatty acid composition of Malaysian palm kernel oil

Fatty acid (common name)	Carbon atom	Abundance (Mean, %)	Structure
Lauric	C12:0	48.3	$CH_3(CH_2)_{10}COOH$
Myristic	C14:0	15.6	$CH_3(CH_2)_{12}COOH$
Oleic	C18:1	15.1	$CH_3(CH_2)_7\mathbf{CH=CH}(CH_2)_7COOH$
Palmitic	C16:0	7.8	$CH_3(CH_2)_{14}COOH$
Caprylic	C8:0	4.4	$CH_3(CH_2)_6COOH$
Capric	C10:0	3.7	$CH_3(CH_2)_8COOH$
Stearic	C18:0	2.0	$CH_3(CH_2)_{16}COOH$
Linoleic	C18:2	2.7	$CH_3(CH_2)_4\mathbf{CH=CH}(CH_2)\mathbf{CH=CH}(CH_2)_7COOH$
Caproic	C6:0	0.3	$CH_3(CH_2)_4COOH$

Source: Pantzaris and Basiron (2002).

3.1.2 Materials

Refined, bleached and deodorized (RBD) PKO and glycerol (99% purity) were obtained from Emery Oleochemicals (M) Sdn. Bhd, Selangor, Malaysia. PKO (saponification value 245 mg KOH/ g oil) is a highly saturated oil, which is the extract from the nut of the oil palm fruit (*Elaeis guineensis Jacq.*). It consists of a mixture of C6 to C18:2 fatty acids of about >80% saturated fatty acids. The major fatty acid compositions are: lauric acid (C12:0, 48.3%), myristic acid (C14:0, 15.6%), oleic acid (C18:1, 15.1%), palmitic acid (C16:0, 7.8%), caprylic acid (C8:0, 4.4%), capric acid (C10:0, 3.7%), stearic acid (C18:0, 2.0%), linoleic acid (C18:2, 2.7%) and caproic acid (C6:0, 0.3%) (Pantzaris & Basiron, 2002). The same batch of PKO and glycerol were used throughout the study without further purification to minimize the compositional variations.

Phthalic anhydride (PA, 2-benzofuran-1,3-dione, $C_8H_4O_3$, M_w = 148.10 g mol^{-1}) was from Hanwha Chemical (M) Sdn. Bhd., Malaysia and lithium hydroxide (LiOH, M_w = 23.95 g mol^{-1}, J. T. Baker) was from Center Valley, PA, USA. Potassium hydrogen phthalate (KHP, $C_8H_5KO_4$, M_w = 204.23 g mol^{-1}) was from R&M, Essex, UK. Deuterated chloroform ($CDCl_3$, M_w = 120.38 g mol^{-1} 99.8 atom % D) and phenolphthalein (3,3-bis(4-hydroxyphenyl)isobenzofuran-1(3*H*)-one, $C_{20}H_{14}O_{24}$, M_w = 318.33 g mol^{-1}, ACS) were from Merck. Potassium hydroxide (KOH, M_w = 56.11 g mol^{-1}, ChemAR 85% essay) was from Systerm, Selangor, Malaysia. Tetrahydrofuran (THF, C_4H_8O, M_w = 72.11 g mol^{-1}) of gel permeation chromatography grade, stabilized with 0.025% butylated hydroxytoluene (BHT) was from Fisher Scientific (M) Sdn. Bhd., Malaysia. Toluene (C_7H_8, M_w = 92.14 g mol^{-1}) and ethanol (denatured alcohol, C_2H_5OH, M_w= 46.07 g mol^{-1}) were from R&M, Essex, UK. All materials were used as received.

3.1.3 Formulation of Alkyd

Alkyd resin is an oil-based polyester, which is synthesized by reacting polyhydric alcohol and polybasic acid. The most commonly used polyhydric alcohol and polybasic acid are glycerol and phthalic anhydride (PA) respectively. A general rule of thumb for alkyd formulation is that the amount of polyhydric alcohol varies between 5 to 40 wt. %. If it exceeds 40 wt. %, the unreacted polyhydric alcohols in the system will give rise to the adsorption of moisture. Whereas, if the content is less than 5 wt. %, the molecular weight of the finished alkyd resin is difficult to improve (Hattori et al., 2007).

While for polybasic acids, the desirable amount varies from 10 to 50 wt. %. Excess amount of polybasic acid of more than 50% by weight may cause an increase in side reactions during synthesis, which will be accountable for the gel formation at high temperature. Moreover, the extra amount of polybasic acid can affect the tackiness of the finished alkyd, resulting in alkyd resin with low tackiness. **Table 3.2** defines the commonly used symbols in alkyd technology while **Table 3.3** lists the alkyd's formulation and the related equations.

Table 3.2: Commonly used symbols and definitions in alkyd technology

M	molecular weight $(= W/m = FE)$
m	number of moles $(= W/M = e/F)$
m_0	total moles present at start of reaction ($\Sigma m_0 = \Sigma e_A + \Sigma e_B$)
E	equivalent weight $(= W/e = M/F)$
e	number of equivalents $(= W/E = Fm)$
e_0	total equivalents present at start of reaction
e_A	number of acid equivalents
e_B	number of hydroxyl equivalents
F	functionality $(= M/E = e/m)$
W	weight

Source: Patton (1962).

Table 3.3: Formulation of AlkydPKO65

Component	Wt.%	W (g)	E	e_0 (mol)	e_A (mol)	e_B (mol)	F	m_0 (mol)
PKO	63.4	750	233.7	3.21	-	-	-	-
Glycerol from PKO	-	-	-	-	-	3.21	3	1.0700
Fatty acid from PKO	-	-	-	-	3.21	-	1	3.2100
Glycerol	16.4	194	30.7	6.32	-	6.32	3	2.1067
PA	20.2	239	74.1	3.23	3.21	-	2	1.6050
Total (Σ)		1183	-	12.75	6.42	9.53	-	7.99

Here, the oil length was first set to 65% and the amount of polyhydric alcohol and the polybasic acid were fixed to ~16 wt. % and 20 wt. % respectively. By doing this, the alkyd constant (K) or Patton's gel point was from $K = \Sigma m_0 / \Sigma e_A$ = 7.99/6.42 = 1.24. K is defined as the point when gelation is expected to occur. According to Patton (1962), in order to ensure that no gelation occurs, this value should be larger than 1.00 so that gelation would not occur at 100% of reaction conversion. Referring to **Table 3.4**, at K value of 1.24, AlkydPKO65 is expected to have no gelation at 100% reaction conversion.

Next, the percentage of oil or oil length refers to the oil portion of an alkyd expressed as a percentage of the finished alkyd weight. Alkyds of different oil lengths have different properties suitable for different applications. For instance, alkyds with long oil length is used for brushing application due to their good flow-ability and ease of grinding. On the other hand, a short oil length alkyd is more suitable for spraying application because it has the lacquer type of dry properties and high viscosity. The medium oil length alkyds have properties somewhere in between short and long oil length alkyds. They can be used in paints along with long oil length alkyd to improve metal adhesion. In this work, AlkydPKO65 is a long oil length alkyd with relatively low viscosity was prepared to be emulsified and encapsulated.

R value refers to the excess of hydroxyl groups (–OH) over the –COOH groups present in the alkyd cook. It is defined as the ratio of e_B to e_A as listed in **Table 3.4**. AlkydPKO65 was formulated with excess of –OH groups to avoid premature gelation during the alkyd synthesis and the expected hydroxyl value in the finished alkyd is expressed as mg KOH in 1 g of alkyd.

Acid value or acid number is defined as the amount of KOH (in mg) required to neutralize the free carboxylic groups (–COOH) in 1 g of alkyd. Initial acid value of an alkyd cook is calculated based on the number of acids equivalent (e_A) value of the dibasic acid introduced in the cook. The final acid value and amount of –COOH groups was determined experimentally as described in Section 3.1.5.1.

Finally, the alkyd reaction usually releases a simple by-product molecule (commonly water) during the molecular bonding of polyhydric alcohol and polybasic acid. When the alkyd is cooked from oil (PKO) that is already esterified, water evolved was from the esterification of the PA with glycerol (9 weight units per equivalent of anhydride). Therefore, the expected weight of water collected from the alkyd cook can also be calculated. The complete amount of water collection could mark the completion of the alkyd synthesis.

Table 3.4: Value of parameters and formulation of AlkydPKO65

Parameters	Formula	Calculation
Alkyd constant (K) or Patton gel point	$K = \Sigma m_0 / \Sigma e_A$	$K = \frac{7.99\ mol}{6.42\ mol}$ $= 1.24$
Oil length / percentage of oil	$Oil\ length = \frac{weight\ of\ oil\ (g)}{finished\ alkyd\ (g)}$ OR $= \frac{weight\ of\ oil\ (g)}{total\ reactant\ charged - water\ evolved\ (g)}$	$Oil\ length = \frac{750\ g}{1183-28.89} \times 100\ \%$ $= 65\ \%$
R value	$R = \Sigma e_B / \Sigma e_A$	$R = \frac{9.53\ mol}{6.42\ mol}$ $= 1.48$
Initial acid value / acid number (AN)	$AN_{initial}$ $= 56100.\ e_A\ /\ W_{\text{Total}}$ 56100 = molecular weight of KOH in mg/mol	$AN\ initial = \frac{56100\frac{mg}{mol} \times 6.42\ mol}{1183\ g}$ $= 304.45\ mg\ KOH/\ g\ alkyd$
Final acid value	$AN\ final\ (experimental)$ $= \frac{56.1\ \times N\ \times (V - Vb)}{W}$ $= 15\ mg\ KOH/g\ alkyd$	$Amount\ of\ free - COOH\ groups$ $= \frac{AN\ final}{56100\ mg/mol}$ $= 2.67 \times 10^{-4}\ mg/mol$
Percentage of excess –OH	$\%\ of\ excess - OH\ groups =$ $100\%\ \times (R - 1)$	$\%\ of\ excess - OH\ groups =$ $100\%\ \times (1.48 - 1)$ $= 48\%$
Expected hydroxyl value	$= (\Sigma e_B - \Sigma e_A) \times 56100\ /$ $(\Sigma W - W_{water})$	$= \frac{(9.53\ mol - \ 6.42\ mol) \times 56100}{1183\ g - 28.89\ g}$ $= 151.17\ mg\ KOH/g\ alkyd$
Expected weight of water	$=$ (e_A from PA) $\times$ 9 g/mol	$= 3.21\ mol\ \times 9\ g/mol$ $= 28.89\ g$

3.1.4 Synthesis of AlkydPKO65

The alkyd AlkydPKO65 was synthesized according to the following procedure. 750 g PKO, 107 g glycerol and 0.7 g lithium hydroxide were charged into a reactor flask equipped with a reflux condenser, thermometer and mechanical agitator, as shown in **Fig. 3.1 (a)**. The mixture was heated at 220°C for about 2 h to complete the alcoholysis process. The complete conversion of the oil to monoglycerides was checked by the solubility test of the product in ethanol. Heating was turned off, the temperature was allowed to drop to 180°C and a Dean-stark decanter was attached to the reactor, in order to collect water as a by-product from the esterification process, as shown in **Fig. 3.1 (b)**. Next, 230 g phthalic anhydride and 87 g glycerol were added. The polycondensation was carried out at 210–220°C and the progress of the reaction was monitored by acid number determination according to ASTM D1639-90. The reaction was stopped when the acid number (AN) has dropped to about 5% of the initial value. The product was a viscous liquid and dark brown in color. **Fig. 3.2** summarizes the preparation steps of the alkyd.

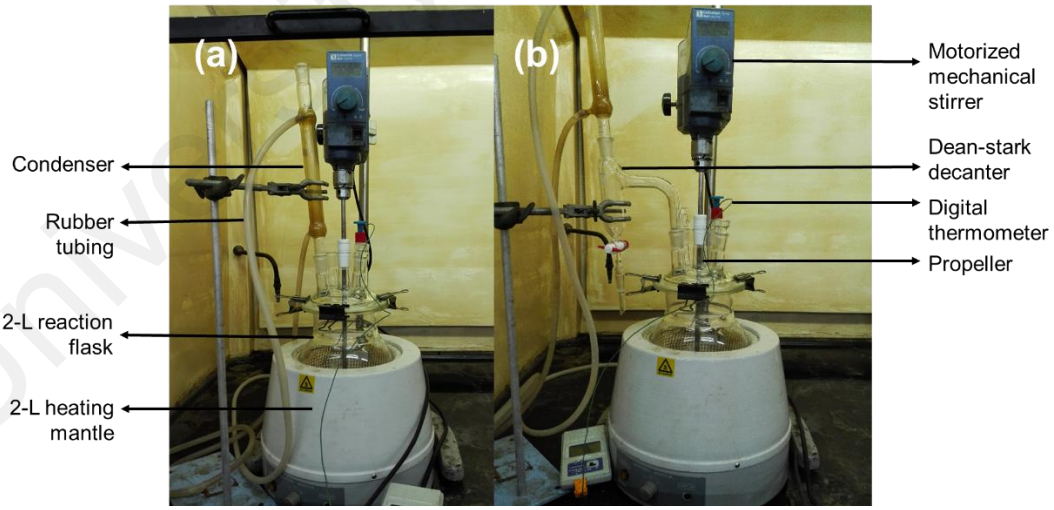

Fig. 3.1: Experimental set up of (a) alcoholysis process (b) esterification process, equipped with Dean-stark decanter to collect water

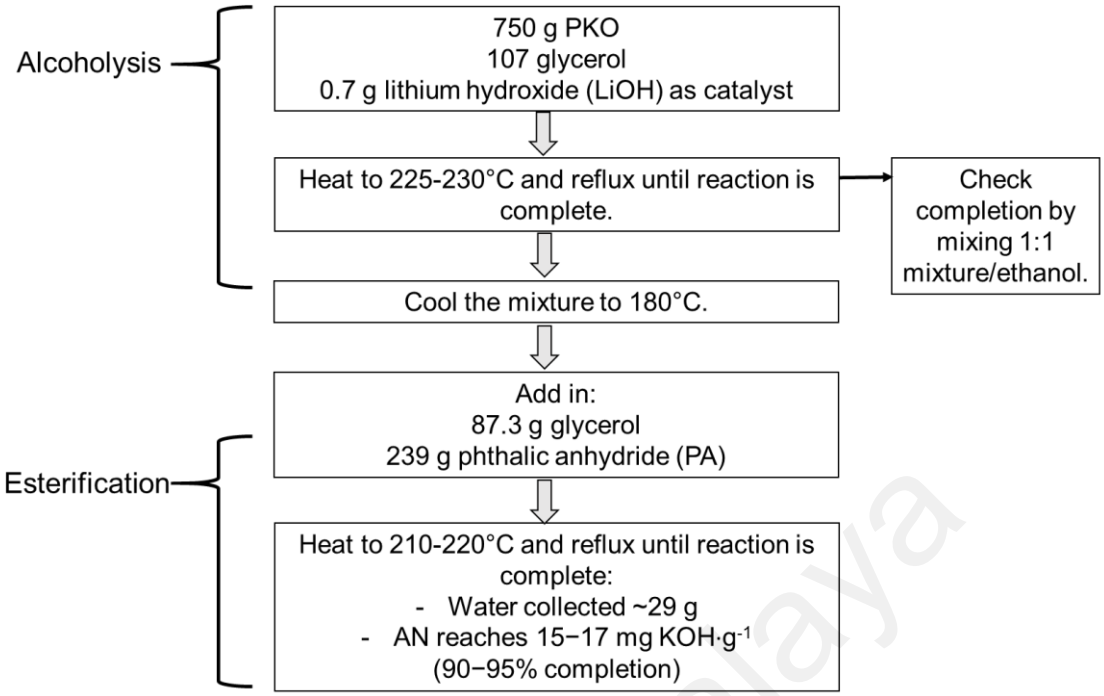

Fig. 3.2: Synthesis of alkyd using palm kernel oil (by alcoholysis and esterification processes)

3.1.5 Characterization of AlkydPKO65

Alkyd usually is characterized by conventional techniques in the same way as its raw material to determine the physical properties such as acid, iodine and hydroxyl values, viscosity, volatile matter content and specific gravity. The results from the acid value, iodine value, hydroxyl value and viscosity indicate the level of free carboxylic groups, level of unsaturation, degree of free hydroxyl groups and the alkyd's processability, respectively. The structural analysis, molecular weight determination, rheological behavior and thermal characterization are carried out by techniques such as Fourier transform infrared (FTIR), nuclear magnetic resonance (NMR), gel permeation chromatography (GPC), rheometry analysis, differential scanning calorimetry (DSC) and thermogravimetric analysis (TGA).

3.1.5.1 Determination of acid value (AN) and amount of –COOH group of alkyd

Acid value or AN is an indication of the amount of KOH (in mg) required to neutralize the free acids contained in 1 g of alkyd. It denotes the level of free carboxylic acid groups

in the alkyd. The decrease of AN is a measure of the usage of the polybasic acids in the esterification process that could thus determine the completion of the polyesterification process.

(a) ***Preparation and standardization of 0.05 N ethanolic potassium hydroxide***

An ethanolic potassium hydroxide solution was prepared by dissolving 2.8 g of KOH in a 1.0 L volumetric flask and the volume was made up to 1.0 L with ethanol. The solution was then standardized using potassium hydrogen phthalate (KHP). The KHP was dried in an oven at 110°C for 2 h and cooled in a desiccator prior usage. About 0.5 g of KHP was weighed into a conical flask and was then completely dissolved with 50 mL of distilled water and ~0.5 mL of 1% phenolphthalein indicator. The KHP solution was titrated with the 0.05 N of ethanolic KOH from a burette, until a tint of pale red persisted in the solution for 30 seconds. Titration was done in duplicate; the volume of KOH was recorded and the normality of KOH solution was calculated based on Eqn. 3.1:

$$\text{Normality of KOH} = \frac{W_{KHP}}{0.2042 \times V_{KOH}} \qquad \textbf{Eqn. 3.1}$$

where W_{KHP} is weight of KHP and V_{KOH} is the volume of KOH solution used to neutralize the KHP.

(b) ***Preparation of sample and blank titration***

About 2 g of alkyd was weighed in a conical flask and dissolved in 50 mL of solvent mixture, which composed of 3:2 parts by volume of toluene and ethanol. Subsequently, the alkyd was titrated with standardized KOH solution that contained ~0.5 mL 1% phenolphthalein indicator. The titration was complete when a tint of pale red persisted in the solution for 30 seconds and the volume of KOH solution required for the titration was recorded. The titration was done in duplicate and the AN was calculated using Eqn. 3.2:

$$\text{Acid number (AN)}_{\text{final}} = \frac{56.1 \times N \times (V - V_b)}{W} \qquad \textbf{Eqn. 3.2}$$

where N is the normality of KOH solution, V and V_b are the volumes (mL) of KOH solution required to titrate the sample and blank respectively. The amount of –COOH groups in alkyd can be calculated according to Eqn. 3.3.

$$\text{Amount of free } -COOH \text{ groups} = (\text{AN}_{\text{final}} / 56100)\ \text{mg·mol}^{-1} \qquad \textbf{Eqn. 3.3}$$

3.1.5.2 Viscosity analysis

The rheological behavior of alkyd resins such as viscosity, the variations of viscosity with time, temperature and shear rate (τ) , the variations of storage modulus, loss modulus and loss factor with frequency, can be determined by capillary and oscillation viscometer or rheometer (Karak, 2012). Here, the viscosity of alkyd was determined using a rheometer (Physica MCR, Anton Paar GmbH, Graz, Austria) with a double gap) accessory (DG 26.7), equipped with a temperature regulator (Viscotherm VT, Anton Paar GmbH, Graz, Austria). Approximately 10–12 mL of alkyd were loaded into the sample holder and measurement was performed at 26°C at shear rate (τ) of 1−100 s^{-1}. The measurement of the viscosity was recorded using Rheoplus/32 software v3.60 (Anton Paar).

3.1.5.3 Attenuated total reflectance-Fourier transform infrared (ATR-FTIR) analysis

The Fourier transformed infrared (FTIR) is widely used in the qualitative and quantitative determination of polymers composition. A fast and well recognized fingerprinting method, it is used to determine functional groups such as carboxyl, ester, hydroxyl, unsaturation and aromatic ring, which are present in the structures of oil and

alkyd, specifically. FTIR spectrometers are used to analyze solids, liquids and gases by means of transmitting the infrared radiation directly through the sample (Perkin Elmer, 2005). The technique of attenuated total reflectance (ATR) overcomes the challenging aspects of FTIR, which are the sample preparation and spectral reproducibility. It is the most widely used FTIR sampling method today that allows qualitative or quantitative analysis of samples. In contrast to the traditional FTIR sampling by transmission, where the sample must be diluted and put onto IR transparent salt, pressed into a pellet or pressed to a thin film, ATR-FTIR requires little or no sample preparation. This significantly speeds up sample analysis (Pike Technologies, 2011).

In this study, a spectrometer, ATR-FTIR (Perkin-Elmer Spectrum 400, Perkin Elmer, Waltham, MA, USA) was used to obtain the FTIR spectra. The spectra of alkyd and PKO were recorded after eight scans, from 4000−450 cm^{-1} at 4 cm^{-1} resolution.

3.1.5.4 Proton nuclear magnetic resonance (^{1}H-NMR) analysis

Proton nuclear magnetic resonance (^{1}H-NMR) can play an important role in understanding the actual structures of a range of polyesters and their precursors. It can be used to structurally identify the oil and the alkyd. It also provides quantitative determination of oil, anhydride and polyol components present in the alkyd (Karak, 2012). In this work, ^{1}H-NMR spectrum of the alkyd and PKO were recorded on the samples dissolved in $CDCl_3$ and analyzed using a JNM-ECX400 II FT-NMR (JEOL, Tokyo Japan) spectrometer, operating at 400 MHz at ambient temperature. The samples were prepared by dissolving ~0.1 g of PKO and alkyd in approximately 3−4 mL $CDCl_3$.

3.1.5.5 Gel permeation chromatography (GPC) analysis

The average molecular weight (M_n) and distribution of multiple molecular weights normally found within a polymer influence both the processability of the material and its mechanical properties. Gel permeation chromatography (GPC) is a secondary method

used for fast determination of molecular weight distribution (MWD, M_w/M_n), after light scattering technique. It is the most frequently used commercial technique due to its ease of use, low cost and short time for analysis (Furches, 2004).

GPC is a form of liquid column chromatography, in which carrier solvent is passed at a constant rate through a column, consisting of cross-linked polymer beads previously allowed to swell in the same solvent (Elgert, 2000). Dilute polymer solutions are placed on top of a column filled with a porous carrier. Molecules with low molecular mass can enter the pores, but not the molecules with higher molecular mass. Medium-sized molecules enter the column with difficulty and remain for shorter times than the molecules with low molecular mass. Higher molar masses are thus eluted first, followed by medium and smaller sized molecules that gives the last peak in the chromatogram. This final peak defines the total permeation limit.

The M_n and MWD of the alkyd are determined by GPC (Viscotek, Malvern Instruments, Worcestershire, UK). Alkyd sample of 0.02 g was dissolved in 10 mL of THF and left overnight before being filtered into the sample vials. A non-sterile nylon filter 25 mm in diameter and 0.22 microns of pore size was used in the filtration process. The GPC was calibrated with monodispersed polyisoprene and 100 µL of sample (0.2% w/v of sample in THF) was injected into the column at 25°C. The chromatograms and integrated data were recorded using OmniSEC 4.6 software.

3.1.5.6 Differential scanning calorimetry (DSC) analysis

Differential scanning calorimetry (DSC) is the most commonly used thermal analysis technique to obtain information about the phase and chemical changes, by measuring the difference between the heat flows from the sample and the reference of a sensor. The measurement gives an enthalpy change, due to the physical and chemical changes, as a function of temperature or time. It is used extensively in polymer science as most

polymers display glass transition, a condition where the material changes from a glassy to a rubbery state, with a simultaneous rise in specific heat capacity. Glass-transition temperature (T_g) measurements are used to characterize polymeric material such as to obtain thermal history, crystallinity, extent of cure and plasticizer content of a polymer. For instance, amorphous polymers normally exhibit crystallization exotherm while thermosetting polymers such as epoxy show curing exotherm (Warrington & Höhne, 2000).

DSC thermogram of the alkyd was recorded using a differential scanning calorimeter (DSC822e, Mettler Toledo GmbH, Giessen, Germany) equipped with a sub-ambient cooling accessory (HAAKE EK/90, Mettler Toledo GmbH, Giessen, Germany). Calibration was carried out using high purity indium before each measurement to ensure accuracy. Approximately 5−10 mg of sample was weighed and sealed in an aluminum pan. The sample was analyzed over a temperature range of -60 to 300°C at a scanning rate of 20°C min^{-1}, under nitrogen atmosphere. T_g was obtained and was defined as the middle point of the inflection in the DSC curves.

3.1.5.7 Thermogravimetric analysis (TGA)

Thermogravimetric analysis (TGA) observes the change in the mass of a material during a controlled temperature ramp. It can be used to determine the types of polymers by comparison of degradation curves. The derivative curve of TGA (dTG) can be used to improve the determination of onset and end point of decomposition in multi-polymer systems (Furches, 2004). The thermal characterization of alkyd resin is generally carried out using this technique, where the patterns and kinetics of degradation and char residues can also be determined (Karak, 2012). The thermal stability of alkyd in certain environments can also be studied using TGA. Here, about 5−8 mg of alkyd sample was analyzed using TGA (TGA 6, Perkin Elmer, Waltham, MA, USA), in a nitrogen

environment at a flow rate of 20 mL min^{-1}. The measurement was carried out from 30°C to 700°C at the heating rate of 20°C min^{-1}.

3.2 Microencapsulation of Alkyd by Amino Resins

For optimization of the alkyd encapsulation process, a number of series of microcapsules were prepared and the detail of each series are listed in **Table 3.5**.

Table 3.5: Details of series of microcapsules

Series of microcapsules	Shell material/s	Melamine used	Method	Core	Others
1	PMUF	Monomer	1	AlkydPKO65	-
2	PUF	-	2	AlkydPKO65	-
A	PUF	-	2	AlkydPKO65	-
B	PMUF	Resin	2	AlkydPKO65	-
C	PUF; PMUF	Resin	3	AlkydPKO65	Sonication, PVA added
D	PMUF	Resin	2	AlkydFA35*	-

*AlkydFA35 is a commercially available alkyd, encapsulated for comparison with AlkydPKO65; PUF= poly(urea-formaldehyde); PMUF= poly(melamine-urea-formaldehyde); Method 1= shell materials were added followed by the emulsification of alkyd; Method 2= alkyd was emulsified prior to addition of shell materials; Method 3 is a modified method 2 with additional sonication (Refer Appendix B).

3.2.1 Materials

Urea (CH_4N_2O, M_w = 60.06 g mol^{-1}, ACS), 1-octanol ($C_8H_{18}O$, M_w = 130.23 g mol^{-1}, ACS), resorcinol (1,3-dihydroxybenzol, C_6H_4-1,3-$(OH)_2$, M_w = 110.11 g mol^{-1}, Riedel de-Haën), ethylene maleic anhydride copolymer (EMA, C_2H_6O, M = 46.07 g mol^{-1}, M_w = 400 000, Riedel de-Haën), ammonium chloride (NH_4Cl, M_w = 53.49 g mol^{-1}, Fluka), melamine ($C_3H_6N_6$ 99%, M_w = 126.12 g mol^{-1}, Aldrich) and poly(vinyl alcohol) (PVA, fully hydrolyzed, $–[CH_2CHOH]–_n$, Sigma) were from Sigma-Aldrich. Formaldehyde (37% aqueous, CH_2O, M_w = 30.03 g mol^{-1}, ChemAR) was from Systerm®, Selangor, Malaysia. Hexamethoxymethyl melamine or Cymel 303® (melamine resin) ($C_{15}H_{30}N_6O_6$, M_w = 390.44 g mol^{-1}) was from Cytec Industries (M) Sdn. Bhd., Selangor, Malaysia.

Deuterated chloroform ($CDCl_3$, M_w = 120.38 g mol^{-1}, 99.8% atom D) and sodium hydroxide (NaOH, M_w = 40.00 g mol^{-1}, Emsure® ISO) were from Merck. AlkydPKO65 was synthesized as described in Section 3.1.2 whereas alkyd AlkFA35 (acid number 55 mg $KOH \cdot g^{-1}$) was obtained from Jadi Imaging Technologies Sdn. Bhd., Malaysia. Acetone (C_3H_6O, M_w = 58.08 g mol^{-1}) and ethanol (denatured alcohol, C_2H_5OH, M_w= 46.07 g mol^{-1}) were from R&M, Essex, UK.

The epoxy resin used was Epikote 240, which is a low-viscosity resin with an epoxy molar mass of 185–190 g per equivalent. Epikure F205 (cycloaliphatic amine) was used as the curing agent. Both the epoxy and its curing agent were from Hexion Inc., Columbus, Ohio, USA. Vinyl polysiloxane (VPS) (silicone rubber) impression material (Take 1 Advanced Putty) was from Kerr Corp., Orange, CA, USA (Lot 71040, 2017-3, part #34070). All materials were used as received.

3.2.2 Synthesis of Microcapsules Filled with Alkyd

The general microencapsulation procedure are as follows (denotes as Method 2 in **Table 3.5**). 25 mL of 2.5 wt. % EMA and 100 mL of distilled water were mixed in a 500 mL beaker, suspended in a water bath at ambient temperature (28−33°C). Pre-weighed amount of alkyd was poured slowly into the aqueous mixture to be emulsified and agitated by a mechanical stirrer with a 4-bladed-propeller at 300−500 rotation per minute (rpm). After 10 min of agitation, 2.50 g urea, 0.25 g ammonium chloride and 0.25 g resorcinol were added into the emulsion. pH of the emulsion was changed to 3.50 by dropwise addition of 10% sodium hydroxide solution and 37% hydrochloric acid. Finally, 6.35 g of formaldehyde solution was added into the emulsion. Temperature of the bath was elevated at 1.5°C min^{-1} rate to 55°C. The experimental setup is shown in **Fig. 3.3**. The polymerization was done for 4 h, until a white slurry in the water was formed. Next, the stirring was reduced to 200 r.p.m and the slurry was let to cool overnight. The slurry was

washed thoroughly with distilled water and rinsed with ethanol to remove unreacted monomers. It was then filtered under suction and dried under fan for 1 h to get the free-flowing microcapsules. Subsequently, they were filtered using sieves (Endecotts, certified acc. to BS410, ISO 3310) with mesh sizes of 50, 150, 200, 300 and 500 microns. The microcapsules of larger than 500 microns and smaller than 50 microns were negligible and discarded. Certain modifications were done for different series as listed in **Table 3.5** and they are described in detail in **CHAPTER 5**. **Fig. 3.4** summarizes the general microencapsulation method.

Fig. 3.3: Experimental set up of microencapsulation process

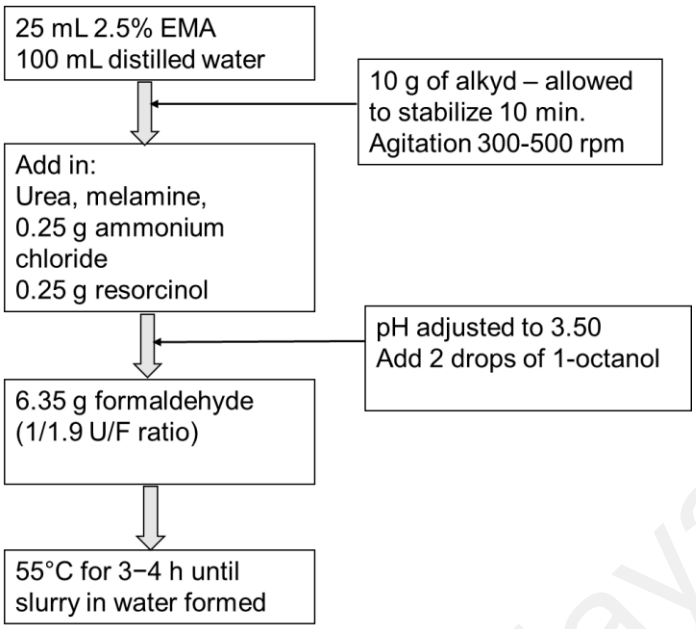

Fig. 3.4: General microencapsulation procedure of alkyd

3.2.3 Spectroscopic Analyses of Core Content

The chemical structure of the alkyd in the microcapsule can be analyzed by different spectroscopic methods such as attenuated total reflectance-Fourier transform infrared spectroscopy (ATR-FTIR) and proton nuclear magnetic resonance (^{1}H-NMR). The microcapsules of 0.2−0.3 g were crushed with a pestle in a mortar. The core content was extracted with acetone and the insoluble shell materials were filtered, washed and dried at 70°C for 24 h in a vacuum oven. For the ^{1}H-NMR analysis, the core content was extracted using deuterated chloroform ($CDCl_3$).

FTIR spectra of the samples were collected from a spectrometer (ATR-FTIR Perkin-Elmer Spectrum 400) with eight scans, in the range of 4000−450 cm^{-1} wavenumbers at 4 cm^{-1} resolution. The spectra of the extracted core were compared with the spectra of the neat alkyd. The spectra of the shell materials were also obtained. All data were processed by Spectrum v6.3.1.0132 (Perkin Elmer) software.

Solution state ^{1}H-NMR spectrum of the extracted core content was recorded on the sample dissolved in $CDCl_3$. The shell was insoluble in $CDCl_3$, thus could not be analyzed

by NMR. The samples were analyzed using a JNM-ECX400 II FT-NMR (JEOL) spectrometer and data were processed by JEOL Resonance software. The successful encapsulation of the alkyd would be verified by the presence of the characteristic signals corresponding to alkyd in the spectrum of the diluted microcapsule extract.

3.2.4 Characterization of Microcapsules

Several experiments were performed to physically characterize the microcapsules are described in the following sub-sections.

3.2.4.1 Yield of microcapsules

The total yield of the microcapsules was calculated from the weight of the product over the total weight of capsules-forming raw materials. The microcapsules could be separated into several fractions of different sizes by sieving. The major fraction (~50%) was in the range of 300−500 μm and was selected for further characterization.

3.2.4.2 Size and particles distribution

The average diameter of the microcapsules was determined on data sets of more than 250 particles using images obtained from a digital microscope, equipped with measuring software (AnMo Electronics, Taipei, Taiwan), based on recommended literatures (Li et al., 2007; Liu et al., 2012; Wang et al., 2013; Yuan et al., 2006).

3.2.4.3 Calculation of core content

Solvent extraction and gravimetric analysis were used to determine the core content of microcapsules. A known weight of microcapsules was crushed with a pestle in a mortar. The core content was extracted with acetone and the insoluble shell materials were filtered, stirred in a mixture of acetone and ethanol for 24 h to ensure no alkyd was left, washed and dried at 70°C for 24 h in a vacuum oven. The extracted core content

(E_{core}) was calculated using Eqn. 3.4, where W_s refers to the weight of sample and W_m refers to the weight of the shell.

$$E_{core} = \frac{(W_s - W_m)}{W_s} \times 100\% \qquad \textbf{Eqn. 3.4}$$

3.2.4.4 Viscosity of core content and selected epoxy resins

The viscosity of alkyd AlkFA35 and epoxy resins (Epikote 828 and Epikote 240) were determined using a rheometer (Physica MCR, Anton Paar GmbH, Graz, Austria) as described before in Section 3.2.3.2. Approximately 10–12 mL of resin was loaded into the sample holder and measurement was performed at 26°C at increasing shear rate of 1−100 s^{-1}.

3.2.5 Differential Scanning Calorimetry (DSC) Analysis

In DSC analysis, the particular temperatures at which peaks are observed, can be used for the identification of components in a mixture (Warrington & Höhne, 2000). Thus, apart from obtaining certain thermal and physical properties of the microcapsules and their core content, DSC can be used to provide evidence that the microcapsules contain the alkyd. Analysis was done using DSC822e (Mettler-Toledo) on the microcapsules and the shell materials, in a nitrogen environment at a flow rate of 20 mL min^{-1}. Samples were scanned from -60°C to 300°C at a heating rate of 10°C min^{-1}. Measurement was calibrated with an indium standard and an intercooler (HAAKE EK/90, Mettler Toledo) was used for sub-ambient temperature.

3.2.6 Thermogravimetric Analysis (TGA)

For thermal stability study of the microcapsules and the core, analyses of each sample were carried out using TGA (TGA 6, Perkin Elmer). About 1−5 mg of each sample were

scanned from 30°C to 700°C at 20°C min^{-1}, in a nitrogen environment at a flow rate of 20 mL min^{-1}.

3.2.7 Simultaneous Thermal Analysis (STA)

Approximately 5 mg of samples from the C and D series were analyzed using simultaneous thermal analyzer (STA 6000, Perkin Elmer, Waltham, MA, USA) due to unavailability of the previous instrument. They were scanned from 30°C to 800°C at 20°C min^{-1}, in a nitrogen environment at a flow rate of 20 mL min^{-1}.

3.2.8 Surface Morphology and Shell Wall Thickness

The morphology of microcapsules was examined using two different field-emission scanning electron microscopes (FESEM) (Hitachi SU8220, Hitachi Hi-Tech Corp., Tokyo, Japan and Quanta FEG 450, FEI, Oxford, UK). Samples were mounted on a single-stub sample holder and some of the microcapsules were sliced with a razor blade to facilitate examination of the interior of the microcapsules. The analysis was carried out under low vacuum using an electron acceleration voltage of 2.0 and 5.0 kV.

3.2.9 Storage of Microcapsules

After the isolation and sieving processes, the microcapsules were kept in tightly sealed vials. They were stored in two refrigerators with the average temperature of 25−26°C and 8−9°C respectively. After a certain period of time, microcapsules were inspected using digital microscope and tested using DSC.

3.3 Microcapsules in Epoxy Matrix: Mechanical Properties and Epoxy/Alkyd Reaction

The prepared microcapsules were embedded to a selected epoxy matrix and certain mechanical properties of the epoxy composite were tested. Next, the curing of epoxy with

alkyd were evaluated by blending the epoxy and alkyd. The blends were cured with amine hardener.

3.3.1 Mold Preparation

Bar- and disc-shaped molds were prepared using VPS impression material (silicone rubber). The base material was mixed with its catalyst in a 1:1 ratio. They were kneaded until a dough was formed. The soft dough was pressed and quickly shaped to form the required shape of mold. The mold hardened within 1−1.5 min. It was cured after 4 min at room temperature (25−26°C). Gloves were used to prevent heat transfer from hands that would accelerate the curing process. The mold was used to cast the epoxy resins.

3.3.2 Samples Preparation for Mechanical Tests

B2 and C2 microcapsules of 1, 3 and 6 wt. % were mixed with 5.0 g epoxy resin, in small beakers. The mixtures were stirred for 5 min. Then, 2.9 g of amine hardener (58 parts resin per hundred resin (p.h.r) were added to each mixture and carefully stirred for 5 min. As the epoxy resin started to react with the hardener, the mixtures gradually thickened. They were transferred to rectangular silicone rubber molds with a dimension of 25 mm × 2 mm × 2 mm to produce five samples for a three-point-bend test. Another set of 2 samples with the specified amount of microcapsules, were prepared with dimension of 2 mm diameter and 8 mm height according to modified ASTM E 384:1990 for micro-indentation hardness (Vickers) test. The excess mixture was removed using spatula. The samples were cured for 24 h at ambient temperature followed by 100°C for 2 h to complete the curing process. The same procedure was employed to make neat epoxy samples as controls for each respective tests.

3.3.3 Morphology and Dispersion of Microcapsules in Epoxy Matrix

To ensure good distribution of microcapsules in the epoxy matrix, all samples were visually inspected using digital microscope prior to testing (AnMo Electronics, Taiwan). For further observation using FESEM, after the thickened mix was transferred to the mold, it was cooled in liquid nitrogen for 2 min and quickly sliced using a razor blade. The sliced pieces were then cured at 100°C for 2 h, followed by examination using FESEM (Hitachi SU8220) at suitable voltage and magnifications.

3.3.4 Three-Point Bend Test

The samples prepared in Section 3.4.2 were subjected to a three-point-bend test. The test was carried out using a universal testing machine (AG-X Shimadzu, Shimadzu Corp., Kyoto, Japan). The setup consists of two rods of 2 mm in diameter, mounted parallel with 20 mm distance. Then, 5 kN load cell were applied at a crosshead speed of 1 mm min^{-1} until 5% strain. Each reported flexural strength was the average of four repeated samples.

3.3.5 Micro-Indentation Hardness (Vickers) Test

The Vickers test was performed on a microhardness measuring machine (HMV-2, Shimadzu Corp., Kyoto, Japan) with test force of 98.07 mN (HV 0.01). Each sample was subjected to three indentations at different spots for 5 s duration per indent and the three readings were averaged.

3.3.6 Preparation and Characterization of Epoxy/Alkyd (EA) Blends

To probe the viability of the healing reactions, small amounts of alkyd were blended with epoxy and hardener at different ratios. They were cured at room temperature for 24 h and at 100°C for 2 h. Each of the un-cured blend was dropped and sandwiched between two PET plastic and left to cure at room and elevated temperature (100°C). The cured

film were analyzed using ATR-FTIR (Perkin-Elmer Spectrum 400), with 4 cm^{-1} resolution from eight scans at 4000−450 cm^{-1} wavenumber.

3.4 Summary

Overall, an alkyd as the bio-based polymer, served as potential healing agent for epoxy matrix, was synthesized, followed by its encapsulation using amino resins. It was done using *in situ* polymerization of PUF and PMUF forming the shell around the droplets of the emulsified alkyd. The microcapsules were characterized and incorporated to the epoxy matrix. The effect of its inclusion on the mechanical properties were studied. Finally, the potential reaction of alkyd and epoxy was examined through blending experiment. The findings of this study will be presented in three parts according to the three main research objectives determined previously.

CHAPTER 4: ALKYD RESIN FROM PALM KERNEL OIL

4.1 Alkyd Synthesis

The alkyd was synthesized by alcoholysis and esterification processes. The acid number decreased with increasing reaction time as shown in **Fig.4.1**. The initial acid number of 305 mg KOH g^{-1} was reduced to 15 mg KOH g^{-1} in 450 min, indicating the reaction has achieved >95% completion.

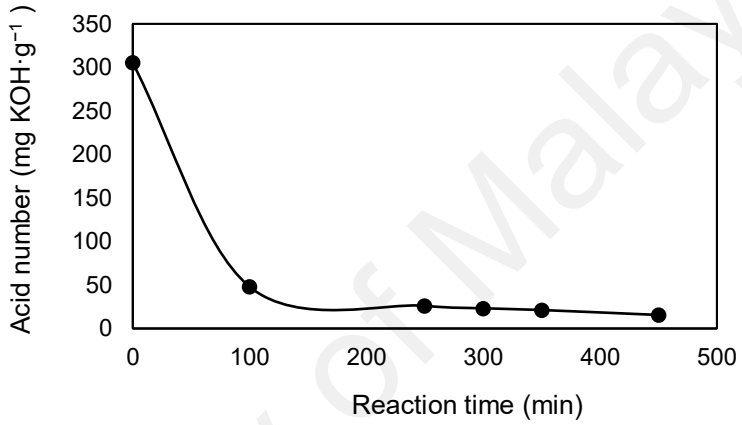

Fig. 4.1: Acid number change vs. esterification time

4.2 ^{1}H-NMR Spectroscopy

The proton-NMR (^{1}H-NMR) spectra of PKO and alkyd are shown in **Fig. 4.2** and the assignment of the peaks is given in **Table 4.1**. For PKO, peaks at 0.8 and 1.3 ppm represent the methyl and methylene protons from the hydrocarbon chain of fatty acids. The unsaturated fatty acids in PKO such as oleic and linoleic acid are reflected from the resonance of the allylic and vinylic protons at 2.0 and 5.3 ppm respectively. Other peaks observed at 1.6 ppm, 2.3 ppm and 4.1-4.3 ppm correspond to the methylene protons that directly attached to the carbon and oxygen atom of the ester unit.

AlkydPKO65 shows the similar spectrum as its starting materials. Peaks *a, b, c, d, e* and *g* represent the fatty acid chains contained in the PKO. Significant amount of ester

linkages present in the alkyd has resulted in broader peaks at 3.6 to 4.4 ppm (labelled as *f)*, compared to the peaks of PKO. Two peaks at 7.5 ppm and 7.6 ppm from the alkyd are attributed to the aromatic protons from PA (labelled as *h*). Based on this spectrum, a plausible structure of AlkydPKO65 was derived and is shown in **Fig. 4.3**, with the assignments of peaks from the selected fatty acids chain. It is useful to note that the structure proposed is one of the plausible structure. The two fatty acids shown are randomly chosen for proton-NMR peaks assignment and may not represent the dominant species.

Table 4.1: Peak assignments for ^{1}H-NMR spectrum of PKO and AlkydPKO65

Palm kernel oil (PKO)		AlkydPKO65	
Chemical shifts (ppm)	Proton assignment	Chemical shifts (ppm)	Proton assignment
0.8	-R-C***H***$_3$-	0.8	-R-C***H***$_3$-
1.3	-R-C***H***$_2$-R-	1.3	-R-C***H***$_2$-R-
1.6	-OOC-C***H***$_2$-C***H***$_2$-	1.6	-OOC-C***H***$_2$-C***H***$_2$-
2.0	-C=C-C***H***$_2$-	2.0	-C=C-C***H***$_2$-
2.3	-OOC-C***H***$_2$-	2.3	-OOC-C***H***$_2$-
4.1-4.3	-COO-C***H***$_2$-	3.6-4.4	-COO-C***H***$_2$-
5.3	-***HC***=C***H***-	5.3	-***HC***=C***H***-
		7.51, 7.69	aromatic –C***H***=C***H***-

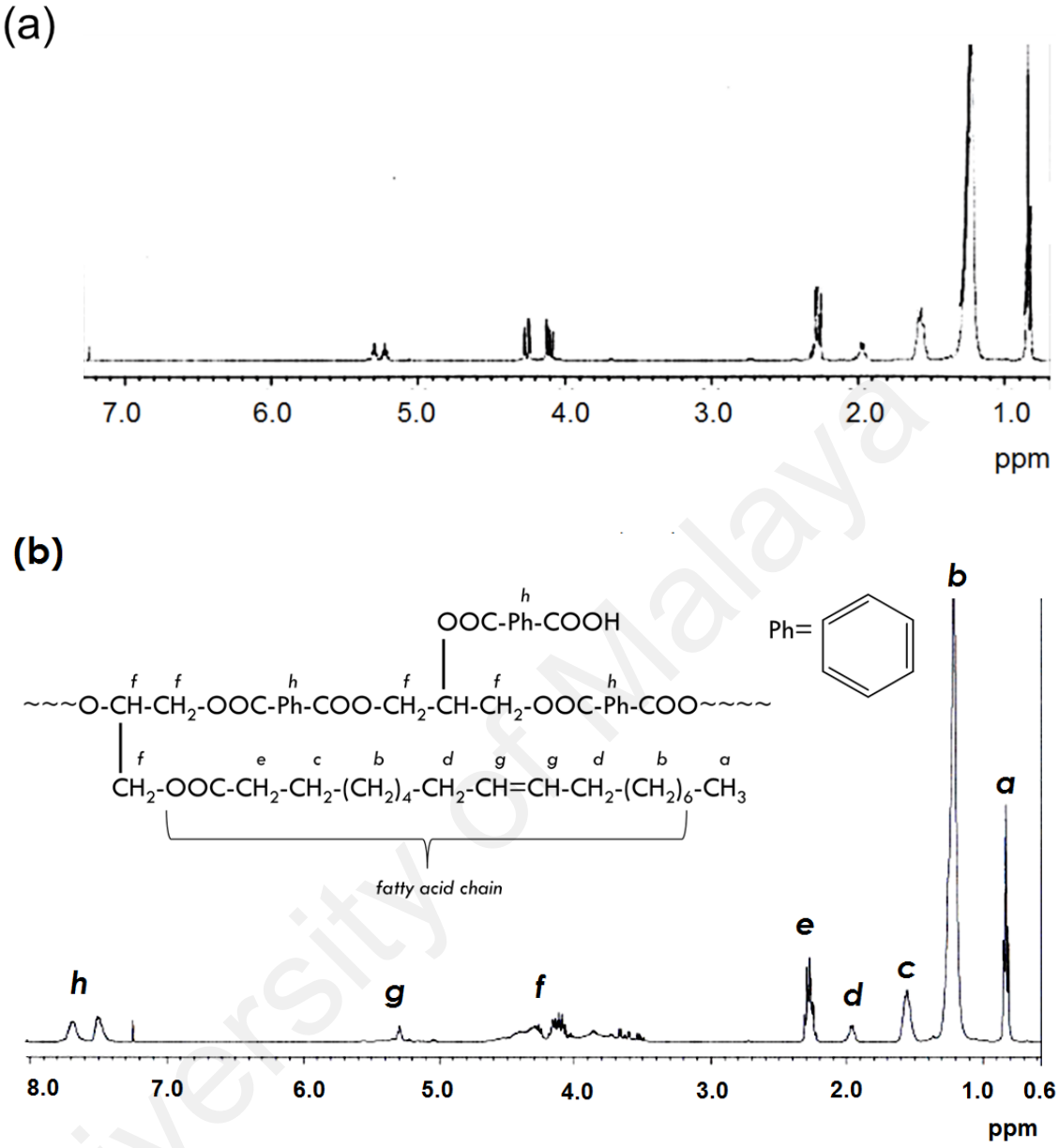

Fig. 4.2: ^{1}H-NMR spectra of (a) PKO (b) AlkydPKO65

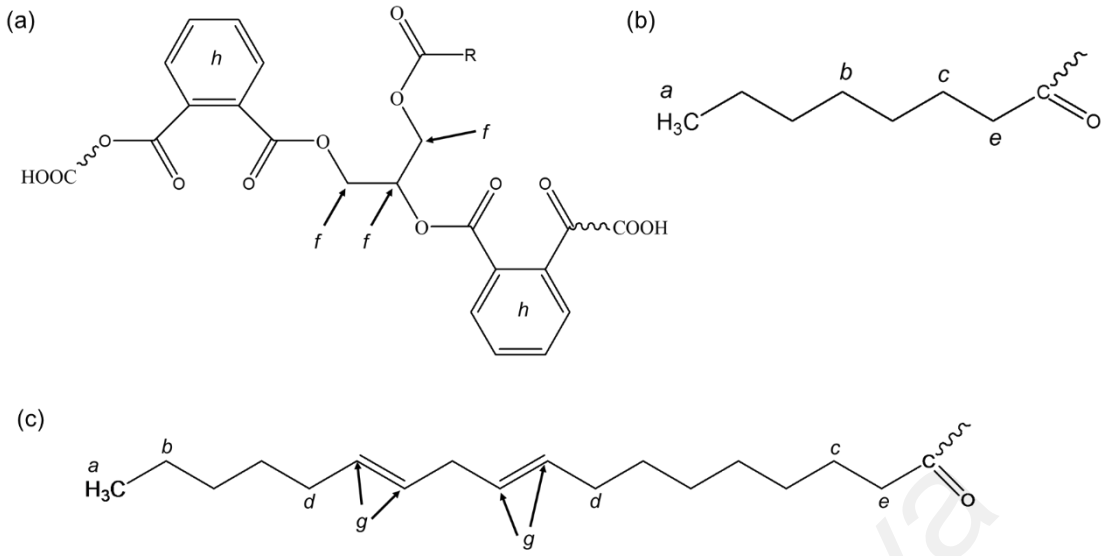

Fig. 4.3: (a) Plausible structure of AlkydPKO65 (b) saturated caprylic acid (c) unsaturated linoleic acid

4.3 ATR-FTIR Spectroscopy

Fig. 4.4 (a) shows the FTIR spectrum of PKO which is the characteristics of a triglyceride structure. The absorption bands of the hydrocarbon chains of fatty acids observed at 2924 cm^{-1} and 2854 cm^{-1} were attributed to C–H stretching of $–CH_3$ and $–CH_2$ groups, 1462 cm^{-1} was due to C–H bending of $–CH_2$ group, 1378 cm^{-1} was due to C–H bending of $–CH_3$ and 722 cm^{-1} was due to $–CH_2$ rocking. Ester linkages in PKO are represented by peaks at 1744 cm^{-1} which is due to C=O stretching of ester and peaks at 1156 cm^{-1} and 1111 cm^{-1} that are attributed to C–O stretching of ester.

The FTIR spectrum of AlkydPKO65 is shown in **Fig. 4.4 (b).** The characteristic peaks observed are as follows: broad band at 3449 cm^{-1} (O–H stretching), sharp peaks at 2923 and 2854 cm^{-1} (C–H stretching) and strong peak at 1727 cm^{-1} (C=O of carboxyl groups), small peaks at 1600 and 1581 cm^{-1} (aromatic ring) and 1459 and 1378 cm^{-1} (C–H and C–R bending modes). The small peaks at 1072, 1119 and 1268 cm^{-1} (C–O groups) and the weak peak at 743 cm^{-1} (aromatic =C–H bending).

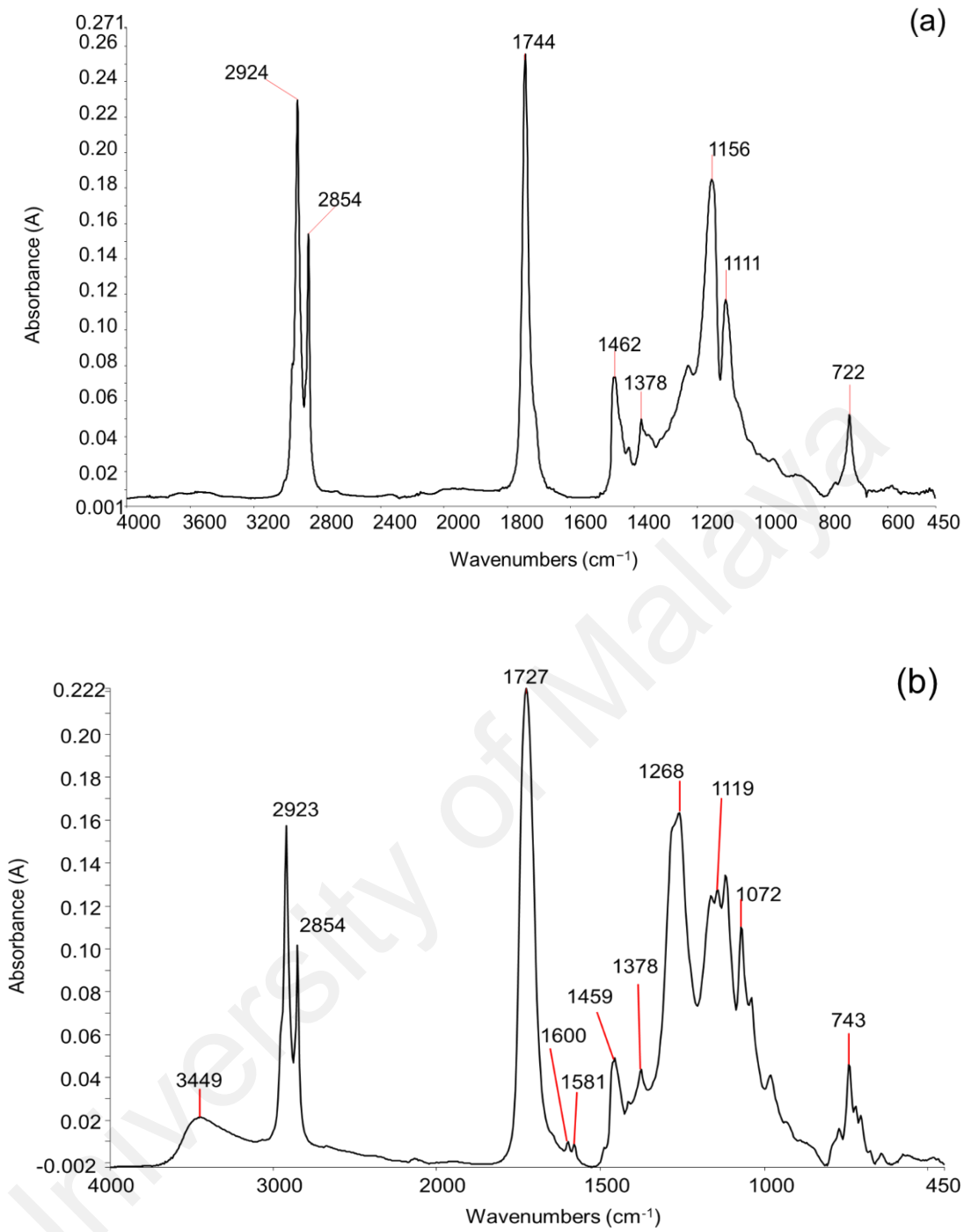

Fig. 4.4: FTIR spectra of (a) PKO (b) AlkydPKO65.

The alkyd shows additional peaks at 3449 cm^{-1} and 1268 cm^{-1} as exhibited in **Fig. 4.4 (b)**. During the alcoholysis process, triglycerides in PKO were converted to a predominant mixture of monoglycerides through reaction with glycerol. This reaction contributes to high amount of –OH groups in the system. Subsequently, the –OH groups were consumed in the esterification reaction with PA, therefore producing a significant

amount of ester linkages as shown by the strong –C−O stretching peak of the ester groups at 1268 cm^{-1}. Even with the consumption of –OH groups during esterification, the –OH stretching at 3483 cm^{-1} in the spectrum was relatively strong as AlkydPKO65 was formulated with 48 % excess of –OH groups. The additional small peaks at 1600 cm^{-1} and 1581 cm^{-1} were attributed to the aromatic rings from the incorporated PA. The strong, sharp –C=O peak of triglycerides ester has also shifted from 1744 to 1727 cm^{-1}. Finally, a plausible synthetic route of the alkyd is presented in **Fig. 4.5**.

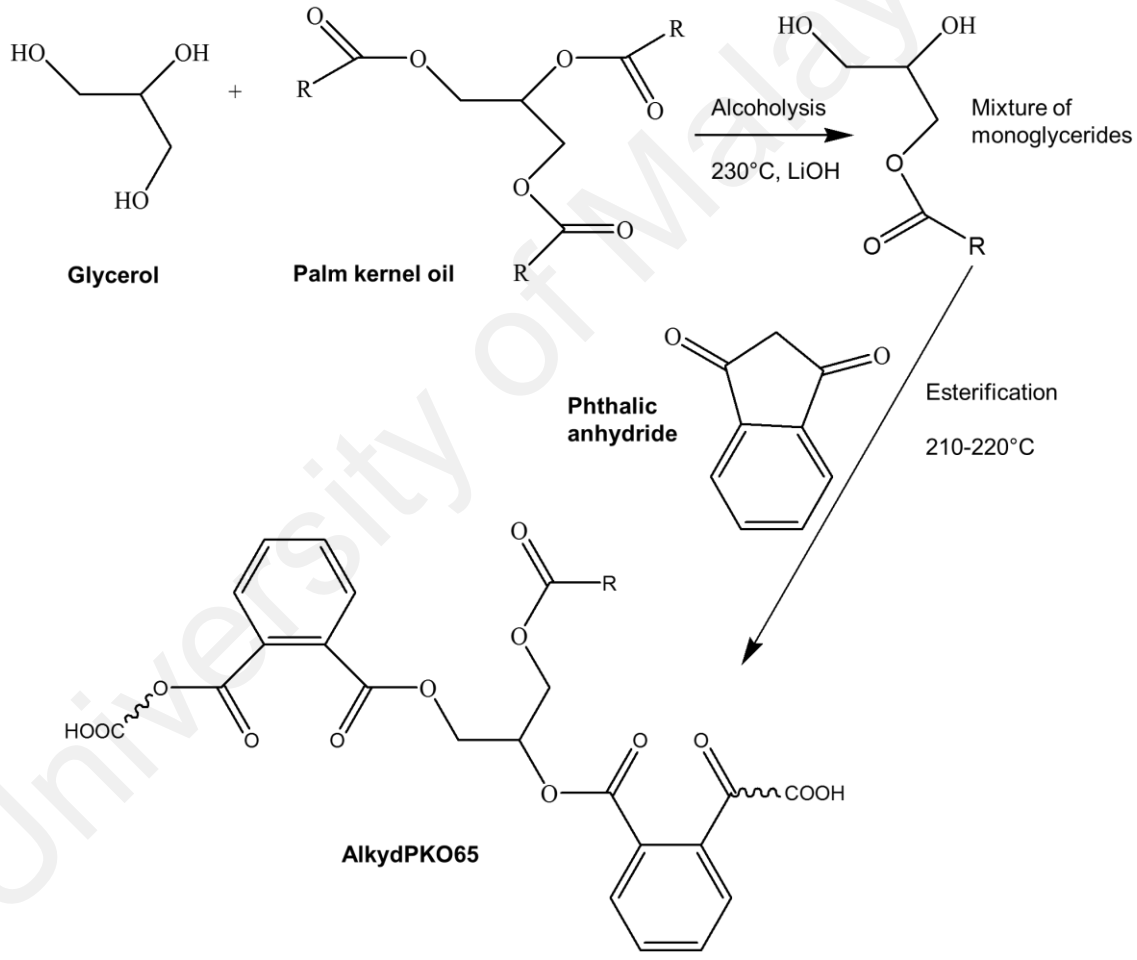

Fig. 4.5: Plausible synthesis route of AlkydPKO65; R= fatty acid chains from PKO

4.4 Viscosity of Alkyd

The correct rheological properties including the viscosity of alkyd resin are essential for their effective utilization across a variety of fields. These properties are mainly

influenced by the presence of the chain entanglement, coiling, different inter- and intramolecular attractive forces, cross-linking density, rigidity and by molecular weight distribution (Karak, 2012). In this work, the viscosity of alkyd was determined using a rheometer, with a rotating disc.

Typical microencapsulation process or *in situ* emulsion polymerization of the amino resins was performed at temperature of 55−70°C. The chosen temperature for microencapsulation in this work was 55°C. Therefore, the viscosity of the potential core content was tested at 55°C, at increasing shear rates (0 −100 s^{-1}). At elevated temperature, the viscosity of AlkydPKO65 decreases by 84% to 0.33 ± 0.04 Pa·s, as shown in **Table 4.2**.

Table 4.2: Viscosity of AlkydPKO65

Sample	Temperature (°C)	Viscosity (η, Pa·s)	
		At 100 s^{-1}	At 0−100 s^{-1}
AlkydPKO65	25	2.14 (0.01)	2.07 (0.01)
	55	−	0.33 (0.04)

4.5 Molecular Weight Determination

The gel permeation or size exclusion chromatograms of AlkydPKO and epoxy resin used as matrix host for microcapsules are presented in **Fig. 4.6**. The chromatogram of alkyd shows a peak at a slightly lower elution volume, at 32.4 mL, indicating a slightly higher molecular weight compared to the epoxy resin (elution volume of 33.3 mL). The number average molecular weight (M_n), weight average molecular weight (M_w) and polydispersity for the resins are listed in **Table 4.3**.

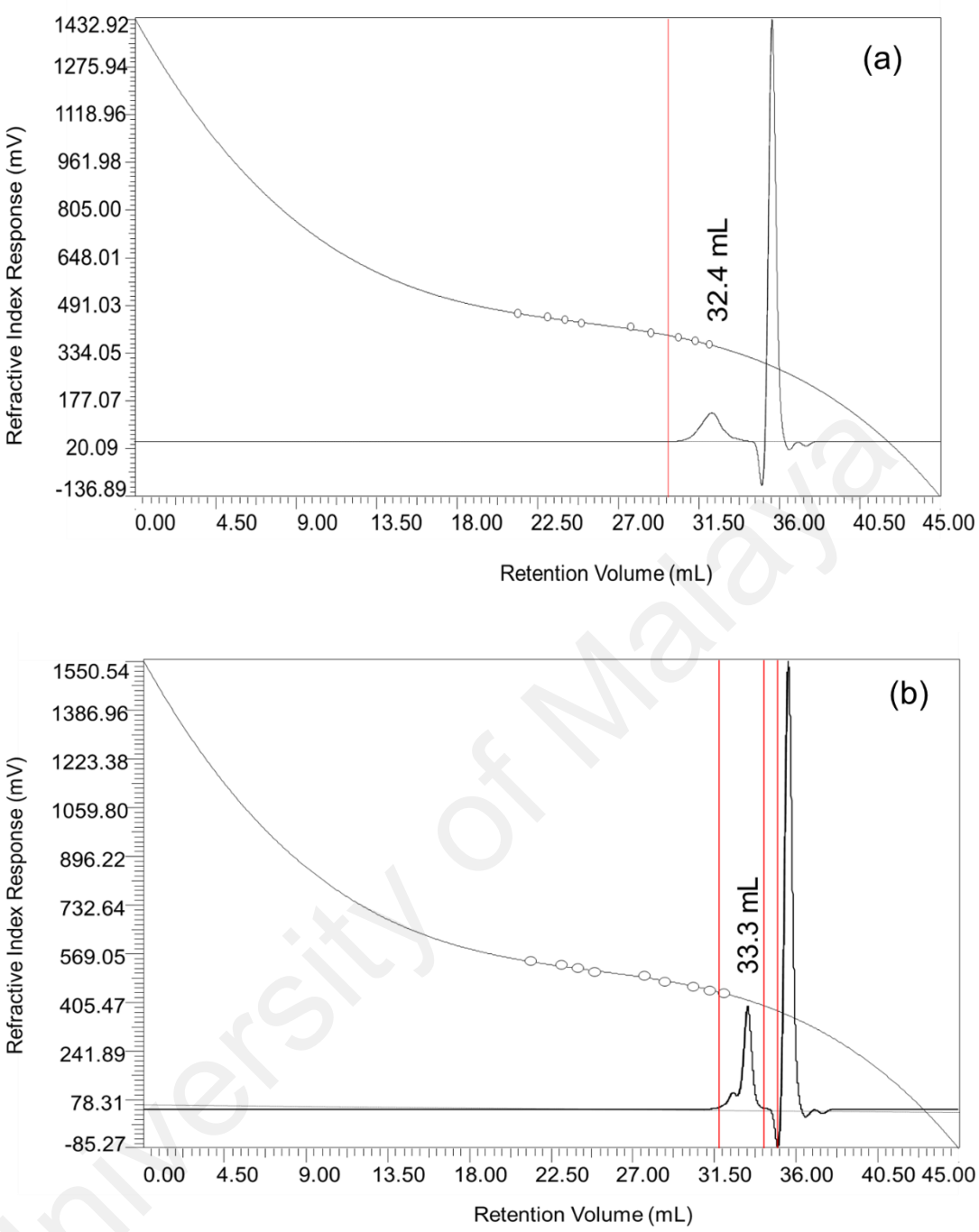

Fig. 4.6: GPC curves of (a) AlkydPKO65 (b) Epikote™ 240

Table 4.3: M_n, M_w and polydispersity index (PDI) of alkyd and epoxy resins

Sample code	Concentration (% w/v)	M_n	M_w	PDI= M_w/ M_n
AlkydPKO65	0.2	642	1042	1.63
Epikote™ 240	0.2	248	321	1.29

4.6 Thermal Analysis

AlkydPKO65 showed high thermal stability with a single step degradation profile, as exhibited by the TG profile in **Fig. 4.7**. The onset degradation temperature of alkyd was around 252°C. At 342°C, the alkyd has already 50% degraded and it decomposed completely at 550−600°C.

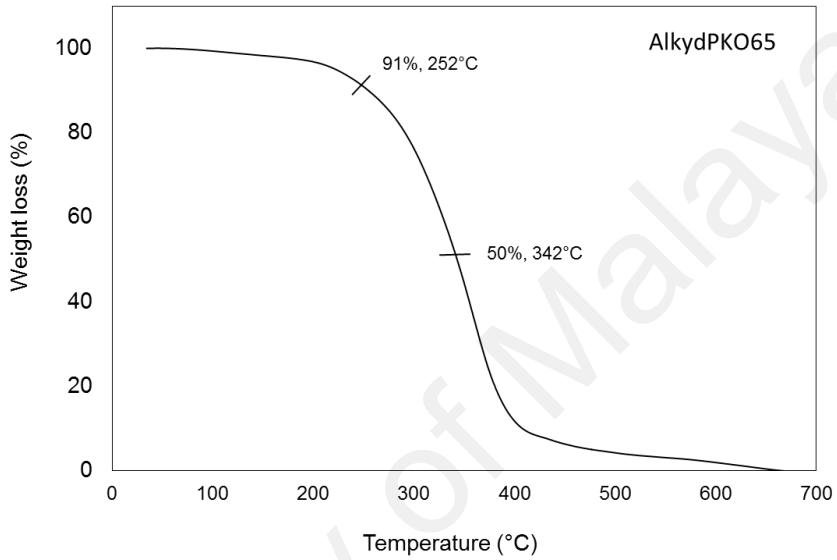

Fig. 4.7: TGA thermogram of AlkydPKO65

Fig. 4.8 shows the DSC thermogram of AlkydPKO65, which displays a glass transition temperature (T_g) at around -13°C (midpoint). The T_g indicates the transformation of the alkyd from a glassy to a rubbery state and it can be a useful identification characteristic in microencapsulation work. The sub-ambient T_g is expected as alkyd is a liquid at room temperature and it was on the shoulder of a broad endothermic peak. This endothermic peak at −15°C to 15°C was attributed to the melting (T_m) of alkyd, which indicates phase transition from solid (alkyd crystallized after cooling) to liquid.

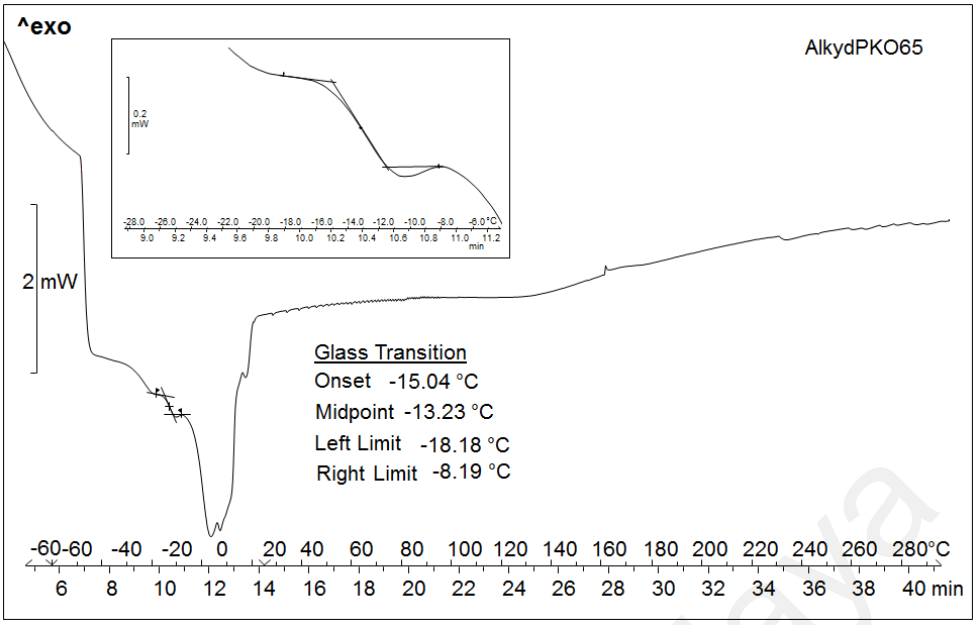

Fig. 4.8: DSC thermogram of AlkydPKO65; inset: enlarged T_g area

4.7 Summary

In this chapter, a selected long oil length alkyd has been synthesized. The plausible chemical structure and the synthesis scheme were determined, as well as several of its physical properties. Its thermal properties were also examined and the characterization data is summarized in **Table 4.4**. The alkyd is ready for encapsulation as will be discussed in the next chapter.

Table 4.4: Characterization data of AlkydPKO65

Characteristic	Value
Oil length (%)	65
Acid value (mg KOH g^{-1} alkyd)	15
Hydroxyl value* (mg KOH g^{-1} alkyd)	151
Viscosity (Pa·s)	2.14 (At 25°C); 0.33 (At 55°C)
Molecular weight (M_n, M_w)	642, 1042
Thermal properties (°C)	
• T_d onset	252
• $T_{d\ 50\%}$	342
• T_g midpoint	−13
• T_m	−15−15

* Calculated

CHAPTER 5: MICROENCAPSULATION OF ALKYD BY AMINO RESINS

5.1 Synthesis of Microcapsules

The general process described in Section 3.3.2 produced poly(urea-formaldehyde) (PUF) and poly(melamine-urea-formaldehyde) (PMUF) microcapsules with alkyd core over a size range of 50-500 microns. Yield of the preparation, as defined by the ratio of the mass of recovered microcapsules to the total mass of alkyd and shell constituents are in the range of 15−65 %. The microcapsules were spherical and free flowing after drying. Under high shear condition, microcapsules could fractured resulting in lower yields as agitation increases. Similar observation has been reported in Brown et al. (2003).

In this work, the *in situ* polymerization of amino resins to encapsulate the alkyd could be described in three phases. During phase 1, after about 60 min of reaction, alkyd droplets separate from aqueous medium when agitation stops, as shown in **Fig. 5.1 (a)**. Urea (U) and formaldehyde (F) or melamine (M)-urea and formaldehyde react and form methylol ureas, which further condenses under acidic condition to form the shell materials. The encapsulation of alkyd takes place simultaneously during the formation of crosslinked UF/ MUF polymer. At this point, melamine, urea and formaldehyde are soluble in water. When the pH is changed to acidic and heated to 55°C, the oligomers react to form poly(UF) or poly(MUF).

In the second phase, which was after 120 min of reaction, microcapsules have already formed, with a density lower than the medium. Clumping will occur if the agitation stops. As shown in **Fig. 5.1 (b)**, the reaction solution turns milky due to the formation of emulsion. The number of polar groups will gradually reduce as the molecular weight of polymer increases. After attaining a certain molecular weight, hydrophilicity of UF/ MUF polymer will reduce. This will separate the polymers from the aqueous phase and they

will get deposited on the suspended or emulsified alkyd droplets. Similar observations were observed and explained in literatures (Brown et al., 2003; Kouhi et al., 2013).

In the final phase (**Fig. 5.1 (c)**), which was after 180−240 min, the reaction mixture started to turn clear as the UF/ MUF nanoparticles were attached to the microparticles of the alkyd. This process continues and a thin shell is formed over the alkyd's droplet. The density of the particles now are higher than that of the medium and they will form a white slurry and settle at the bottom of the beaker when the agitation stops. **Fig. 5.1 (d)** shows the final product of microcapsules after washing and filtration processes. The process of UF/MUF condensation to form the shell of microcapsules can be illustrated as in **Fig. 5.2**.

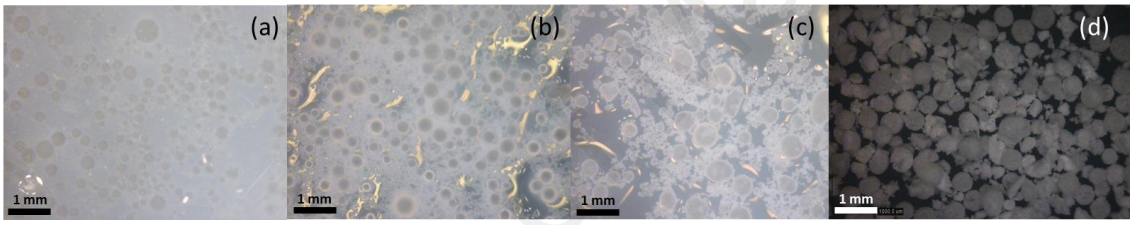

Fig. 5.1: Digital microscope images of reaction medium after (a) 60 min (b) 120 min (c) 180−240 min; (d) microcapsules after washed and filtered

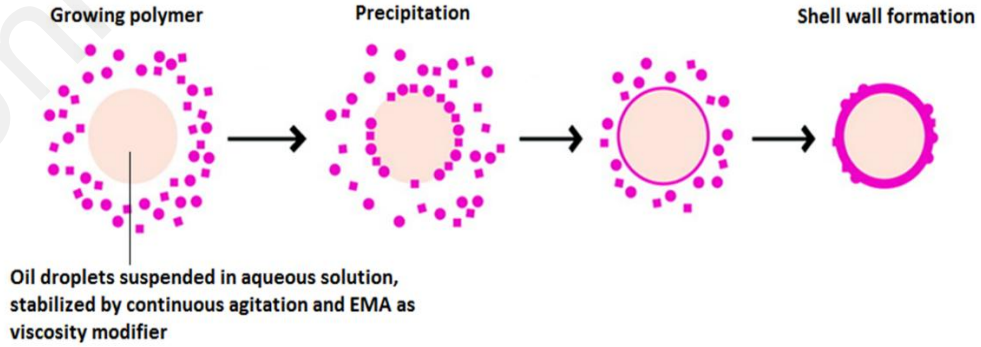

Fig. 5.2: A suspension or emulsion polymerization where polymer is deposited at an aqueous/organic interface, yielding a polymer shell wall around a stabilized droplet that becomes the core solution. From Esser-Kahn et al. © 2011 ACS

Fig. 5.3 (a) shows the reactions of urea with formaldehyde to form mono- and di-methylol urea. The methylol group could react with amino group to form methylene linkage and with other methylol group to form ether linkage **Fig. 5.3 (b)**. In addition, it could also react with –OH groups of resorcinol as in **Fig. 5.3 (c)**.

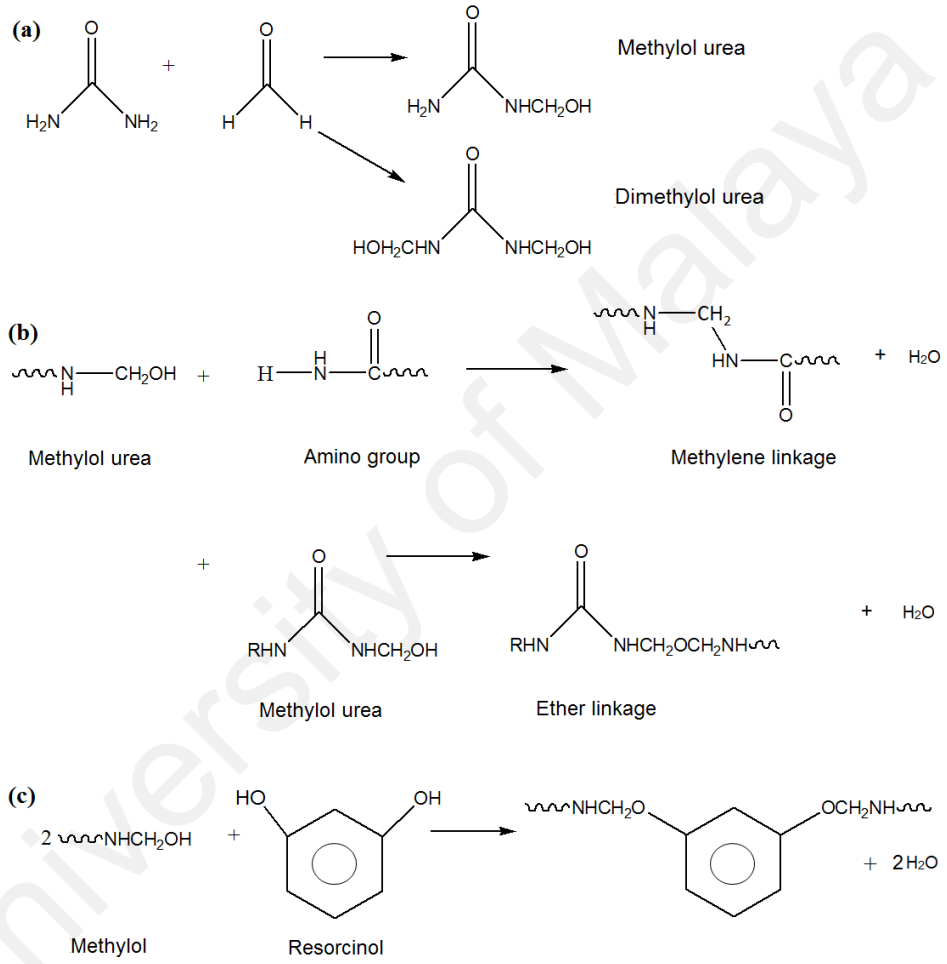

Fig. 5.3: (a) Reactions of urea and formaldehyde to form mono- and di-methylol urea (b) reactions between methylol urea to form linkages (c) reaction between methylol and resorcinol (as crosslinking agent)

Fig. 5.4 (a) shows the melamine resin, Cymel 303®, which has up to six methylated groups and can react with both methylol and hydroxyl groups. The methylated melamine could also react with the hydroxyl group on the surface of alkyd droplets.

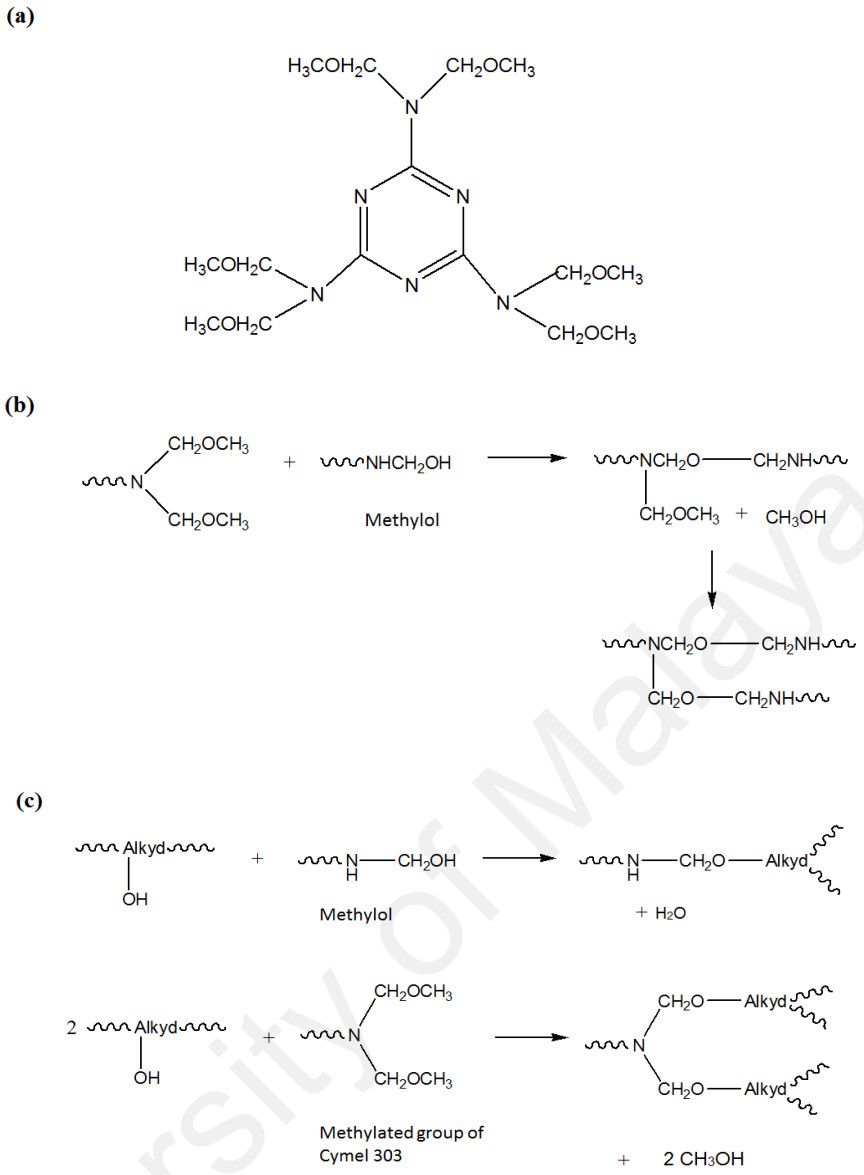

Fig. 5.4: (a) Chemical structure of melamine resin (Cymel 303®); (b) plausible crosslinking reaction of melamine resin; (c) plausible crosslinking reaction of alkyd with methylol urea and –N-CH_2-O-CH_3 of melamine resin

5.2 Influence of Reaction Parameters on the Microencapsulation

To obtain a good yield of alkyd microcapsules, several important parameters of encapsulation were investigated and elaborated in the following sections. Two methods, namely Method 1 and Method 2 were adopted. **Fig. 5.5** summarizes the encapsulation steps and highlights the differences between the two. Method 1 was based on reference (Brown et al., 2003).

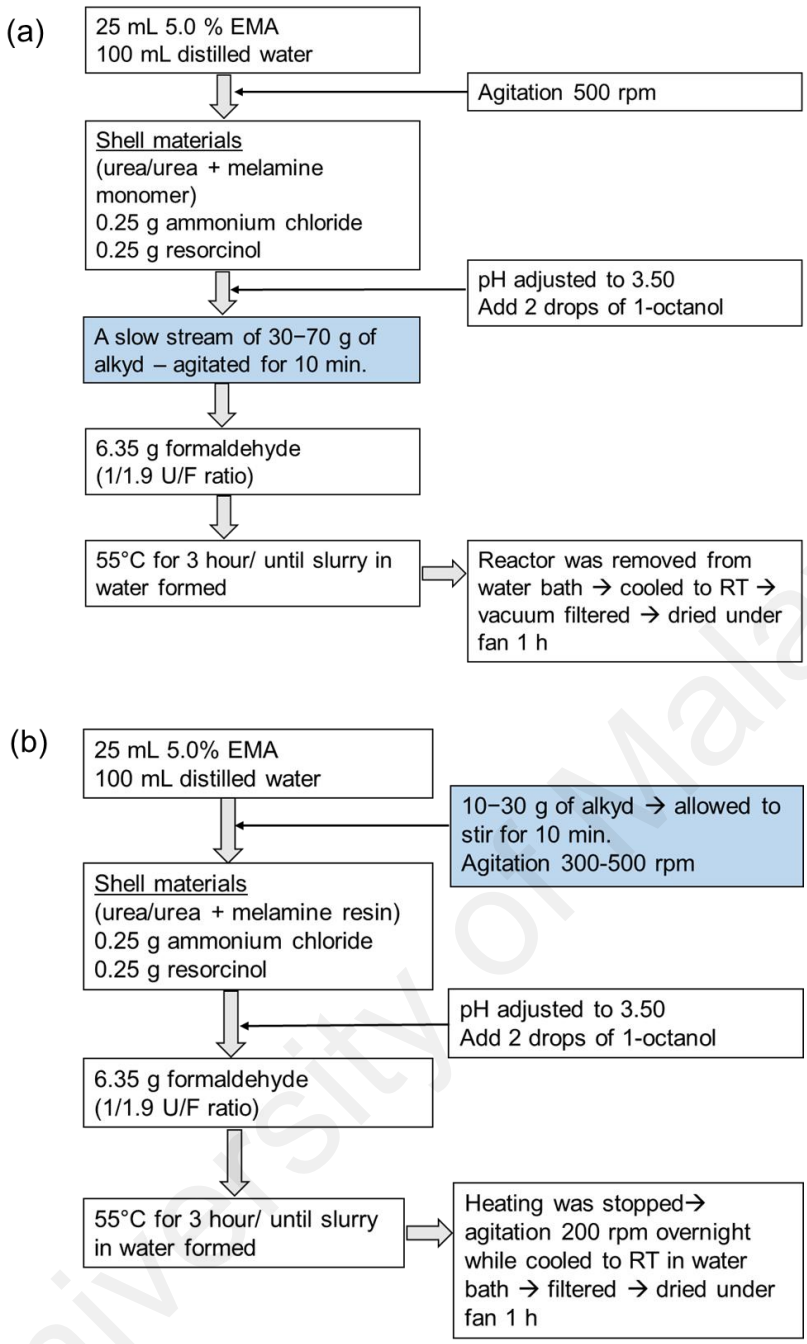

Fig. 5.5: Microencapsulation procedures of alkyd (a) Method 1 (b) Method 2.

5.2.1 Core/Shell Weight Ratio Variation in Method 1

Brown and his colleague has used a 6.2: 1 core/shell weight ratio in the *in situ* polymerization of UF (Brown et al., 2003). This ratio has been adopted by a number of other researchers (Noh & Lee, 2013; Then et al., 2011a; Tong et al., 2010). The effect of different core/shell weight ratios (samples 1-A to 1-F) on the surface morphology of

microcapsules were investigated. The microcapsules were prepared using Method 1 and the ratio was varied from 6.0 to 13.9 as tabulated in **Table 5.1**.

Table 5.1: Formulation and characterization data of PMUF microcapsules, prepared using Method 1

Sample	Core/shell (wt. ratio)	Core (g)	Shell materials (g)			Yield (%)	MCs description
			U	F	M		
1-A	6.0	30	2.35	6.35	0.32	25	Fragile, not free flowing
1-B	8.0	40	2.35	6.35	0.32	34	Fragile, not free flowing
1-C	9.0	45	2.35	6.35	0.32	42	Fragile, not free flowing
1-D	10.0	50	2.35	6.35	0.32	32	Fragile, not free flowing
1-E	12.0	60	2.35	6.35	0.32	52	Fragile, not free flowing
1-F	13.9	70	2.35	6.35	0.32	40	Fragile, not free flowing

U: urea; M: melamine (pure 99 %); F: formaldehyde of 37% aqueous; EMA: ethylene (maleic anhydride); 2.5 wt. % of EMA were used as emulsifier for this series.

Fig. 5.6 shows the digital microscope images of Series 1 microcapsules becoming smoother with the increase of core material. Increasing the core material could increase the number of droplets in the emulsion, while size of the droplets remains the same, since the stirring rate was kept constant at 500 rpm. When the number of droplets increases, the surface area increases and deposition of PMUF nanoparticles on the droplets surface becomes more even, thus the yield of capsules increases. Less agglomerated PMUF was also being observed when core content was increased. However, if the core was in excess, (as in 1-F where amount of shell material was relatively less) thinner wall of the encapsulated particles were obtained. This explains why 1-F microcapsules were easily ruptured and the yield decreased. At room temperature, they ruptured in 1 day. Alkyd core diffused out, causing the capsules to stick to each other and appeared yellowish, which was the color of the alkyd. **Fig. 5.7 (a)** shows the 1-E microcapsules as round-spherical in shape with smooth surface. Blown up micrograph (**Fig. 5.7 (b)**) shows thin

deposition of PMUF nanoparticles on the microcapsules surface. Generally, the microcapsules produced a typical UF rough outer surface but differs upon core loading content. In this series although in the beginning, there were microcapsules produced, all of them tend to be fragile after 1-2 days and were no longer free flowing.

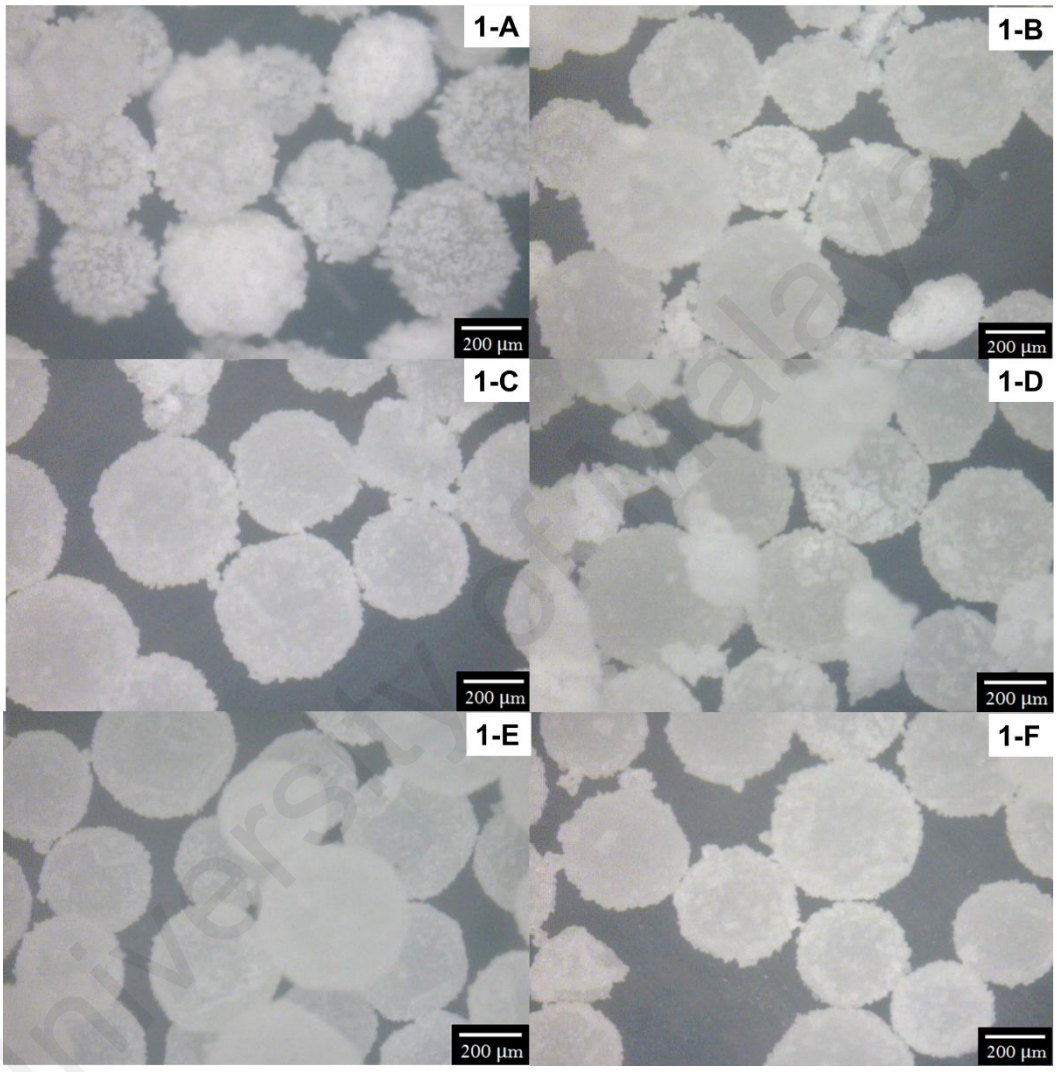

Fig. 5.6: Digital microscope images of PMUF microcapsules (Series 1), prepared at different core/shell weight ratios

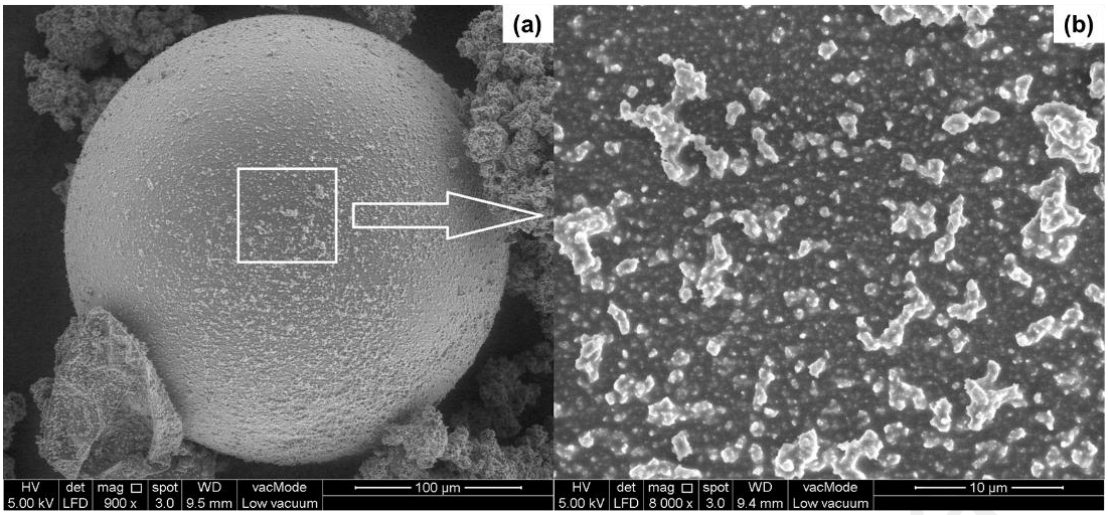

Fig. 5.7: (a) Smooth surface of 1-E microcapsule (b) magnified shell surface of PMUF microcapsule by Method 1

5.2.2 Core/Shell Weight Ratio Variation in Method 2

With reference to **Table 5.2**, samples 2-A to 2-C were synthesized using Method 2, where the alkyd was emulsified before addition of the urea and formaldehyde. Shell was formed through the polycondensation reaction of urea-formaldehyde. The core/shell weight ratios were varied from 6.2 to 2.1. Lower ratios were chosen in this series because at high amount of alkyd core, the microcapsules formed were too fragile and ruptured during processing and consequently very few microcapsules were stable enough for isolation. Referring to **Fig. 5.8**, some microcapsules that were successfully isolated can be seen in 2-B, but the sample was contaminated by some agglomerated UF particles. 2-C shows the microcapsules with minimum UF particles, whereas 2-A consisted of fragile microcapsules with lots of UF debris. Apparently the size of the microcapsules did not decrease with the decrease of core content and was still maintained in the range of 300 to 500 microns.

The microcapsules were further investigated with FESEM to check their surface morphology. They appeared round-spherical shape as shown in the micrograph (**Fig. 5.9 (a)**), having rough shell that consisted of the high molecular weight of PUF. The blown

up image (**Fig. 5.9 (b)**) shows that the PUF formed layers on top of each other from the polycondensation of urea and formaldehyde.

Table 5.2: Formulation and characterization data of PUF microcapsules, prepared using Method 2

Sample	Core/shell (wt. ratio)	Core (g)	Shell materials (g)		Yield (%)	MCs description
			Urea	Formaldehyde		
2-A	6.2	30	2.50	6.35	-	Fragile, not free flowing
2-B	2.7	15	2.50	6.35	9	Fragile, not free flowing
2-C	2.1	10	2.50	6.35	17	Adequately coated, free flowing

Formaldehyde: aqueous solution of 37 %; EMA: ethylene (maleic anhydride); EMA used was 2.5 % for all samples.

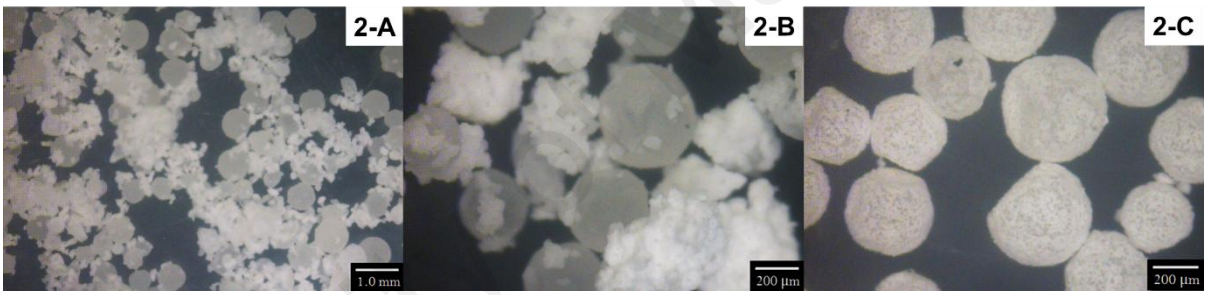

Fig. 5.8: Digital microscope images of PUF microcapsules (Series 2) prepared with Method 2

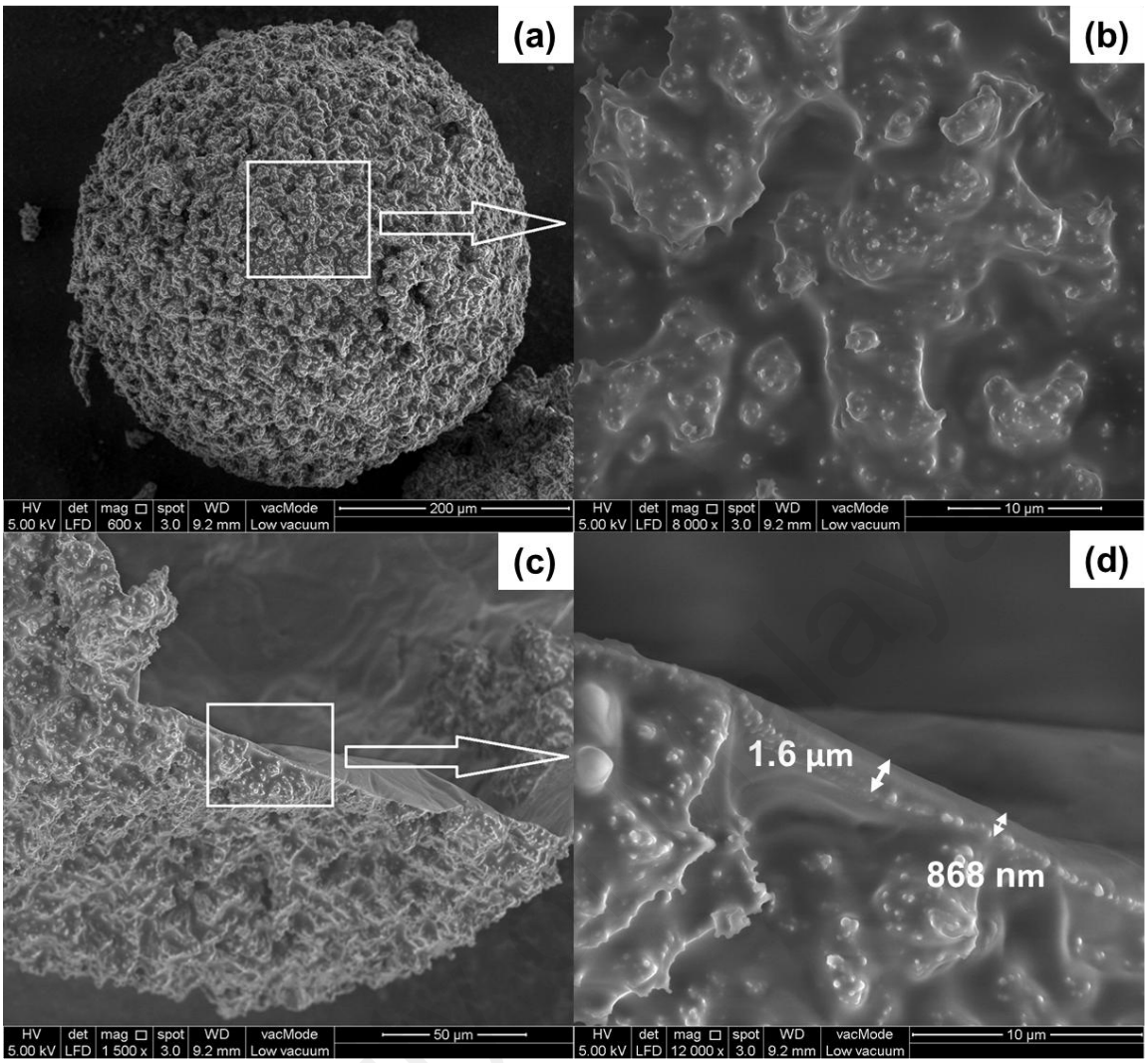

Fig. 5.9: FESEM micrographs of sample 2-C microcapsule and its shell surface morphology

Reduction of core material and difference in procedure could produce significant differences in the capsules. Sample 2-A was at nearly similar ratio of core to shell as 1-A, except no melamine was used. Sample 2-A has produced mainly the agglomerated UF resin particles. When the core content was reduced (sample 2-B), about 9% of microcapsules were formed. Further reduction of the core-shell ratio in sample 2-C has led to the formation of 17% of microcapsules. All the microcapsules have similar spherical shape with rough outer shell surface consisting of a layer of nanoparticles of amino resin. **Fig. 5.9 (c)** shows a ruptured microcapsule (sample 2-C) where the outer surface of the shell was rough. The inner shell had a thickness of 800 nm to 1.6 microns (**Fig. 5.9 (d)**).

5.2.3 Agitation Rate

Agitation rate has been shown to affect the size distribution of microcapsules with high agitation rate resulting in smaller core droplets (Blaiszik et al., 2009; Brown et al., 2003). However, very high agitation rate above 500 rpm would lead to frequent collisions causing deposition of the PUF and alkyd on the stirrer and reactor's wall, leading to poor yield. In this study, the agitation rate was maintained between 300 rpm to 500 rpm. As shown in **Table 5.3**, the mean diameter of the microcapsules changed from 412 μm to 360 μm as the agitation rate was increased from 300 to 500 rpm. **Fig. 5.10** shows the size distribution of microcapsules, which was from 300 microns to 600 microns. The microcapsules produced were poly-dispersed and sieved to separate the residue particles before being used in further processes.

Table 5.3: Characterization data of PUF microcapsules – Series A

Code	EMA (Wt. %)	Agitation rate (rpm)	Yield (%)	Core content (%)	Mean diameter (micron)	Descriptions of MCs
A1	2.5	500	17	93.9 (1.3)	360 (50)	Free flowing, thin shell.
A2	2.5	400	40	89.9 (0.5)	403 (56)	Free flowing.
A3	2.5	300	15	88.0 (0.0)	412 (66)	Free flowing with some agglomerated particles.
A4	1.0	400	0	-	-	No individual microcapsules. Big lumps of white particles.
A5	5.0	400	0	-	-	Fragile, thin wall, sticky and not free flowing.

Alkyd core used=10 g throughout the series; values in parentheses are standard deviation.

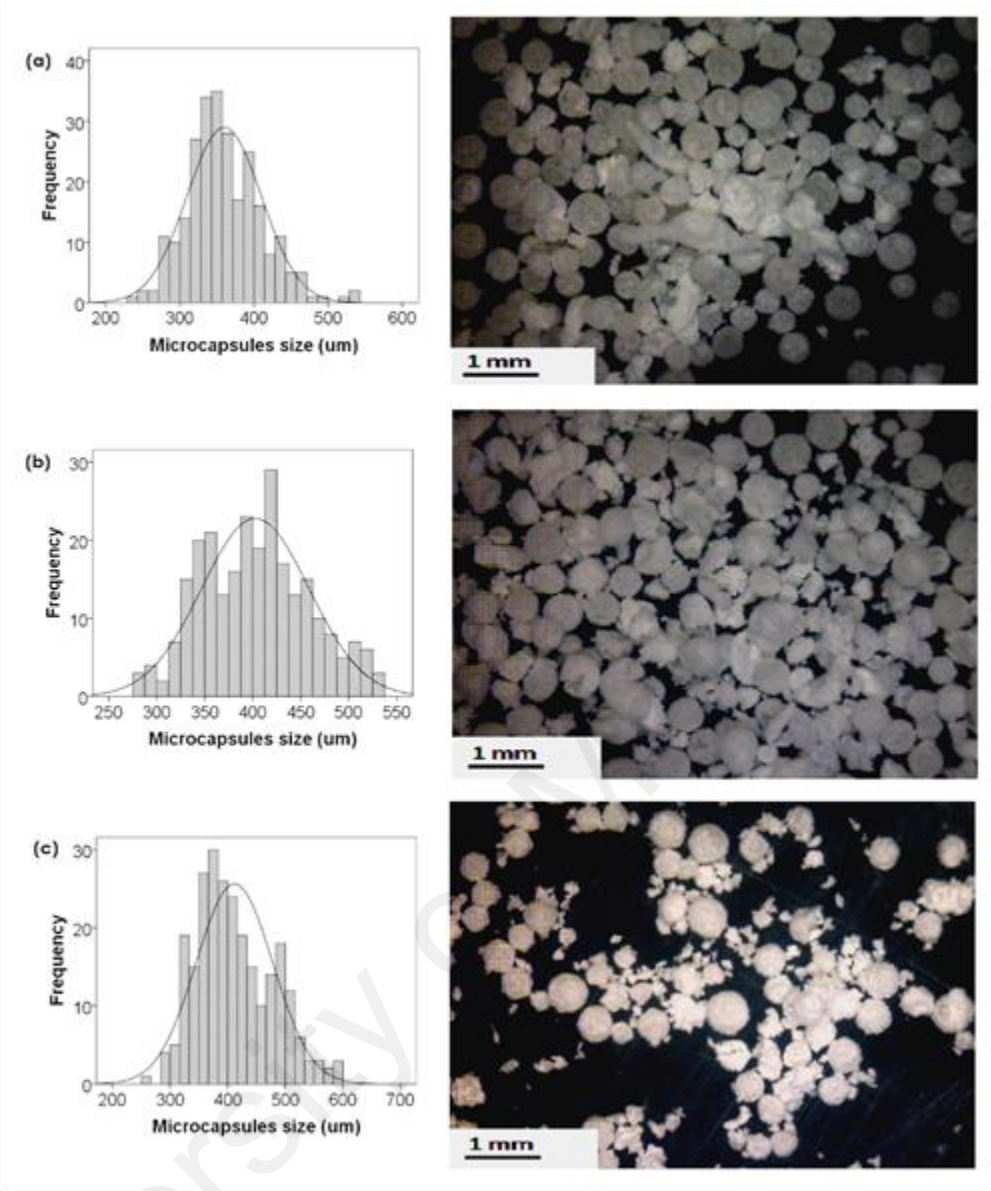

Fig. 5.10: Size distribution (left) and digital microscopic images of microcapsules (right, 50×), prepared at different agitation rates (rpm): (a) 500; (b) 400; (c) 300

Sample A1 prepared at agitation rate of 500 rpm has produced 17% yield of the microcapsules. As exhibited in **Fig. 5.11**, these microcapsules have relatively thin wall and contain up to 94 % core, whereas, sample A2, which was made with agitation rate of 400 rpm produced a higher yield (40 %) with more stable and more free flowing microcapsules. The faster stirring dispersed the alkyd into smaller droplets. However, extremely high stirring rate can lead to collisions between the droplets leading to agglomeration of the microcapsules, thus lowering the yield (Chen et al., 2015). On the other hand, sample A3 prepared with lower agitation rate (300 rpm) produced

microcapsules with a slightly thicker shell (core content was 88 %) and lower yield of 15 %. Lowering the agitation rate resulted in bigger alkyd droplets and the urea and formaldehyde would be in excess, which presumably had polymerized to form the agglomerated residues. **Fig. 5.12** shows that the size of microcapsules is inversely proportional with agitation rates. Several studies had described similar observation (Brown et al., 2003; Xiao et al., 2007; Yuan et al., 2006).

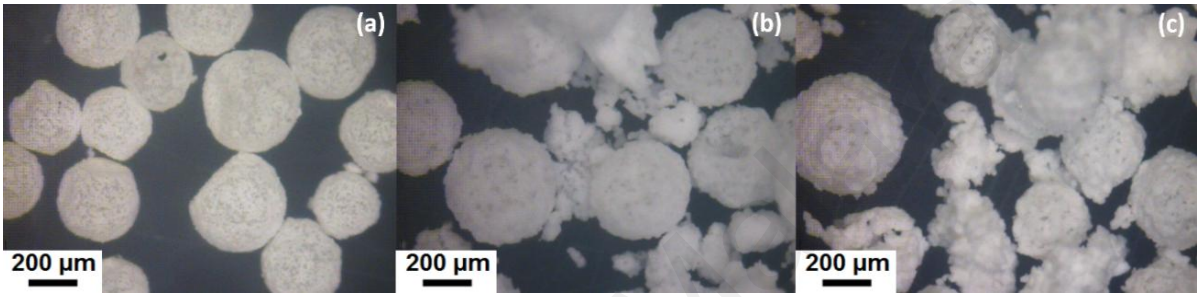

Fig. 5.11: Digital microscope images of PUF microcapsules (200×): (a) A1 (b) A2 (c) A3

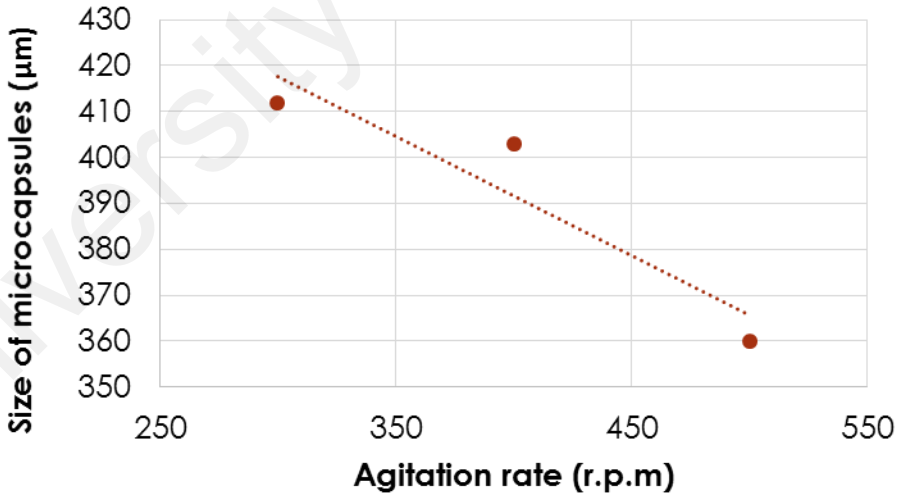

Fig. 5.12: Size of microcapsules with agitation rate

5.2.4 Concentration of Emulsifier and Viscosity of the Aqueous Phase

Fig. 5.13 shows the appearances of samples A4, A2 and A5 that were synthesized in 1.0, 2.5 and 5 % EMA respectively. Sample A4 has produced agglomerated mass with no distinctive microcapsule as seen in **Fig. 5.13 (a)**. Whereas, in **Fig. 5.13 (c)**, the microcapsules (A5) have thin shells with surfaces sticking to each other; they were fragile and could not be separated as free flowing microcapsules. Only sample A2 (**Fig 5.13 (b)**) synthesized in 2.5 % EMA could successfully be isolated as stable free flowing microcapsules. Presumably, the higher concentration of EMA leads to higher solution viscosity. Thus, insufficient PUF prepolymer was able to be deposited onto the alkyd droplet and consequently, thin shell was formed. **Fig. 5.14** shows the viscosities of EMA aqueous medium increased with the rise in the concentration of EMA, irrespective of temperatures. The concentration of EMA solutions at 55°C were 1.5 (±0.04), 2.1 (±0.07) and 5.0 (±0.15) mPa·s respectively. Therefore, it can be concluded that the concentration of emulsifier affects the viscosity of the aqueous phase (medium of encapsulation) and consequently the shell wall of microcapsules.

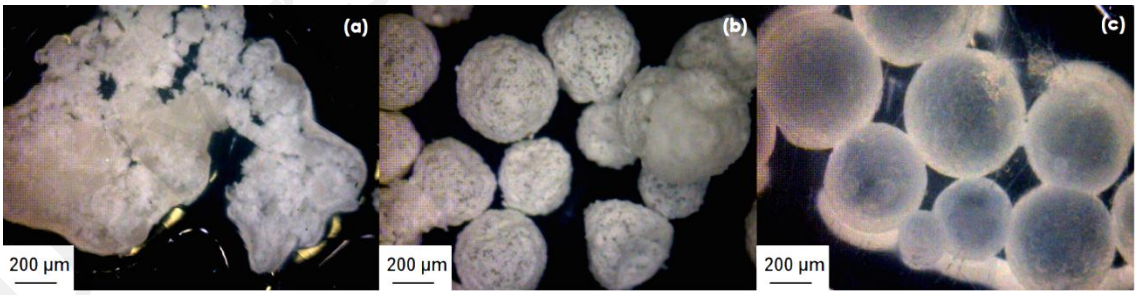

Fig. 5.13: Digital microscopic images of microcapsules (200×) synthesized at different EMA concentrations (wt. %): (a) 1.0; (b) 2.5; (c) 5.0

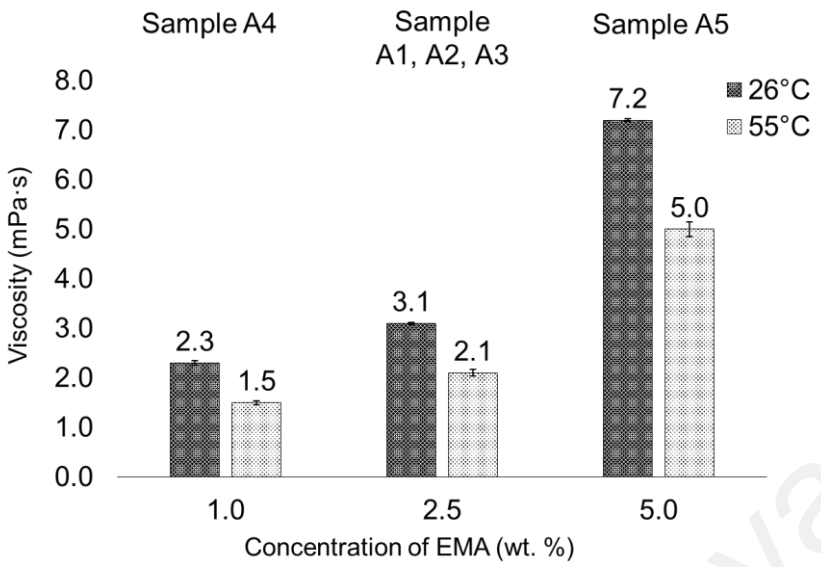

Fig. 5.14: Viscosity of the solution of EMA as the aqueous phase of the microencapsulation process, at 26°C and 55°C

5.2.5 Melamine/Urea Ratio

With reference to the results in **Table 5.4**, sample A2 that used urea and formaldehyde (without melamine resin) produced microcapsules that were low in yield (40%). With the addition of a small amount of melamine resin, at M/U ratio of 0.03, the yield of microcapsules has increased as in B1 to 65%. In addition, the microcapsules have become more robust. This could be explained by the crosslinking ability of the melamine resin that has up to six -N–CH_2OCH_3 groups per molecule. The plausible reactions of the melamine resin are previously shown in **Fig. 5.4 (b) and (c)**. Further increase in M/U ratio to 0.06 and 0.12 as in samples B2 and B3 saw a drop in the yield of microcapsules to 60 % and 49 % respectively. The larger amount of melamine resin has increased the crosslinking reactions with the urea-formaldehyde prepolymer in the aqueous medium, forming more agglomerated particles and consequently fewer microcapsules. As presented in **Fig. 5.15**, sample B4 at M/U ratio of 0.29, started to lose their spherical shape and formed mixtures of microcapsules and the irregular-shape agglomerated particles, which explains the drop in yield to 34 %. The melamine-modified PUF

microcapsules in the B series were poly-dispersed with a size range of 200-550 μm as shown in **Fig. 5.16**.

Table 5.4: Characterization data of PMUF microcapsules – Series B and D

Sample	M/U (wt. ratio)	M (g)	U (g)	Yield (%)	Core-content (wt. %)	Mean diameter (μm)	Description of MCs
Ref./A2	0	0	2.50	40	89.9 (0.5)	403 (56)	Spherical, free flowing
B1	0.03	0.08	2.49	65	94.8 (0.3)	383 (56)	Spherical, free flowing
B2	0.06	0.16	2.47	60	92.0 (1.3)	380 (60)	Spherical, free flowing
B3	0.12	0.30	2.45	49	91.9 (0.4)	384 (55)	Spherical, free flowing
B4	0.29	0.70	2.40	34	63.1 (0.4)	-	Less spherical, free flowing MCs with rougher outer surface
D1	0.03	0.08	2.49	46	91.6 (0.3)	396 (62)	Spherical, free flowing

M: melamine resin; U: urea. The same amount of formaldehyde was used in all cases. Values in parentheses are the standard deviation)

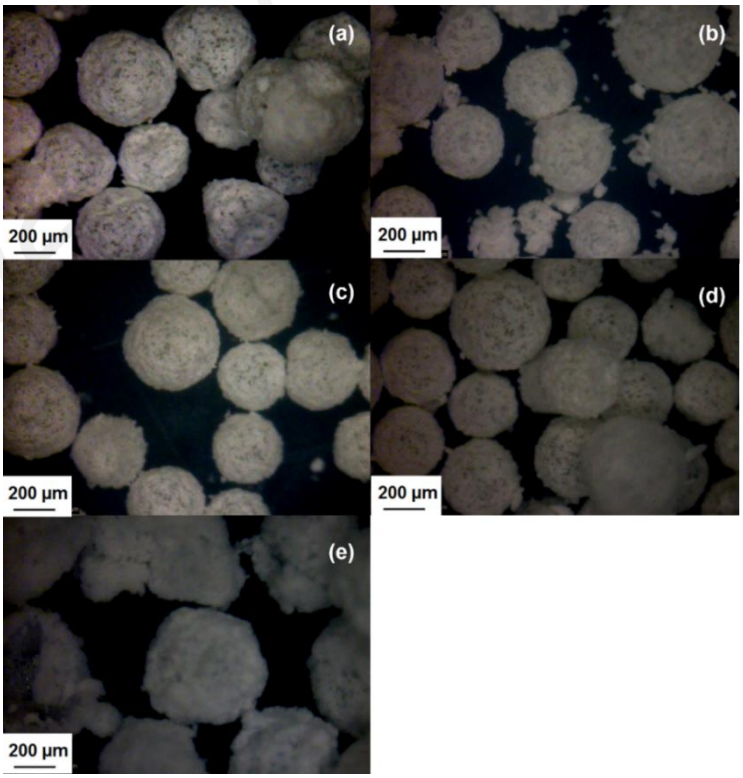

Fig. 5.15: Digital microscopic images of microcapsules with increasing M/U ratio: (a) 0; (b) 0.03; (c) 0.06; (d) 0.12; (e) 0.29

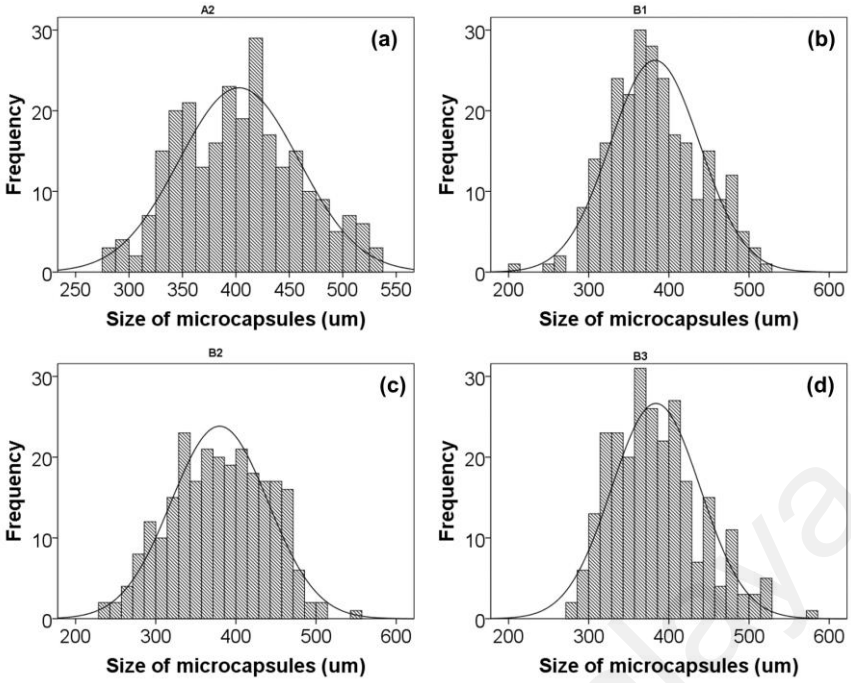

Fig. 5.16: Size distributions of microcapsules in B series compared to A2 microcapsules: (a) A2; (b) B1; (c) B2; (d) B3.

5.2.6 Different Alkyd as Core Content

In this work, another alkyd, AlkydFA35 with higher viscosity (14 Pa·s) and acid value than that of AlkydPKO65 (2 Pa·s) was encapsulated to produce D1 microcapsules. Comparing D1 and B2 microcapsules, both microcapsules were not significantly different in diameter size, considering the high standard deviation of each microcapsules series. D1 microcapsules have slightly bigger mean diameter (396 ± 62 μm) compared to B2 microcapsules (380 ± 60 μm), which contained AlkydPKO65 (refer **Table 5.4**). The size distributions of D1 ranging from 300 to 600 μm and they were also poly-dispersed as exhibited in **Fig. 5.17**. D1 formed the typical spherical and free flowing PMUF microcapsules (**Fig. 5.18**), with ~92% of alkyd loading and 46% yield. AlkydFA35 has much higher acid free carboxylic group (based on its acid number) and may promote higher crosslinking with residual epoxy in epoxy matrix, which would be useful for healing reaction. **Table 5.5** tabulates the viscosity values of alkyd and epoxy resins tested.

Table 5.5: Viscosity of core content and epoxy resins

Resin	Viscosity (Pa·s, 26°C)	Viscosity (Pa·s, 55°C)	Acid number (mg KOH/ g alkyd)
AlkydPKO65	2.14 ± 0.01	0.33 ± 0.04	15
AlkydFA35	13.95 ± 0.01	1.25 ± 0.05	55
Epikote 828	10.36 ± 0.01	0.38 ± 0.04	-
Epikote 240 (matrix host)	0.62 ± 0.01	0.10 ± 0.01	-

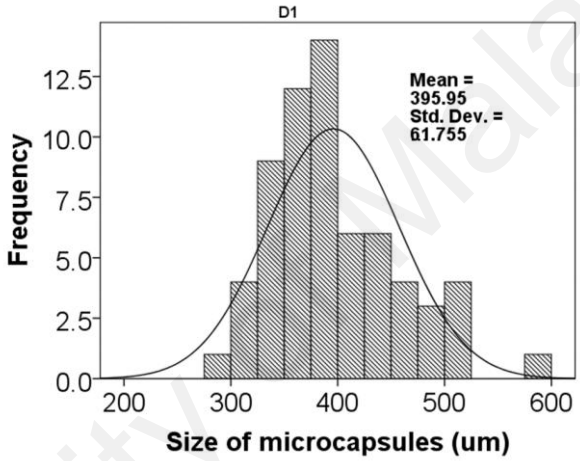

Fig. 5.17: Size distribution and mean diameter of D1 microcapsules

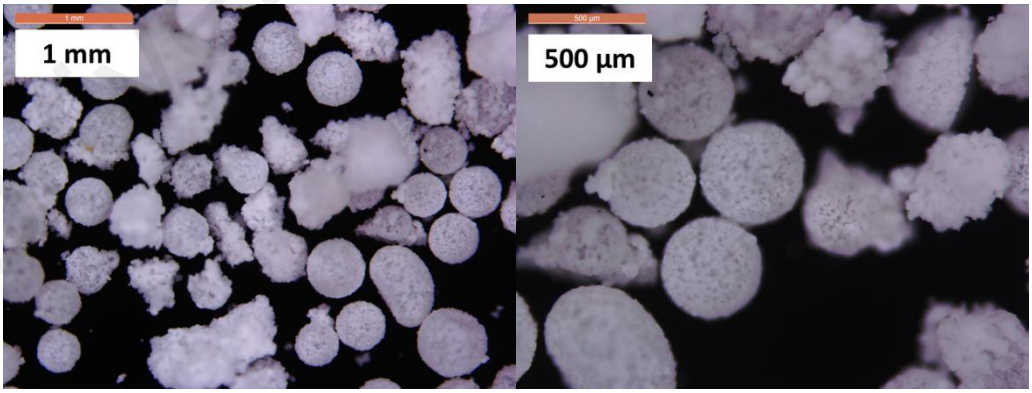

Fig. 5.18: Optical microscope images of D1 microcapsules at low and high magnifications

In addition, the viscosity of Epikote 828 is in agreement with the literature value (refer **Table 2.1**). It is one of the most common epoxy resin encapsulated for the development

of self-healing epoxy. AlkydPKO65 has far lower viscosity than Epikote 828 thus the use of diluent may not be necessary. Epikote 240 is a low viscosity epoxy resin, which has similar epoxy per weight equivalent as Epikote 828. Thus, it was chosen to be used as the matrix material in this study. Microcapsules were incorporated into this resin and it was cured with amine hardener. The low viscosity made the incorporation process easier and air entrapment was less or reduced.

5.2.7 Sonication

Sonication was introduced to further reduce the size of the dispersion of the oil phase, hence the size of the microcapsules. Method 3 was adopted with additional sonication at 15% intensity for 3 min (Appendix B), performed after 10 min alkyd was agitated. The microcapsules produced are coded as C1-C4 and the results are summarized in **Table 5.6**. Here, EMA concentration has to be optimized, other than the usage of the additional co-stabilizer (3% PVA). C1 microcapsules is a sonicated version of A2 and C2 is a sonicated version of B2, which both resulted white and free flowing powder. C1 produced smaller and clustered microcapsules compared to A2, as revealed by FESEM **Fig. 5.19 (a-b)**. The encapsulation was also verified with the occurrence of T_g of alkyd in the microcapsules when scanned with DSC (Appendix E).

Table 5.6: Characterization data of microcapsules prepared with sonication

Sample	M/U (Wt. ratio)	M (g)	U (g)	EMA (Wt. %)	Yield (%)	Core-content (wt. %)	Description of physical MCs	DSC analysis
C1	0	0	2.50	2.5	5	NA	White & free flowing powder	T_g of alkyd was observed.
C2	0.06	0.16	2.47	5.0	48	54 (3.1)	White & free flowing powder	T_g of alkyd was observed.
C3	0.06	0.16	2.47	3.5	NA	NA	A mixture of clumped and free flowing white powder	T_g of alkyd was observed (not clear).
C4	0.06	0.16	2.47	2.5	NA	NA	Clumped, white particles	T_g of alkyd was not observed.

M: melamine resin; U: urea; EMA: ethylene (maleic anhydride); the same amount of formaldehyde was used in all cases (6.35 g of 37 % formaldehyde solution); NA: not available; 10 mL of 3% poly(vinyl alcohol) (PVA) was used as co-stabilizer; value in parenthesis is standard deviation.

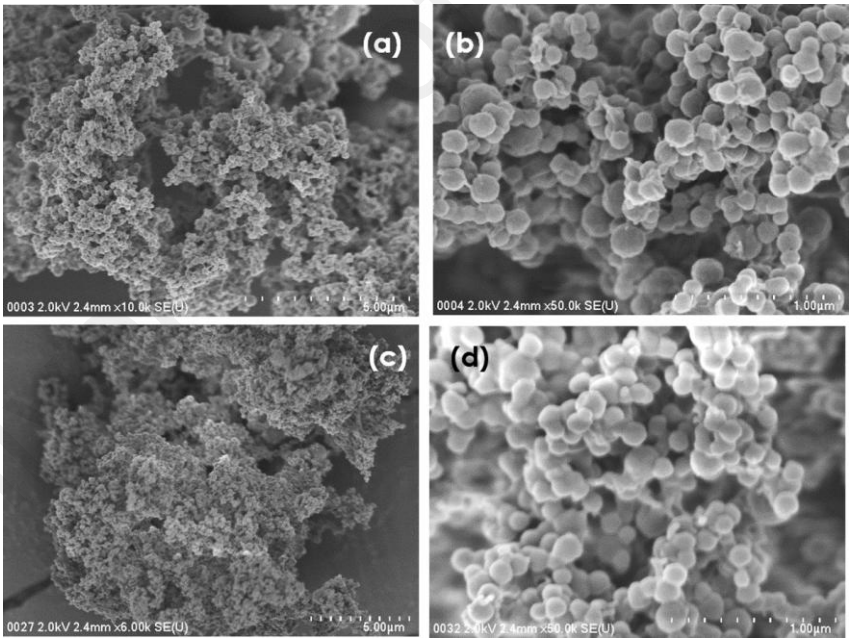

Fig. 5.19: FESEM micrographs of microcapsules prepared with sonication: (a-b) C1 (c-d) C2

At 2.5% EMA concentration, sample C4 yielded clumped white particles. Increase of EMA concentration to 3.5% in sample C3 yielded a mixture of clumped and free flowing powder. Further increase of EMA to 5.0% (sample C2) finally yielded free flowing microcapsules. DSC analysis confirmed the T_g of alkyd were also observed in samples

C2 and C3, proving the successful encapsulation. FESEM analysis of sample C2 revealed the formation of smaller and clustered microcapsules compared to B2, as shown in **Fig. 5.19 (c-d).**

5.3 Spectroscopic Characterizations of Alkyd and Microcapsules

In this section forward, only selected microcapsules from A, B, C and D series were used for further characterizations. Structural analysis of the extracted core content of A2, B2, C2 and D1 microcapsules were done using ATR-FTIR. Each of them showed a good match with the neat alkyd, confirming the successful encapsulation (refer **Fig. 5.20** and **Fig. 5.21**). The characteristic peaks of alkyd are observed; O−H broad peak at 3580 cm^{-1}, strong –C=O peak at 1730 cm^{-1} due to carboxyl group, small twin peaks at 1600 and 1500 cm^{-1} attributed to aromatic ring from PA that formed the alkyd and C−O of esters at 1270 cm^{-1}.

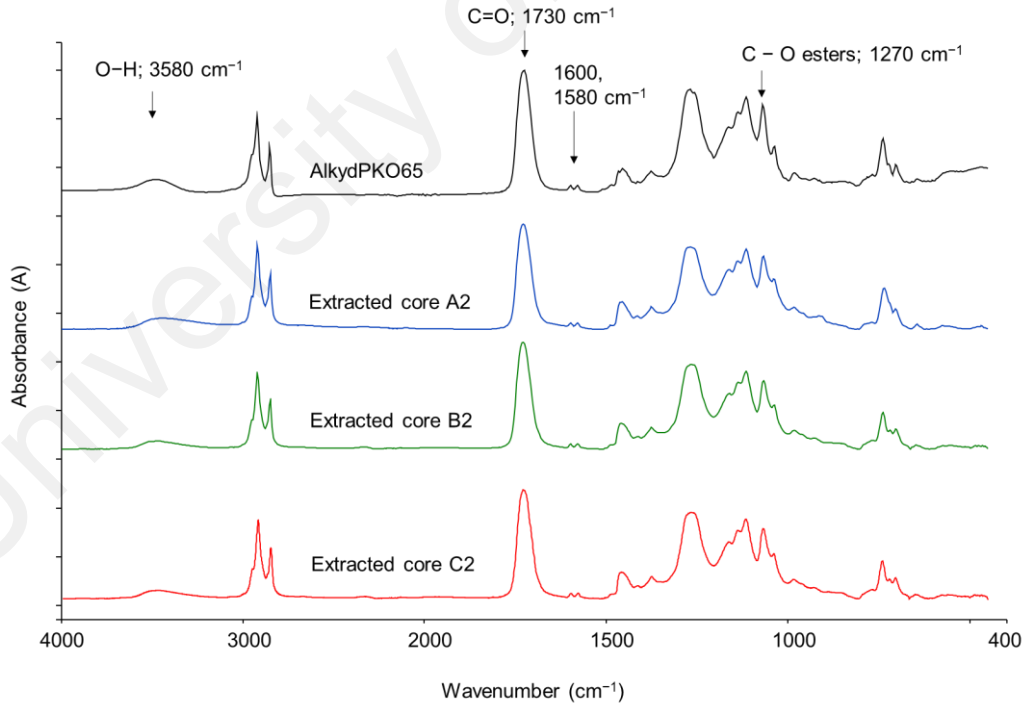

Fig. 5.20: ATR-FTIR spectra of AlkydPKO65 and the extracted core of A2, B2 and C2 microcapsules

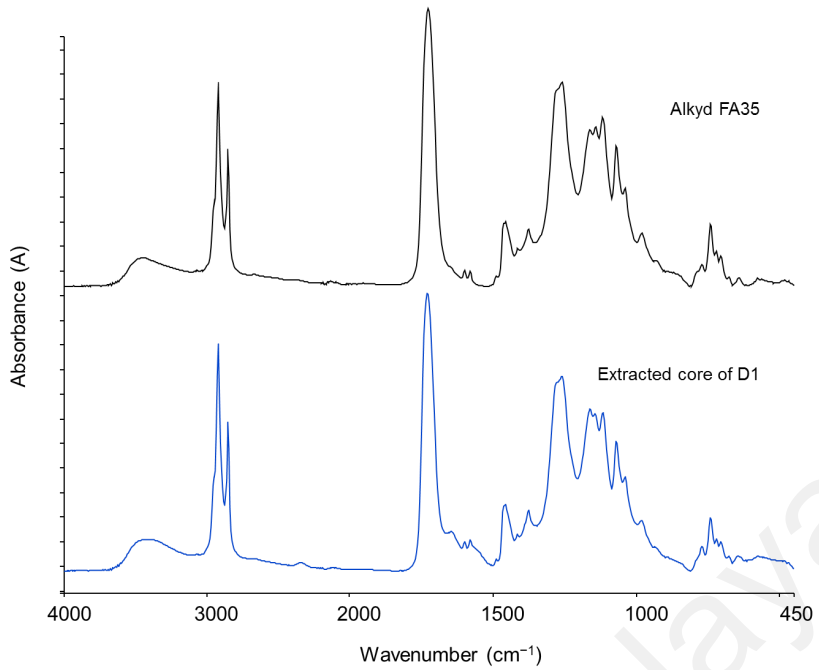

Fig. 5.21: ATR-FTIR spectra of AlkydFA35 and the extracted core of D1 microcapsules

In addition, the extracted shell materials of A2, B2 and C2 microcapsules also showed the characteristic peaks of PUF/PMUF. As shown in **Fig. 5.22**, peaks at 2900 & 2800 cm^{-1} attributed to CH and peaks at 1600 cm^{-1} and 1500 cm^{-1} due to NH and C−N respectively, are observed together with N−H of amine at 3300 cm^{-1}. The spectrum of extracted shell of C2 had an extra peak at 1730 cm^{-1} due alkyd residue from the extraction process. All polymerized shell materials showed no appearance of characteristic peak of melamine resin, at 814 cm^{-1} due to the triazine ring out-of-plane vibrations of 3 C−N. This suggests that all melamine resins had been utilized in the formation of the shells. The FTIR spectra for other microcapsules also showed similar characteristic peaks of alkyd and PUF as shown in Appendix C.

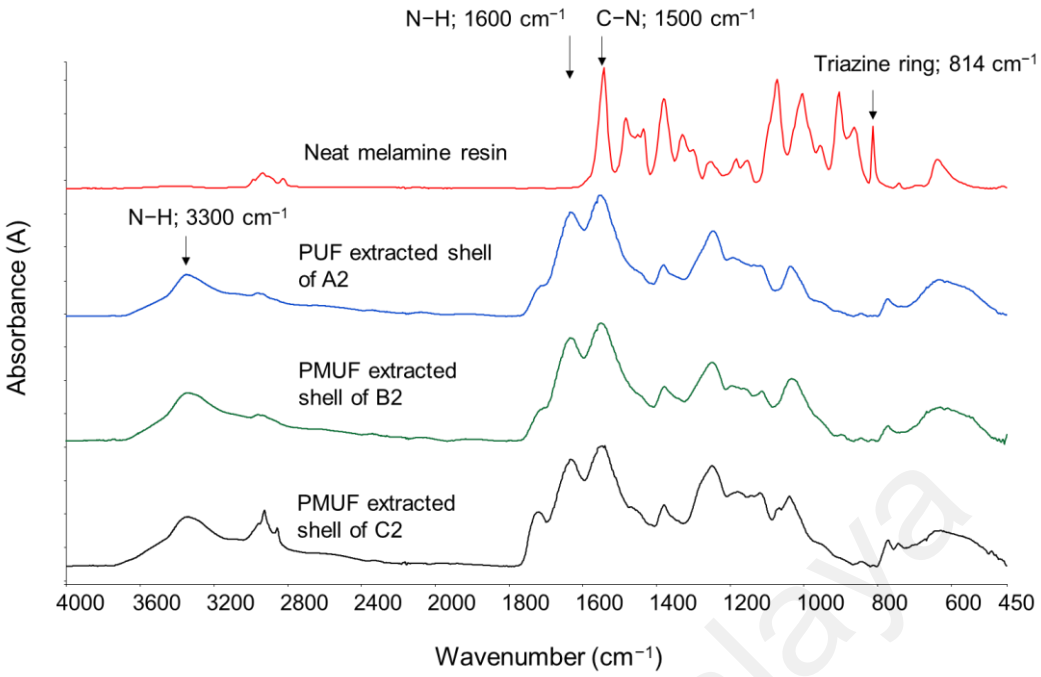

Fig. 5.22: ATR-FTIR spectra of the neat melamine resin and the extracted shell materials of A2, B2 and C2 microcapsules

^{1}H-NMR spectra of the core extracted from A2, B2 and C2 microcapsules showed identical match with the spectrum of AlkydPKO65, which also verified the alkyd's encapsulation (**Fig. 5.23**). The chemical shifts of each of the core are as follows (δ, ppm): 0.8, 1.3, 1.6, 2.0, 2.3, 3.6-4.4, 5.3, 7.51 and 7.69. The assignment of the peaks is similar to the spectrum of alkyd as described in Section 4.2.

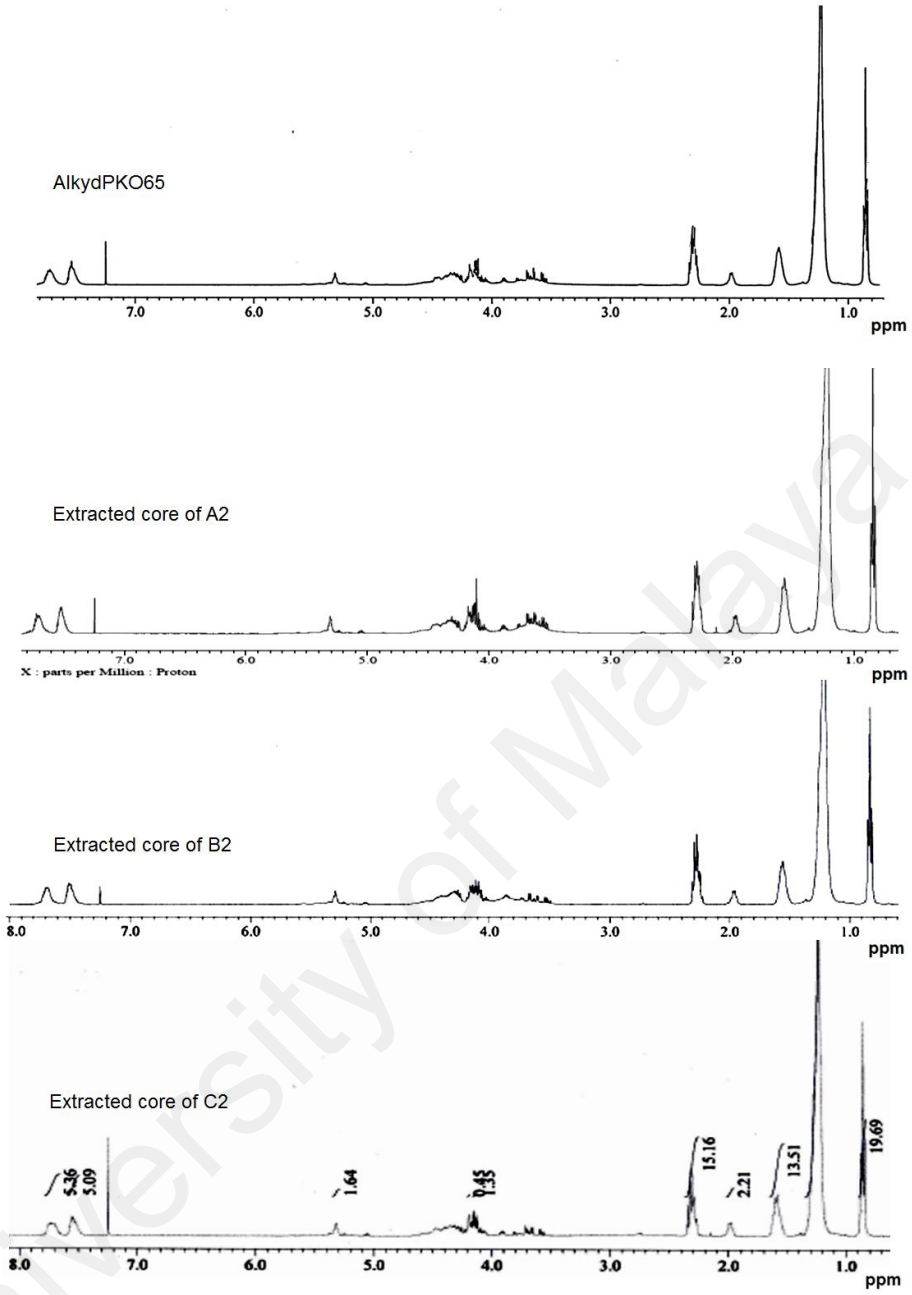

Fig. 5.23: ^{1}H-NMR spectra of AlkydPKO65 and the extracted core of A2, B2, C2 microcapsules

5.4 Thermal Analysis

The thermal stability of microcapsules plays an important role in their applications in self-healing composites or coating. Thermal properties of microcapsules, their shell and core content were analyzed using DSC and TGA.

5.4.1 Differential Scanning Calorimetry (DSC)

Fig. 5.24 shows the DSC diagram of the neat alkyd, microcapsules samples A2 and B2 and the respective amino shells. **Fig. 5.24 (a)** shows the thermogram of neat alkyd with one broad endothermic broad at peak −15°C to 15°C, which corresponds to the melting of the alkyd and a glass transition temperature (T_g) at −13°C.

Two endothermic peaks appeared in the DSC curves of A2 and B2. The first endothermic peaks at 0°C to 15°C were due to the melting of alkyd content in the microcapsules, which were similar to the thermogram of neat alkyd. The second ones appeared at higher temperature range with sharp melting peaks (T_m) at 148°C and 192°C respectively, which correspond to the melting of PUF and PMUF shell walls. The T_m of microcapsules were higher than the T_m of PUF and PMUF shell alone. Both A2 and B2 also showed T_g at −13.0°C and −11.6°C respectively, which correspond to the T_g of encapsulated alkyd.

The higher T_g and T_m of B2 compared to the T_g and T_m of A2 indicates the possibility of some reactions between the melamine resin with the –OH group on the surface of alkyd droplet. These reactions might also have shifted the T_m of the extracted shell materials; from 130°C to 148°C for A2 and from 156°C to 192°C for B2. A small amount of melamine resin was introduced in sample B2 to increase the amount of crosslinking reactions, in order to achieve a more robust shell. The shell however, was not 100% crosslinked hence the T_m, increased from 148°C to 192°C.

A subtle endothermic peak observed at ~85°C in PUF extracted shell (**Fig. 5.24 (d)),** was attributed to evaporation of water and free formaldehyde. Other two endothermic peaks at 210°C and 242°C were due to the decomposition of shell material. The PMUF extracted shell also showed a broad endothermic peak near 220°C due to the decomposition of UF/MUF (**Fig. 5.25 (e)**) (Camino et al., 1983). The DSC

characterization data for other microcapsules can be found in Appendix E. The observation of the T_m and T_g in the microcapsules verifies the encapsulation of alkyd.

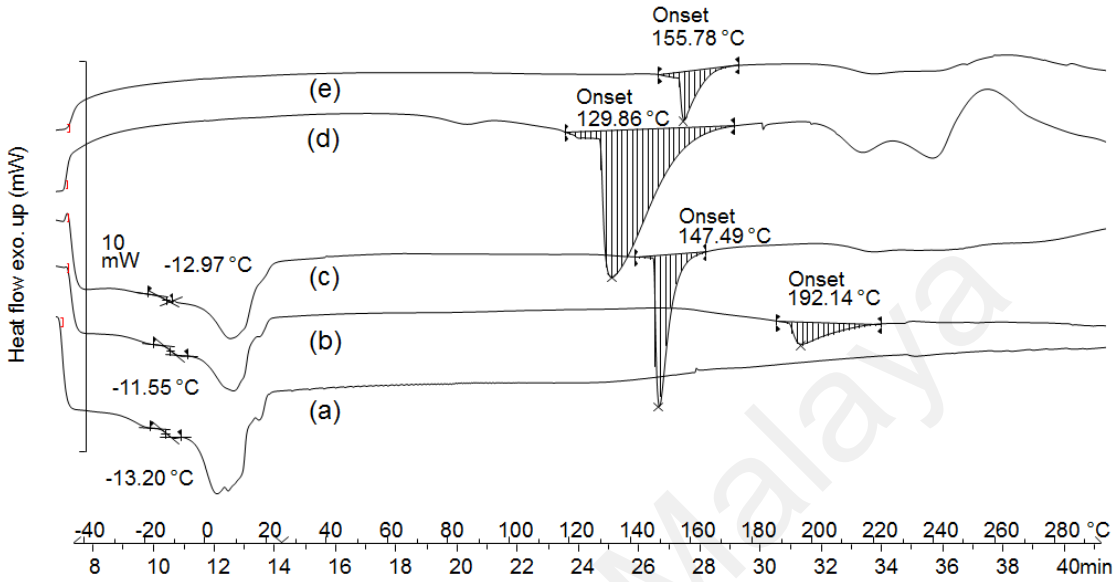

Fig. 5.24: DSC thermograms of (a) AlkydPKO65 (b) B2 (c) A2 (d) PUF shell (e) PMUF shell

5.4.2 Thermogravimetric Analysis (TGA)

Fig. 5.25 shows the thermal degradations of B2 microcapsules, the neat alkyd and the PMUF shell. B2 was thermally stable up to 258°C and subsequently decomposed completely within the range of 260−550°C. Degradation of PMUF occurred around 220−300°C, while the alkyd started to break down around 250°C. The thermal degradations of the core and shell occurred in overlapping temperature ranges; consequently, TGA could not be used to determine the amount of core and shell accurately. The TGA data of the other samples are summarized in **Table 5.7**. All microcapsules were thermally stable up to ~250°C. $T_{50\,\%}$ is the temperature at 50% weight loss and the results showed that half of the microcapsules thermally degraded around 325°C to 375°C.

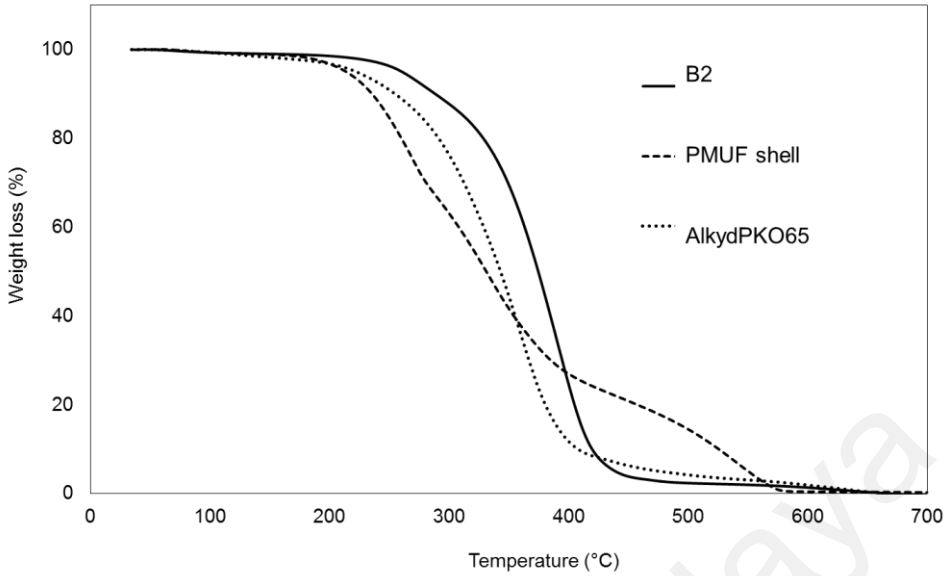

Fig. 5.25: TGA thermograms of B2 microcapsules, neat alkyd and PMUF shell

Table 5.7: TGA data of PUF and PMUF microcapsules

Sample	T_d onset (°C)	$T_{50\%}$ (°C)
A1	250	355
A2	250	352
A3	230	348
B1	250	375
B2	258	375
B3	245	369
B4	200	341
C2*	216	325
D1*	207	350
AlkydPKO65	250	342
PUF shell	220	310
PMUF shell	220	331

***T_d*:** onset degradation temperature; * measurement with STA.

5.5 Morphology of Microcapsules

As shown in **Fig. 5.26 (a)**, the PMUF microcapsule is spherical in shape. **Fig. 5.26 (b)** shows the magnified region of the rough outer surface, which consisted of PMUF nanoparticles. The examination on a broken microcapsule shows that the microcapsule

had smooth inner surface and rough outer surface, as shown in **Fig. 5.28**. The rough outer surface could provide good bonding with the film matrix, which will facilitate in breaking the microcapsules under stress due to cracking (Suryanarayana et al., 2008).

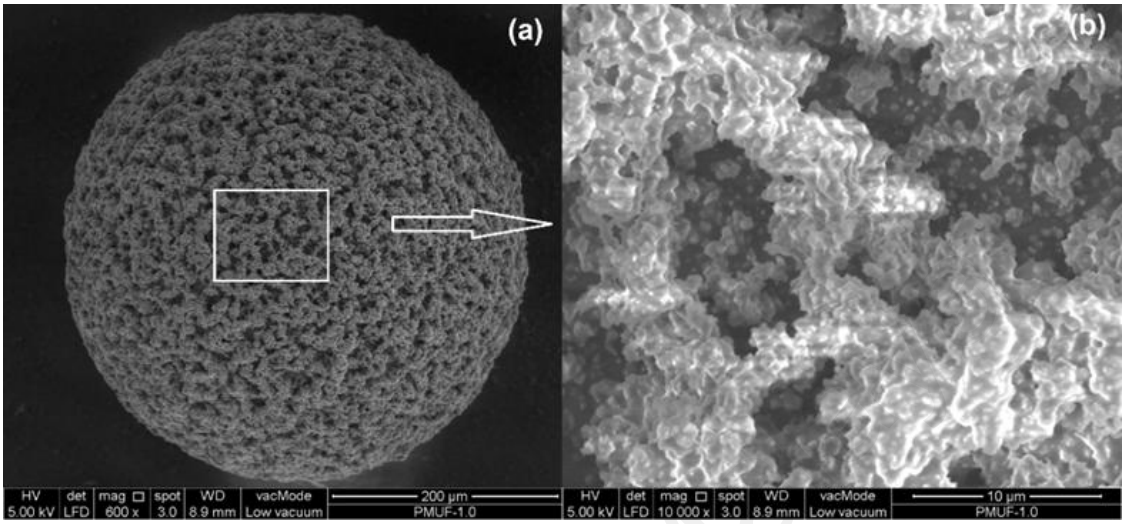

Fig. 5.26: FESEM micrographs of B2 microcapsule at: (a) 600×; (b) 10 000× magnifications

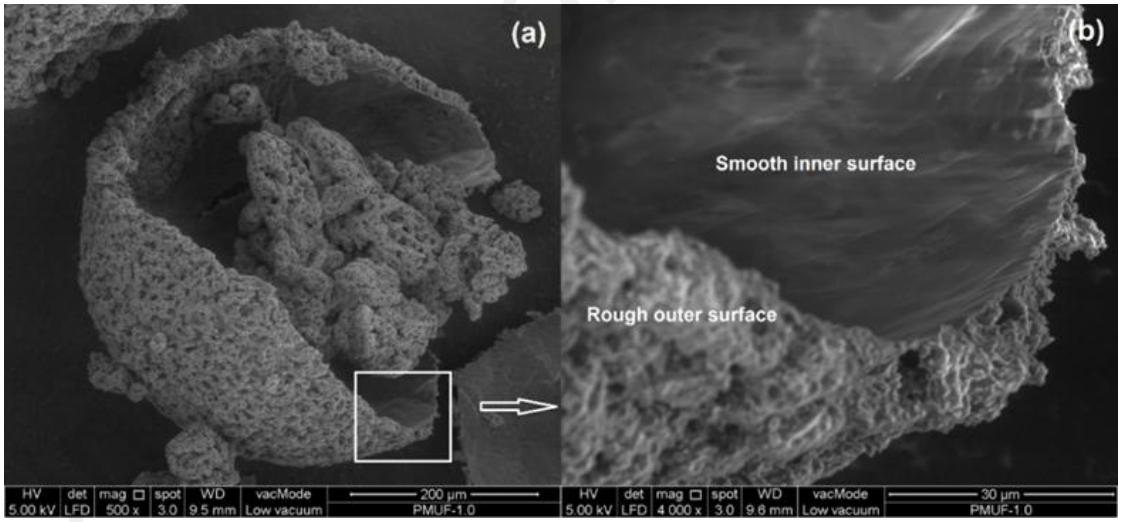

Fig. 5.27: FESEM micrographs of ruptured B2 microcapsule at: (a) 500×; (b) 4000× magnifications

5.6 Storage Stability of Microcapsules

Storage study is necessary to evaluate the performance of microcapsules to be able to store the healing agent until the time it is needed. In this work, microscopy observation within a certain period of time was done, accompanied by thermal analysis using DSC.

Fig. 5.28 (a) shows the digital microscope images of B2 microcapsules when they were freshly synthesized, which were spherical in shape and free flowing. After being stored for a month at 25˚C, the microcapsules began to be less spherical. The alkyd could has diffused out of the capsules, resulted in wet and sticky microcapsules as shown in **Fig.5.28 (b)**. At **(c)**, they became worse as most of them were already ruptured. On the contrary, when stored at 10˚C, the microcapsules lasted longer, retained their spherical shape and were still free flowing (**Fig. 5.28 (d)**). As shown in **Fig. 5.29**, DSC analysis shows that there were no significant difference in T_g of A2 and B2 after 8 and 12 months of storage at 10˚C, respectively. A marginal difference of T_m values were also observed after 8 and 12 months of storage at 10˚C for both microcapsules. These observations indicate that the microcapsules can be safely stored at 10˚C to preserve their quality up to 8-12 months. The details of the storage are summarized in **Table 5.8**.

Table 5.8: Summary of storage conditions of A2 and B2 microcapsules

Characteristics	A2 microcapsules	B2 microcapsules
Yield (wt. %)	40	64
Storage stability at 26°C	5 months	25 days
Storage stability at 10°C	12 months	8 months
Mean diameter (μm)	403 ± 56	380 ± 60
Core content (%)	89.9 ± 0.5	92.0 ± 1.3
T_g (°C)	-13.0 after 6 months	-11.0 after 2 months
	-13.4 after 12 months	-11.7 after 8 months
T_m (°C)	148 after 6 months	192 after 2 months
	157 after 12 months	176 after 8 months

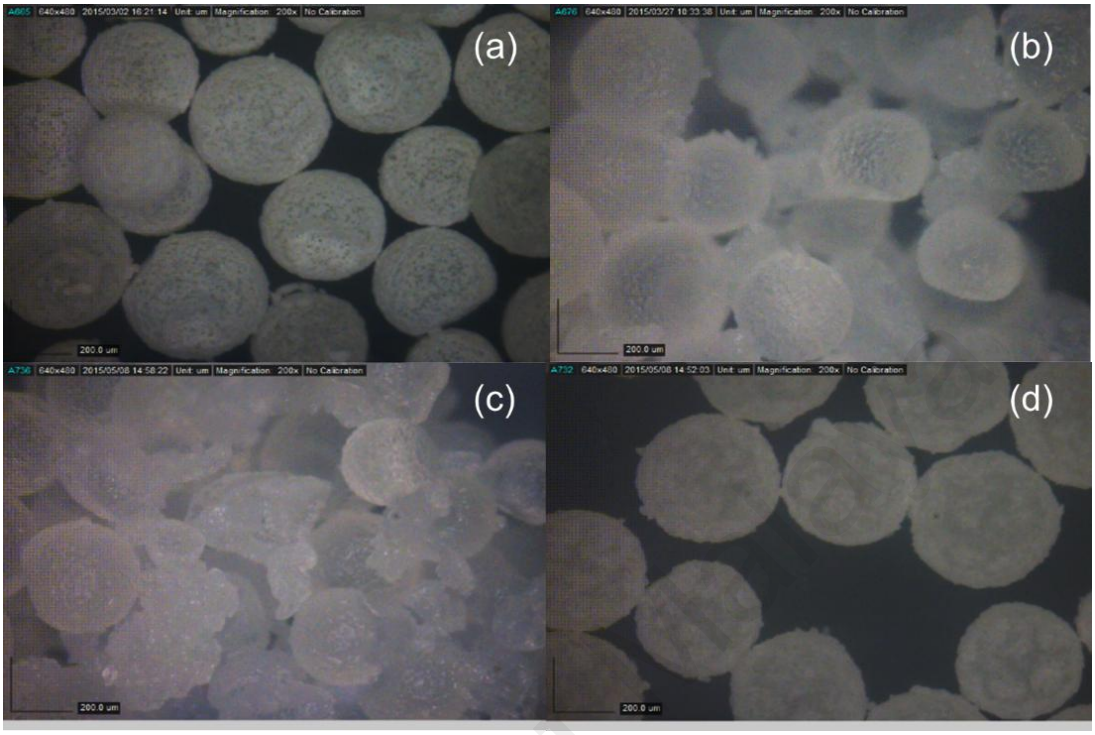

Fig. 5.28: Digital microscope images of B2 microcapsules at: (a) freshly prepared (b) 1 month at 26°C (c) 5 months at 26°C (d) 5 months at 10°C

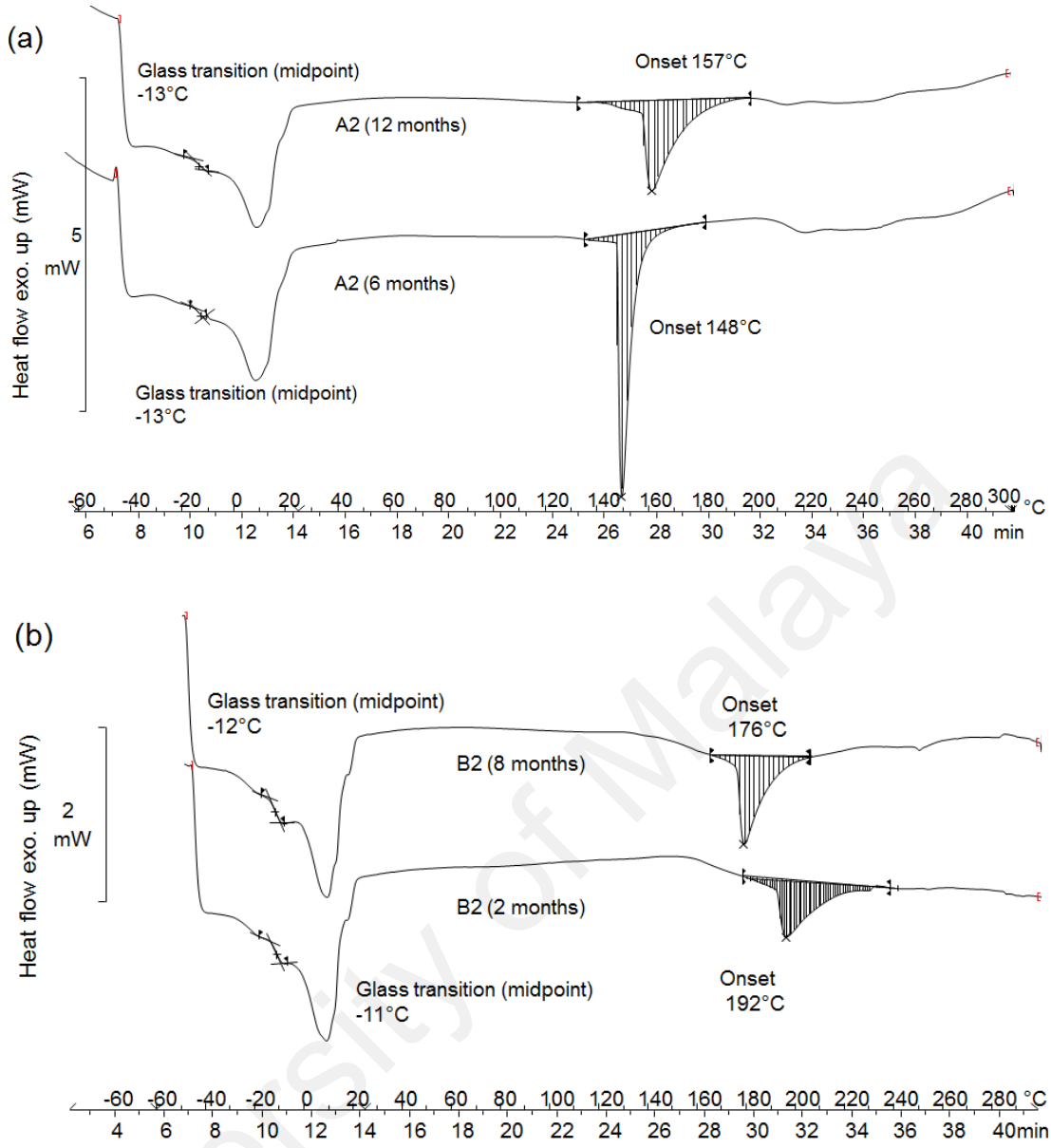

Fig. 5.29: DSC thermograms of A2 and B2 microcapsules after certain period of times stored at 10°C

5.7 Summary

This chapter has identified influence of several factors to get the optimized and most yielded method for alkyd encapsulation. The characterizations of the microcapsules were described in details including thermal, morphology and storage stability. In the next chapter, the microcapsules performance in a selected epoxy system is discussed.

CHAPTER 6: MICROCAPSULES IN EPOXY MATRIX AND EPOXY/ALKYD REACTION

6.1 Microcapsules Distribution in Epoxy Matrix

Fig. 6.1 shows the optical microscope images of microcapsules B2, which embedded in the selected epoxy matrix. The microcapsules retained their spherical shape, even after epoxy curing process with amine hardener at 100°C.

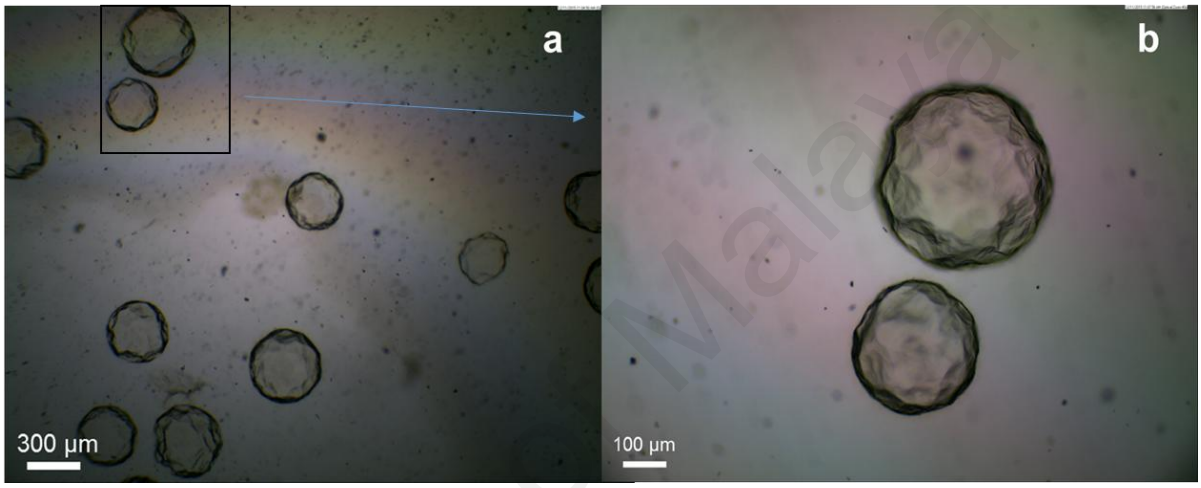

Fig. 6.1: Optical microscope images of B2 microcapsules that were embedded in the epoxy matrix (a) 40× (b) 100×

C2 microcapsules are those prepared with sonication to help disperse the alkyd emulsion in order to reduce the size of resultant microcapsules. Before being embedded into the epoxy matrix, C2 were sieved to separate them into two fractions of size, 50−500 µm and <50 µm. As shown in **Fig. 5.19** (in previous chapter), C2 were smaller than B2 and existed in clusters. To help distribute the microcapsules evenly in the matrix, the mixture of epoxy with microcapsules, was put in a sonication bath before it hardened. **Fig. 6.2 (a)** shows the distribution of the bigger fraction of C2 microcapsules, which spread individually as well as in groups, throughout the matrix. The smaller fraction, below 50 µm, also consists of small microcapsules, dispersed in the host matrix as shown in **Fig. 6.2 (b)**. This indicates that the sonication introduced before hardening of the epoxy has helped separate the agglomerated microcapsules to some extent.

Further inspection of the sliced matrix using FESEM revealed the cavities previously occupied by B2 microcapsules **(Fig. 6.3)**. The size distributions of C2 microcapsules observed is rather large as shown in **Fig. 6.4. Fig. 6.4 (a-b)** show bigger microcapsules incorporated into the matrix, while **Fig. 6.4 (c-d)** show smaller individual and groups of microcapsules embedded in the matrix. The sonication of the epoxy mixture before setting has not fully dispersed the clustered of small capsules. Nevertheless, the microcapsules and the matrix also show good bonding through the embedment of the microcapsules' rough shell with the epoxy matrix, as observed by FESEM shown in **Fig. 6.3 (b)** and **6.4 (b)**.

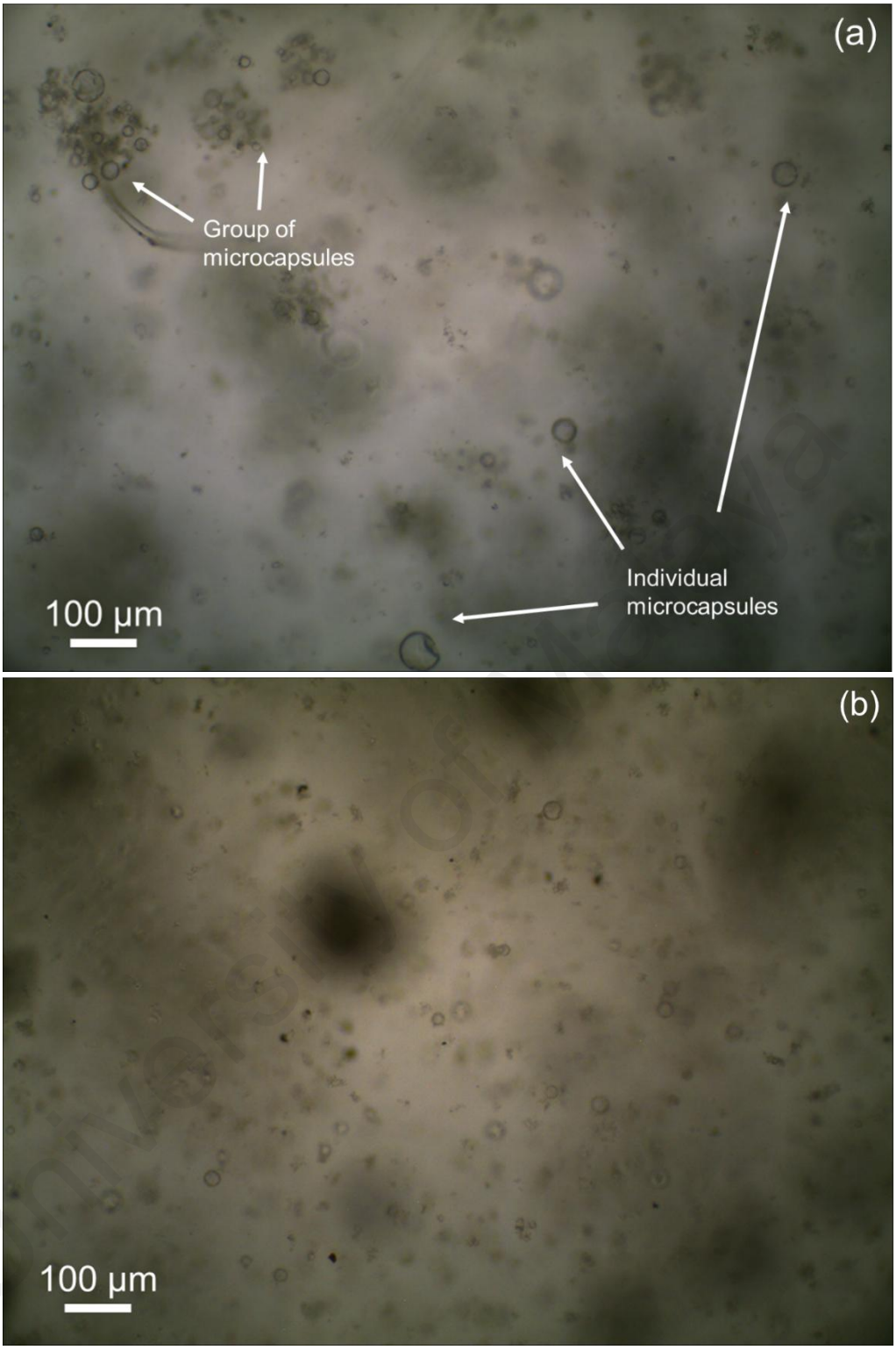

Fig. 6.2: Optical microscope images of C2 microcapsules embedded in epoxy matrix: (a) 50 – 500 µm (100×) (b) <50 µm (100×)

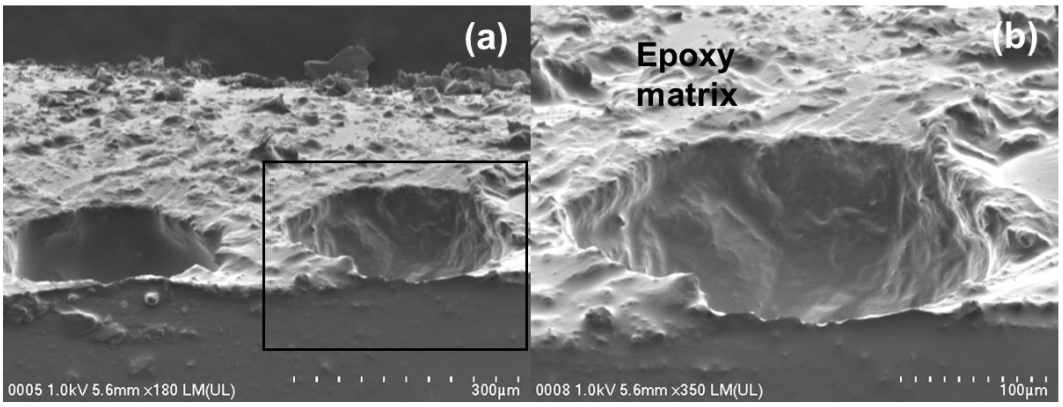

Fig. 6.3: FESEM micrographs of sliced epoxy matrix showing cavities previously occupied by B2 microcapsules: (a) 180× (b) 350×

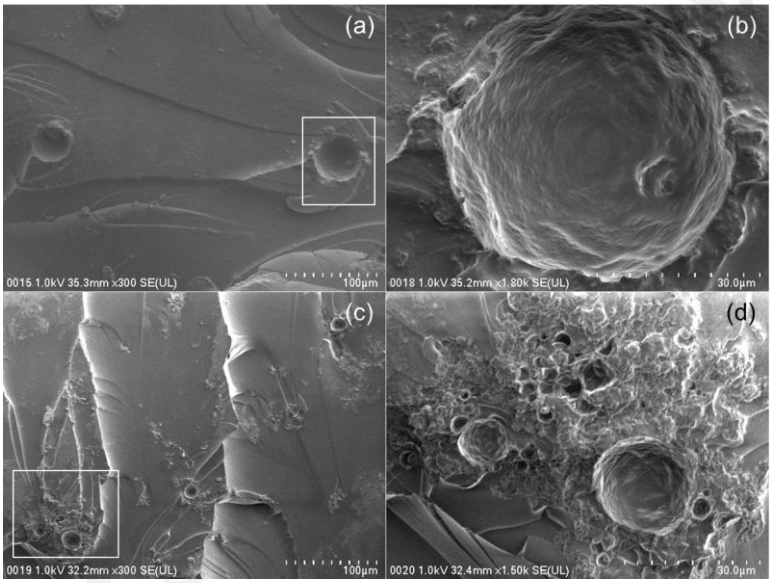

Fig. 6.4: FESEM micrographs of sliced epoxy matrix showing cavities previously occupied by C2 microcapsules: (a) 300× (b) 1800× (c) 300× (d) 1500×

6.2 Flexural and Micro-Indentation Hardness of Epoxy Matrix Loaded with 1%–6% Microcapsules

The effects of B2 loading into the epoxy matrix on flexural strength and Vickers micro-indentation hardness are shown in **Fig. 6.5**. The epoxy matrix without microcapsules served as the control. Overall, the incorporation of 1 and 3 wt. % microcapsules did not have significant effect on the flexural strength and micro-indentation hardness of the epoxy matrix.

First, the incorporation of 1% of B2 microcapsules has increased 11% of the flexural strength of neat epoxy. Further increment to 3% only slightly reduced the flexural strength of 2%. Further addition of microcapsules to 6% evidently lowered the flexural strength of the neat epoxy. These observations suggested the optimum loading of microcapsules with alkyd healing agent is from 1-3%. At 1% loading, the improved flexural strength may be due to the good dispersion of the microcapsules in the matrix, as evidenced from microscopy analysis **(Fig. 6.6)**. It has also been reported that inclusion of dispersed rubbery particles into epoxy polymer can increase their toughness without significantly diminishing the other desirable engineering properties (Kinloch et al., 2005; Kinloch et al., 1983; Yuan et al., 2008). Another possible reason for the good flexural properties may be due to the good matrix-microcapsules interaction. The outer shell of the microcapsules is made up of rough PUF surface that could provide physical bonding. However, the size of the microcapsules (mainly 300-500 μm) is relatively bigger than the typical microcapsules for epoxy matrix (White et al., 2001; Yuan et al., 2008), resulting in low surface area for matrix-capsules interaction. Therefore, this might limit the inclusion of the microcapsules to only 3% maximum. Excessive loading of microcapsules could possibly lead to capsules-capsules agglomeration, thus the low flexural strength observed.

On the contrary to the flexural strength, loading of 1, 3 and 6% of the microcapsules generally did not affect the micro-indentation hardness of the neat epoxy. The difference may lie in the way of hardness was measured. As hardness property was measured by micro-indentation method, it only measures the hardness of surface and not of the interior of the samples (Furches, 2004). Therefore, the microcapsules inclusion into the neat epoxy matrix might not affect much of its micro-indentation hardness.

In a nutshell, the amount and distribution of microcapsules in the polymer matrix would greatly influence the mechanical behavior of the composites and this must be

optimized to achieve the best balance between incorporating self-healing property while retaining good mechanical performance of the composites.

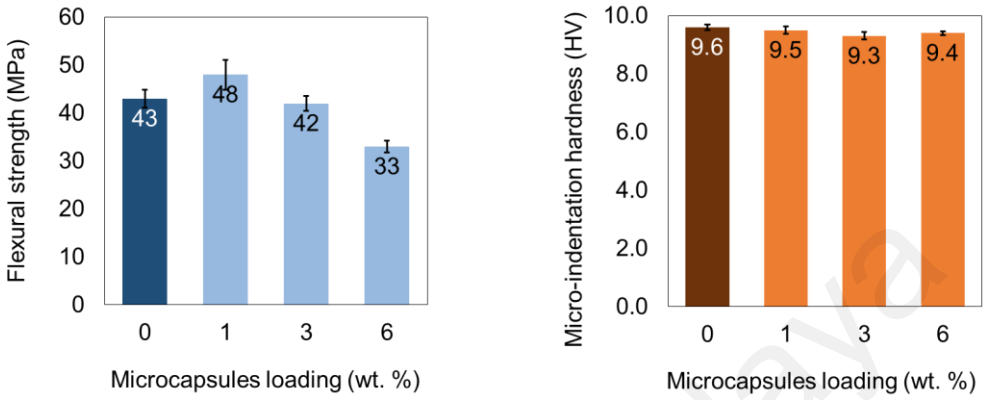

Fig. 6.5: Effect of the microcapsules loading on the flexural strength and micro-indentation hardness (Vickers) of the epoxy matrix

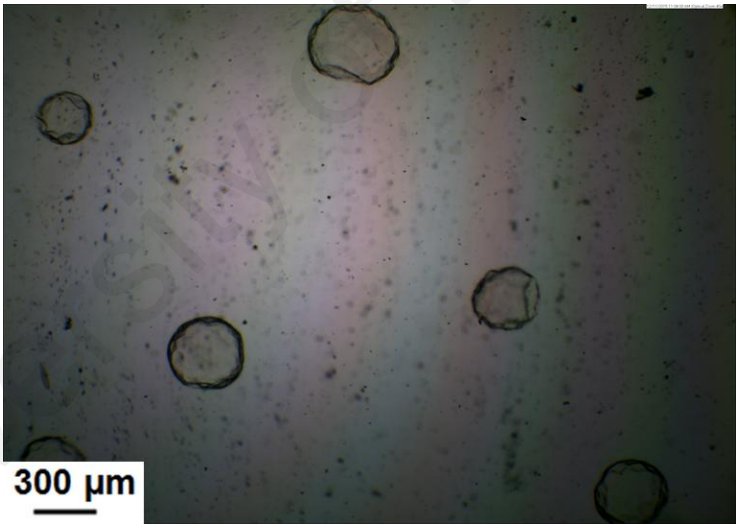

Fig. 6.6: Epoxy matrix with 1% of B2 microcapsules

6.3 Reactions of the Alkyd Blended with Epoxy Resin and Hardener

The alkyd, epoxy resin and its hardener were blended by different equivalent ratios as shown in **Table 6.1**. The blends, EA2 and EA3, were formulated with excess equivalent (Eq.) of epoxy resin. Mixing was carried out manually and all the blends were able to cure to non-sticky solid at room temperature (rt) in 24 h. Similar observation was obtained

with EA samples cured at elevated temperature. The plausible reaction of the alkyd and the epoxy resin is shown in **Fig. 6.7**. The carboxylic acid groups of the alkyd could also react with the amino group of the hardener.

Table 6.1: Reactions of alkyd, epoxy and amine hardener in different blends

Sample	Eq. wt. ratio of epoxy/amine/alkyd	Epoxy/Alkyd wt. ratio	Epoxy (g)	Amine (g)	Alkyd (g)	After 24 h at rt
Control	1/1/0	100/0	1	0.58	0	Cured, solid
EA1	1/0.8/0.02	100/39	1	0.44	0.39	Cured, solid
EA2	1/0.8/0.01	100/20	1	0.44	0.20	Cured, solid
EA3	1/0.7/0.01	100/20	1	0.39	0.20	Cured, solid

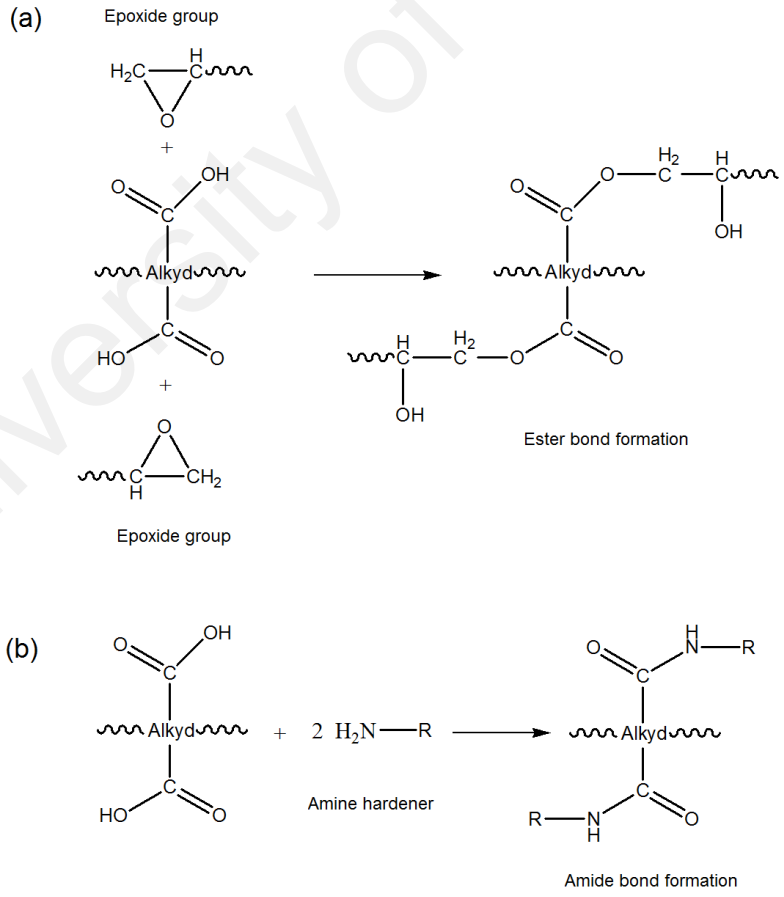

Fig. 6.7: Scheme of plausible reactions of carboxylic groups of alkyd with (a) epoxy and (b) amino group

Fig. 6.8 shows the FTIR spectra of neat alkyd, neat epoxy resin and the samples that were cured at room temperature for 24 h. The spectrum of neat epoxy resin showed a strong adsorption at 2900–2800 cm^{-1} due to C–H stretching. The adsorption peaks at 1607 and 1508 cm^{-1} were attributed to C=C stretching and C–C stretching of aromatic ring, respectively. The strong peaks at 1240–1030 cm^{-1} were due to C–O–C stretching of ether group. The adsorption at 914 cm^{-1} was attributed to the oxirane group. The spectra of the cured blends (EA1, EA2 and EA3) showed the peak at 914 cm^{-1} has diminished as the epoxy group was consumed in reactions. The carboxylic acid groups of alkyd at 1727 cm^{-1} has shifted to 1734 cm^{-1} in the cure samples, presumably due to conversion to ester.

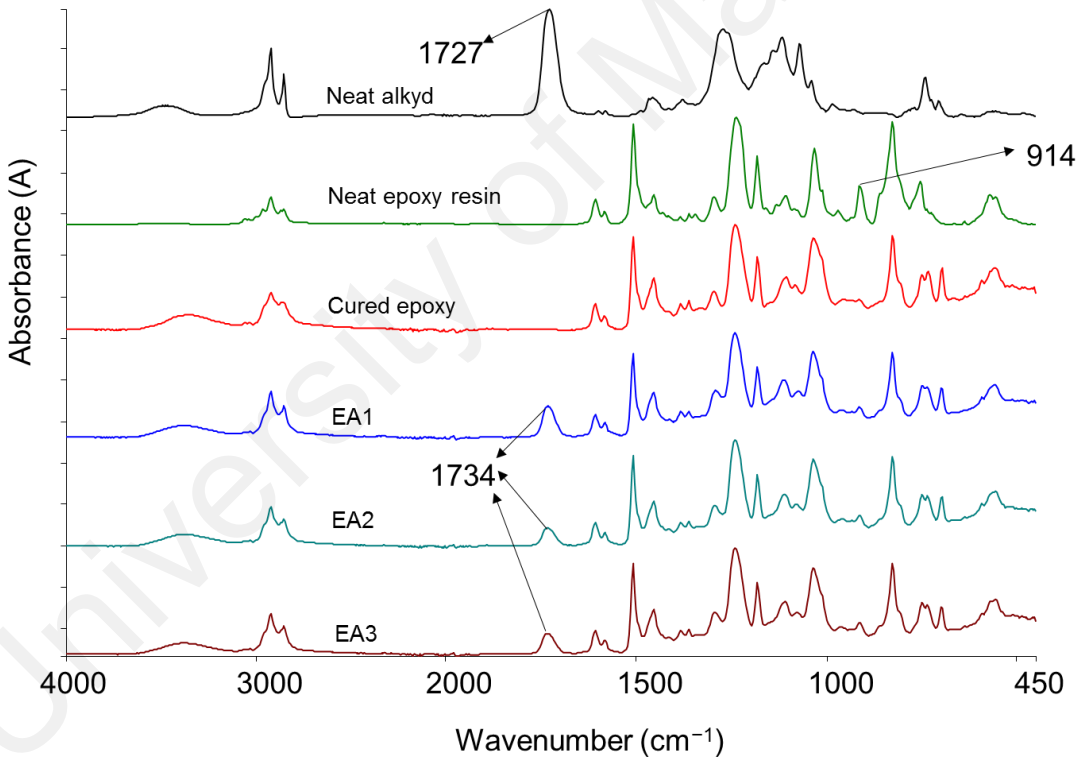

Fig. 6.8: FTIR spectra of neat alkyd, epoxy resin and cured epoxy, EA1, EA2 and EA3 samples

6.4 Summary

Chapter 6 has presented and discussed the incorporation of the microcapsules into a selected epoxy matrix. The microcapsules can be randomly distributed in the matrix, although sonication was needed for smaller microcapsules to ensure good dispersion. Flexural strength and micro-indentation hardness of the epoxy matrix were not jeopardized by the incorporation of 1−3% of B2 microcapsules. The FTIR of epoxy/alkyd blends showed a diminished peak of epoxide group and occurrence of ester bond that suggests the crosslinking reaction.

CHAPTER 7: CONCLUSION AND FUTURE WORK

A long oil with medium viscosity (2.14 Pa·s), with low acid value (15−17 mg KOH/ g alkyd) was successfully synthesized using alcoholysis and esterification of a palm kernel oil. The spectroscopic analyses of the alkyd confirmed the formation of alkyd from PKO. Thermal characterizations of the alkyd showed its stability up to 250°C, a glass transition at −13°C and a broad melting point at 0−15°C.

UF and MUF resin were used as a polymeric shell to encapsulate the synthesized alkyd. Melamine resin was used to modify the UF shell in order to obtain more robust and high yield of microcapsules. For alkyd encapsulation, 0.03−0.12 M/U ratio is suggested. Melamine resin addition has increased shell robustness and thermal stability to ~260°C. The best yielding formulation was with 10 g alkyd as core with 2.1 core/shell weight ratio. The alkyd needs to be emulsified prior to addition of shell materials, with 400 rpm of agitation rate and 2.5 % EMA, which acts as emulsifier or viscosity adjuster. Sonication was used to obtain smaller microcapsules for certain application. Microcapsules obtained were free flowing, have smooth inner shell and rough and layered outer shell. The core loading were 86−91 %, 63−95 % and 54 % for A2, B2 and C2 microcapsules respectively. They were thermally stable to 250°C, 260°C and 216°C for respective microcapsules.

The microcapsules formed could survived the incorporation process into the epoxy matrix and their distribution in the matrix was random. Generally, the embedment of B2 microcapsules did not affect the flexural strength and micro-indentation hardness of the epoxy matrix, if not more than 3 wt. %. Self-healing was proposed via the crosslinking reaction of alkyd and epoxy, as evidenced by FTIR analyses of the EA blends and the healed epoxy coating and the preliminary microscopic examinations of the healed scratched-epoxy coating.

The scope of this study was limited in terms of the storage stability of the microcapsules. B2 needs cold storage to keep them in good shape probably due to the high viscosity and polar nature of the alkyd due to excess hydroxyl content. The shell can be adjusted to be thicker to improve the stability of the microcapsules. A2 with slightly thicker shell gives better storage stability at 25°C but the yield of production was low. C2 is stable at room temperature but the yield of production was low and their clustered condition needs pre-sonication prior to embedment into the epoxy matrix.

The mechanical properties of the matrix carried out in this work were based on two tests due to time constraint. Further mechanical tests such as tensile and impact tests can be done to investigate more on the influence of the microcapsules incorporation to the epoxy matrix. More research is required to determine the self-healing efficiency of the epoxy matrix; the efficiency of epoxy coating healing at different temperatures. The quantitative healing efficiency of epoxy composites also can be measured using suitable mechanical properties, such as lap-shear test and fracture toughness. The quantitative corrosion test also may be applicable for the protective epoxy coating, which can produce improved proof of self-healing. The optimization method to get proper smaller size microcapsules also seems necessary due to requirement for coating application. The small size of microcapsules is important for ease of dispersion and formation of thin layer of coatings. It is also to maintain the good adhesion of coating on substrates.

Another interesting prospect is to study the effect of the introduction of alkyd with higher COOH content to promote faster crosslinking with epoxy. A different type of alkyd with higher acid value can be synthesized and its effect on the epoxy-alkyd crosslinking can be studied. The kinetics of curing of alkyd with the epoxy can also be studied to optimize the healing reaction in the epoxy matrix. Modified alkyds with unsaturation could also be investigated for potential healing agent.

REFERENCES

Ahdash, A., Hamzah, E., Ourdjini, A., & Abdolahi, A. (2014). Characterizations of zeolite, polyaniline and zeolite/polyaniline as antifouling materials for marine applications. *Advanced Materials Research, 845*, 91-95.

Ai, H., Jones, S. A., & Lvov, Y. M. (2003). Biomedical applications of electrostatic layer-by-layer nano-assembly of polymers, enzymes and nanoparticles. *Cell Biochemistry and Biophysics, 39*(1), 23-43.

Alebrahim, R., Haris, S. M., Mohamed, N. A. N., & Abdullah, S. (2015). Vibration analysis of self-healing hybrid composite beam under moving mass. *Composite Structures, 119*, 463-476.

Assanvo, E. F., Gogoi, P., Dolui, S. K., & Baruah, S. D. (2015). Synthesis, characterization and performance characteristics of alkyd resins based on Ricinodendron heudelotii oil and their blending with epoxy resins. *Industrial Crops and Products, 65*, 293-302.

ASTM E384-11 (2011) Standard Test Method for Knoop and Vickers Hardness of Materials, ASTM International, West Conshohocken, PA, www.astm.org

ASTM D445-15a (2015) Standard Test Method for Kinematic Viscosity of Transparent and Opaque Liquids (and Calculation of Dynamic Viscosity), ASTM International, West Conshohocken, PA, 2015, www.astm.org

ASTM E384-16 (2016) Standard Test Method for Microindentation Hardness of Materials, ASTM International, West Conshohocken, PA, www.astm.org

ASTM D790-15e2 (2015) Standard Test Methods for Flexural Properties of Unreinforced and Reinforced Plastics and Electrical Insulating Materials, ASTM International, West Conshohocken, PA, www.astm.org

ASTM D1639-90(1996)e1 (1996) Standard Test Method for Acid Value of Organic Coating Materials (Withdrawn 2005), ASTM International, West Conshohocken, PA, www.astm.org

Basiron, Y. (2007). Palm oil production through sustainable plantations. *European Journal of Lipid Science and Technology, 109*(4), 289-295.

Basiron, Y., & Weng, C. K. (2004). The oil palm and its sustainability. *Journal of Oil Palm Research, 16*(1), 1-10.

Benjapornkulaphong, S., Ngamcharussrivichai, C., & Bunyakiat, K. (2009). Al_2O_3-supported alkali and alkali earth metal oxides for transesterification of palm kernel oil and coconut oil. *Chemical Engineering Journal, 145*(3), 468-474.

Binder, W. H. (2013). *Self-healing Polymers: From Principles To Applications.* Weinheim: Wiley-VCH Verlag GmbH & Co. KGaA.

Blaiszik, B. J., Caruso, M. M., McIlroy, D. A., Moore, J. S., White, S. R., & Sottos, N. R. (2009). Microcapsules filled with reactive solutions for self-healing materials. *Polymer, 50(4),* 990-997.

Blaiszik, B. J., Kramer, S. L. B., Olugebefola, S. C., Moore, J. S., Sottos, N. R., & White, S. R. (2010). Self-healing polymers and composites. *Annual Review of Materials Research, 40,* 179-211.

Bose, R. K., Lafont, U., Vega, J. M., Garcia, S. J., & Swaag, S. v. d. (2013). Methods to monitor and quantify (self-) healing in polymers and polymer systems. In W. H. Binder (Ed.), *Self Healing Polymers: From Principles to Applications*. Weinheim: Wiley-VCH Verlag GmbH & Co.

Boura, S. H., Peikari, M., Ashrafi, A., & Samadzadeh, M. (2012). Self-healing ability and adhesion strength of capsule embedded coatings—Micro and nano sized capsules containing linseed oil. *Progress in Organic Coatings, 75*(4), 292-300.

Brown, E. N., Kessler, M. R., Sottos, N. R., & White, S. R. (2003). In situ poly(urea-formaldehyde) microencapsulation of dicyclopentadiene. *Journal of Microencapsulation, 20*(6), 719-730.

Brown, E. N., Sottos, N. R., & White, S. R. (2002). Fracture testing of a self-healing polymer composite. *Experimental Mechanics, 42,* 372-379.

Brown, E. N., White, S. R., & Sottos, N. R. (2004). Microcapsule induced toughening in a self-healing polymer composite. *Journal of Materials Science, 39*(5), 1703-1710.

Camino, G., Operti, L., & Trossarelli, L. (1983). Mechanism of thermal degradation of urea-formaldehyde polycondensates. *Polymer Degradation and Stability, 5,* 161-172.

Caruso, M. M., Blaiszik, B. J., White, S. R., Sottos, N. R., & Moore, J. S. (2008). Full recovery of fracture toughness using a nontoxic solvent-based self-healing system. *Advanced Functional Materials, 18*(13), 1898-1904.

Caruso, M. M., Delafuente, D. A., Ho, V., Sottos, N. R., Moore, J. S., & White, S. R. (2007). Solvent-promoted self-healing epoxy materials. *Macromolecules, 40*(25), 8830-8832.

Chen, M., Liu, J., Liu, Y., Guo, C., Yang, Z., & Wu, H. (2015). Preparation and characterization of alginate–N-2-hydroxypropyl trimethyl ammonium chloride chitosan microcapsules loaded with patchouli oil. *RSC Advances, 5*(19), 14522-14530.

Chen, X., Dam, M. A., Ono, K., Mal, A., Shen, H., Nutt, S. R., . . . Wudl, F. (2002). A thermally re-mendable cross-linked polymeric material. *Science, 295*(5560), 1698-1702.

Chen, X., Wudl, F., Mal, A. K., Shen, H., & Nutt, S. R. (2003). New thermally remendable highly cross-linked polymeric materials. *Macromolecules, 36*(6), 1802-1807.

Cho, S. H., Andersson, H. M., White, S. R., Sottos, N. R., & Braun, P. V. (2006). Polydimethylsiloxane-Based Self-Healing Materials. *Advanced Materials, 18*(8), 997-1000.

Cho, S. H., White, S. R., & Braun, P. V. (2009). Self-healing polymer coatings. *Advanced Materials, 21*(6), 645-649.

Coope, T. S., Mayer, U. F., Wass, D. F., Trask, R. S., & Bond, I. P. (2011). Self-healing of an epoxy resin using scandium (III) triflate as a catalytic curing agent. *Advanced Functional Materials, 21*(24), 4624-4631.

Cosco, S., Ambrogi, V., Musto, P., & Carfagna, C. (2007). Properties of poly (urea-formaldheyde) microcapsules containing an epoxy resin. *Journal of Applied Polymer Science, 105*(3), 1400-1411.

Darby, Sime. (2011). Palm oil facts and figures Retrieved 31/5/2016 from www.simedarbyplantation.com /upload/PalmOilFactsAndFigures.pdf

Diem, H., Matthias, G., & Wagner, R. A. (2010). Amino Resins *Ullmann's Encyclopedia of Industrial Chemistry*. Weinheim: Wiley-VCH Verlag GmbH & Co. KGaA.

Dry, C. (1994). Matrix cracking repair and filling using active and passive modes for smart timed release of chemicals from fibers into cement matrices. *Smart Materials and Structures, 3*(2), 118.

Dry, C. (1996). Procedures developed for self-repair of polymer matrix composite materials *Composite Structures, 35*, 263-269.

Dry, C., & Sottos, N. R. (1993). *Passive smart self-repair in polymer matrix composite materials.* Paper presented at *1993 North American Conference on Smart Structures and Materials* (pp. 438-444).

Dutta, N., Karak, N., & Dolui, S. (2006). Alkyd–epoxy blends as multipurpose coatings. *Journal of Applied Polymer Science, 100*(1), 516-521.

Elgert, K.-F. (2000). Plastics, General Survey, 1. Definition, Molecular Structure and Properties *Ullman's Encyclopedia of Industrial Chemistry*. Weinheim: Wiley-VCH Verlag GmbH & Co. KGaA.

Elias, H. G., & Mülhaupt, R. (2015). Plastics, General Survey, 1. Definition, Molecular Structure and Properties. *Ullmann's Encyclopedia of Industrial Chemistry*. Weinheim: Wiley VCH Verlag GmbH & Co. KGaA.

Ellis, B. (1993). *Chemistry and Technology of Epoxy Resins*. Netherlands: Springer-Science+Business Media, B.V.

Fan, C., & Zhou, X. (2010). Influence of operating conditions on the surface morphology of microcapsules prepared by in situ polymerization. *Colloids and Surfaces A: Physicochemical and Engineering Aspects, 363*(1), 49-55.

Furches, B. J. (2004). Plastics Testing *Kirk-Othmer Encyclopedia of Chemical Technology*. New Jersey, US: John Wiley & Sons, Inc.

Ghazali, H., Ye, L., & Zhang, M.-Q. (2016a). *Lap shear strength and healing capability of self-healing adhesive containing epoxy/mercaptan microcapsules.* Paper presented at Proceedings of PPS-31: The 31st International Conference of the Polymer Processing Society, Jeju, South Korea.

Ghazali, H., Ye, L., & Zhang, M. Q. (2016b). Interlaminar fracture of CF/EP composite containing a dual-component microencapsulated self-healant. *Composites Part A: Applied Science and Manufacturing, 82*, 226-234.

Ghosh, S. K. (2009). *Self-Healing Materials: Fundamentals, Design Strategies, And Applications*. Weinheim: Wiley-VCH Verlag GmbH & Co. KGaA.

Gogoi, P., Boruah, M., Bora, C., & Dolui, S. K. (2014). Jatropha curcas oil based alkyd/epoxy resin/expanded graphite (EG) reinforced bio-composite: Evaluation of the thermal, mechanical and flame retardancy properties. *Progress in Organic Coatings, 77*(1), 87-93.

Green, B. K., & Schleicher, L. (1957). *Oil-containing microscopic capsules and method of making them*. US Patent.

Guo, H., & Zhao, X. (2008). Preparation of microcapsules with narrow-size distribution by complex coacervation: Effect of sodium dodecyl sulphate concentration and agitation rate. *Journal of Microencapsulation, 25*(4), 221-227.

Hamzah, E., & Ahdash, A. S. I. (2016). *Characterizations and performance of zeolite self-healing coating as an antifouling material for marine applications*. Paper presented at the International Symposium on Coatings and Corrosion (ISCC2016), Kuala Lumpur.

Hattori, T., Terakawa, K., Ichikawa, N., Sakaki, T., Choong, D. H., Gan, S. N., & Lee, S. Y. (2007). *Rubber composition for tire and pneumatic tire using the same*. US Patent.

Hayes, S., Jones, F., Marshiya, K., & Zhang, W. (2007). A self-healing thermosetting composite material. *Composites Part A: Applied Science and Manufacturing, 38*(4), 1116-1120.

Hexion.com. (2005). Epikote™ resin 828 product datasheet. Retrieved 30/4/2016 from www.hexion.com/Products/TechnicalDataSheet.aspx?id=3942

Hexion.com. (2006). Technical data sheet Epikure F205. Retrieved 30/4/2016 from https://www.hexion.com/Products/TechnicalDataSheet.aspx?id=26193

Hexion.com. (2007). Epikote™ resin 240 product datasheet. Retrieved 30/4/2016 from www.hexion.com/products/technicaldatasheet.aspx?id=4586

Hia, I. L., Vahedi, V., & Pasbakhsh, P. (2016). Self-healing polymer composites: prospects, challenges and applications. *Polymer Reviews*, 56(2), 225-261.

Hofland, A. (2012). Alkyd resins: From down and out to alive and kicking. *Progress in Organic Coatings, 73*, 274-282.

Ibeh, C. C. (1998). Amino and Furan Resins. *Handbook of Thermoset Plastics*. CA, USA: William Andrew Publishing, Elsevier.

Inagaki, M., Urashima, K., Toyomasu, S., Goto, Y., & Sakai, M. (1985). Work of fracture and crack healing in glass. *Journal of The American Ceramic Society, 68*(12), 704-706.

Issam, A., Khizrien, A. N., & Mazlan, I. (2011). Physical and mechanical properties of different ratios of palm oil-based alkyd/epoxy resins. *Polymer-Plastics Technology and Engineering, 50*(12), 1256-1261.

Jackson, A. C., Bartelt, J. A., Marczewski, K., Sottos, N. R., & Braun, P. V. (2011). Silica-protected micron and sub-micron capsules and particles for self-healing at the microscale. *Macromolecular Rapid Communications, 32*(1), 82-87.

Jiang, Y., Wang, D., & Zhao, T. (2007). Preparation, characterization, and prominent thermal stability of phase-change microcapsules with phenolic resin shell and n-hexadecane core. *Journal of Applied Polymer Science, 104*, 2799–2806.

Jin, H., Mangun, C. L., Stradley, D. S., Moore, J. S., Sottos, N. R., & White, S. R. (2012). Self-healing thermoset using encapsulated epoxy-amine healing chemistry. *Polymer, 53*, 581-587.

Jin, H., Miller, G. M., Pety, S. J., Griffin, A. S., Stradley, D. S., Roach, D., . . . White, S. R. (2013). Fracture behavior of a self-healing, toughened epoxy adhesive. *International Journal of Adhesion and Adhesives, 44*, 157-165.

Jin, H., Miller, G. M., Sottos, N. R., & White, S. R. (2011). Fracture and fatigue response of a self-healing epoxy adhesive. *Polymer, 52*(7), 1628-1634.

Jones, F. N. (2012). *Alkyd Resins* (Vol. 2). Weinheim: Wiley-VCH Verlag GmbH & Co. KGaA.

Jyothi, N. V. N., Prasanna, P. M., Sakarkar, S. N., Prabha, K. S., Ramaiah, P. S., & Srawan, G. (2010). Microencapsulation techniques, factors influencing encapsulation efficiency. *Journal of Microencapsulation, 27*(3), 187-197.

Kamphaus, J. M., Rule, J. D., Moore, J. S., Sottos, N. R., & White, S. R. (2008). A new self-healing epoxy with tungsten (VI) chloride catalyst. *Journal of The Royal Society Interface, 5*(18), 95-103.

Karak, N. (2012). *Vegetable Oil-Based Polymers: Properties, Processing And Applications*. Cambridge, UK: Woodhead Publishing Limited.

Keller, M. W., White, S. R., & Sottos, N. R. (2007). A self-healing poly (dimethyl siloxane) elastomer. *Advanced Functional Materials, 17*(14), 2399-2404.

Kessler, M. R. (2012). Polymer matrix composites: A perspective for a special issue of Polymer Reviews. *Polymer Reviews, 52*(3), 229-233.

Keyvanfar, A., Majid, M. Z. A., Shafaghat, A., Lamit, H., Talaiekhozan, A., Hussin, M. W., . . . Fulazzaky, M. A. (2014). Application of a grounded group decision-

making (GGDM) model: a case of micro-organism optimal inoculation method in biological self-healing concrete. *Desalination and Water Treatment, 52*(19-21), 3594-3599.

Khong, Y. K., & Gan, S. N. (2013). Blends of phthalic anhydride-modified palm stearin alkyds with high carboxylic acid contents with epoxidized natural rubber. *Journal of Applied Polymer Science, 130*(1), 153-160.

Kienle, R. H., & Ferguson, C. S. (1929). Alkyd resins as film-forming materials. *Industrial & Engineering Chemistry*, 21(4), 349-352.

Kinloch, A., Mohammed, R., Taylor, A., Eger, C., Sprenger, S., & Egan, D. (2005). The effect of silica nano particles and rubber particles on the toughness of multiphase thermosetting epoxy polymers. *Journal of Materials Science, 40*(18), 5083-5086.

Kinloch, A., Shaw, S., Tod, D., & Hunston, D. (1983). Deformation and fracture behaviour of a rubber-toughened epoxy: 1. Microstructure and fracture studies. *Polymer, 24*(10), 1341-1354.

Kongsager, R., & Reenberg, A. (2012). Contemporary land-use trasitions: The global oil palm expansion. Department of Geography and Geology, University of Copenhagen.

Konishi, A., Takahashi, M., Kimura, F., & Toguchi, T. (1974). *Microcapsules for carbonless copying paper*, US Patent.

Kouhi, M., Mohebbi, A., Mirzaei, M., & Peikari, M. (2013). Optimization of smart self-healing coatings based on micro/nanocapsules in heavy metals emission inhibition. *Progress in Organic Coatings, 76*(7–8), 1006-1015.

Kruif, C. G. d., Weinbrecka, F., & Vriesc, R. d. (2004). Complex coacervation of proteins and anionic polysaccharides. *Current Opinion in Colloid & Interface Science, 9*, 340-349.

Lamprecht, A., & Bodmeier, R. (2010). Microencapsulation *Ullman's Encyclopedia of Industrial Chemistry*. Weinheim: Wiley VCH Verlag GmbH & Co. KGaA.

Lee, S. Y., Gan, S. N., Hassan, A., Terakawa, K., Hattori, T., Ichikawa, N., & Choong, D. H. (2011). Reactions between epoxidized natural rubber and palm oil-based alkyds at ambient temperature. *Journal of Applied Polymer Science, 120*(3), 1503-1509.

Li, H., Tong, W., Cui, J., Zhang, H., Chen, L., & Zuo, L. (2014). Heat treatment of centrifugally cast high-vanadium alloy steel for high-pressure grinding roller. *Acta Metallurgica Sinica (English Letters), 27*(3), 430-435.

Li, Q., Kim, N. H., Hui, D., & Lee, J. H. (2013a). Effects of dual component microcapsules of resin and curing agent on the self-healing efficiency of epoxy. *Composites Part B: Engineering, 55*, 79-85.

Li, Q., Mishra, A. K., Kim, N. H., Kuila, T., Lau, K.-T., & Lee, J. H. (2013b). Effects of processing conditions of poly (methylmethacrylate) encapsulated liquid curing

agent on the properties of self-healing composites. *Composites Part B: Engineering, 49*, 6-15.

Li, W., Zhang, X.-X., Wang, X.-C., & Niu, J.-J. (2007). Preparation and characterization of microencapsulated phase change material with low remnant formaldehyde content. *Materials Chemistry and Physics, 106*(2), 437-442.

Liu, H., Wang, C., Zou, S., Wei, Z., & Tong, Z. (2012). Facile fabrication of polystyrene/halloysite nanotube microspheres with core–shell structure via Pickering suspension polymerization. *Polymer Bulletin, 69*(7), 765-777.

Liu, X., Sheng, X., Lee, J. K., & Kessler, M. R. (2009). Synthesis and characterization of melamine-urea-formaldehyde microcapsules containing ENB-based self-healing agents. *Macromolecular Materials and Engineering, 294*(6-7), 389-395.

Malinskii, Y. M., Prokopenko, V. V., Ivanova, N. A., & Kargin, V. A. (1969). Investigation of self-healing of cracks in polymers I. Effect of temperature and crosslinks on self-healing of cracks in polyvinyl acetate. *Mekhanika Polimerov, 2*, 271-275.

Mangun, C., Mader, A., Sottos, N., & White, S. (2010). Self-healing of a high temperature cured epoxy using poly (dimethylsiloxane) chemistry. *Polymer, 51*(18), 4063-4068.

McIlroy, D. A., Blaiszik, B. J., Caruso, M. M., White, S. R., Moore, J. S., & Sottos, N. R. (2010). Microencapsulation of a reactive liquid-phase amine for self-healing epoxy composites. *Macromolecules, 43*(4), 1855-1859.

Moake, J. L. (2016). How Blood Clots (Consumer version). Retrieved 31/5/2016 from http://www.msdmanuals.com/home/blood-disorders/blood-clotting-process/how-blood-clots

Mostovoy, S., & Ripling, E. (1966). Fracture toughness of an epoxy system. *Journal of Applied Polymer Science, 10*(9), 1351-1371.

Murphy, E. B., Bolanos, E., Schaffner-Hamann, C., Wudl, F., Nutt, S. R., & Auad, M. L. (2008). Synthesis and characterization of a single-component thermally remendable polymer network: Staudinger and Stille revisited. *Macromolecules, 41*(14), 5203-5209.

Murphy, E. B., & Wudl, F. (2010). The world of smart healable materials. *Progress in Polymer Science, 35*(1-2), 223-251.

Nabuurs, T., Baijards, R., & German, A. (1996). Alkyd-acrylic hybrid systems for use as binders in waterborne paints. *Progress in Organic Coatings, 27*(1), 163-172.

Nesterova, T., Dam-Johansen, K., & Kiil, S. (2011). Synthesis of durable microcapsules for self-healing anticorrosive coatings: A comparison of selected methods. *Progress in Organic Coatings, 70*(4), 342-352.

Nesterova, T., Dam-Johansen, K., Pedersen, L. T., & Kiil, S. (2012). Microcapsule-based self-healing anticorrosive coatings: Capsule size, coating formulation, and exposure testing. *Progress in Organic Coatings, 75*(4), 309-318.

Noh, H., & Lee, J. (2013). Microencapsulation of self-healing agents containing a fluorescent dye. *Express Polymer Letters, 7*, 88-94.

Olaniyi, A. P., Babalola, O. O., & Oyediran, A. M. (2014). Physicochemical properties of palm kernel oil. *Current Research Journal of Biological Sciences, 6*(5), 205-207.

Ong, H. R., Khan, M. M. R., Ramli, R., & Yunus, R. M. (2015). Effect of CuO nanoparticle on mechanical and thermal properties of palm oil based alkyd/epoxy resin blend. *Procedia Chemistry, 16*, 623-631.

Pang, J. W., & Bond, I. P. (2005). A hollow fibre reinforced polymer composite encompassing self-healing and enhanced damage visibility. *Composites Science and Technology, 65*(11), 1791-1799.

Pantzaris, T. P., & Basiron, Y. (2002). The lauric (coconut and palmkernel) oils. In F. D. Gunstone (Ed.), *Vegetable Oils in Food Technology: Composition, Properties and Uses*. UK: Blackwell Publishing.

Patton, T. C. (1962). *Alkyd resins technology: Formulating Techniques And Allied Calculations*. New York: Interscience, John Wiley and Sons, Inc.

Perkin, Elmer. (2005). FT-IR Spectroscopy Attenuated Total Reflectance (ATR). *Technical Note FT-IR spectroscopy.* Retrieved 30/4/2016 from http://www.utsc.utoronto.ca/~traceslab/ATR_FTIR.pdf

Peterson, A. M., Jensen, R. E., & Palmese, G. R. (2009). Reversibly cross-linked polymer gels as healing agents for epoxy− amine thermosets. *ACS Applied Materials & Interfaces, 1*(5), 992-995.

Pham, H. Q., & Marks, M. J. (2005). Epoxy Resins *Ullmann's Encyclopedia of Industrial Chemistry*. Weinheim: Wiley-VCH Verlag GmbH & Co. KGaA.

Pingkarawat, K., Dell'Olio, C., Varley, R., & Mouritz, A. (2015). An efficient healing agent for high temperature epoxy composites based upon tetra-glycidyl diamino diphenyl methane. *Composites Part A: Applied Science and Manufacturing, 78*, 201-210.

Rule, J. D., Brown, E. N., Sottos, N. R., White, S. R., & Moore, J. S. (2005). Wax-protected catalyst microspheres for efficient self-healing materials. *Advanced Materials, 17*(2), 205-208.

Rule, J. D., Sottos, N. R., & White, S. R. (2007). Effect of microcapsule size on the performance of self-healing polymers. *Polymer, 48*, 3520-3529.

Salaün, F., Devaux, E., Bourbigot, S., & Rumeaud, P. (2009). Influence of process parameters on microcapsules loaded with n-hexadecane prepared by in situ polymerization. *Chemical Engineering Journal, 155*, 457-465.

Samadzadeh, M., Boura, S. H., Peikari, M., Ashrafi, A., & Kasiriha, M. (2011). Tung oil: An autonomous repairing agent for self-healing epoxy coatings. *Progress in Organic Coatings, 70*(4), 383-387.

Samadzadeh, M., Boura, S. H., Peikaria, M., Kasiriha, S. M., & Ashrafic, A. (2010). A review on self-healing coatings based on micro/nanocapsules. *Progress in Organic Coatings, 68*, 159-164.

Sauvant-Moynot, V., Gonzalez, S., & Kittel, J. (2008). Self-healing coatings: An alternative route for anticorrosion protection. *Progress in Organic Coatings, 63*(3), 307-315.

Singha, A. S., & Thakur, V. K. (2008). Effect of fibre loading on urea-formaldehyde matrix based green composites. *Iranian Polymer Journal, 17*(11), 861-873.

Sirajuddin, N. A., & Jamil, M. S. M. (2015). Self-healing of poly (2-hydroxyethyl methacrylate) hydrogel through molecular diffusion. *Sains Malaysiana, 44*(6), 811-818.

Sirajuddin, N. A., Jamil, M. S. M., Mat, M. L., & Shah, M. A. (2014). Effect of cross-link density and the healing efficiency of self-healing poly (2-hydroxyethyl methacrylate) hydrogel. *e-Polymers, 14*(4), 289-294.

Song, J. K., Choi, H. J., & Chin, I. (2007). Preparation and properties of electrophoretic microcapsules for electronic paper. *Journal of Microencapsulation, 24*(1), 11-19.

Suryanarayana, C., Rao, K. C., & Kumar, D. (2008). Preparation and characterization of microcapsules containing linseed oil and its use in self-healing coatings. *Progress in Organic Coatings, 63*(1), 72-78.

Takahashi, I., & Ushijima, M. (2007). Detection of fatigue cracks at weld toes by crack detection paint and surface SH wave. *Materials Transactions (Special Issue on Advances in Non-Destructive Inspection and Materials Evaluation), 48*(6), 1190-1195.

Talaiekhozani, A., Keyvanfar, A., Andalib, R., Samadi, M., Shafaghat, A., Kamyab, H., . . . Hussin, M. W. (2014). Application of Proteus mirabilis and Proteus vulgaris mixture to design self-healing concrete. *Desalination and Water Treatment, 52*(19-21), 3623-3630.

Technologies, Pike. (2011). ATR – Theory and Applications: Application Note. Retrieved 30/4/2016 from http://www.piketech.com/files/pdfs/ATRAN611.pdf

Teo, S. Y., Lee, S. Y., Coombes, A., Rathbone, M. J., & Gan, S. N. (2016). Synthesis and characterization of novel biocompatible palm oil-based alkyds. *European Journal of Lipid Science and Technology*, 118(8), 1193–1201

Then, S., Gan, S. N., & Kasim, N. H. A. (2011a). Optimization of microencapsulation process for self-healing polymeric material. *Sains Malaysiana, 40*(7), 795-802.

Then, S., Gan, S. N., & Kasim, N. H. A. (2011b). Performance of melamine modified urea–formaldehyde microcapsules in a dental host material. *Journal of Applied Polymer Science, 122*(4), 2557-2562.

Thies, C. (2005). Microencapsulation *Kirk-Othmer Encyclopedia of Chemical Technology*. New Jersey, US: Wiley Blackwell, John Wiley & Sons, Inc.

Tian, Q., Rong, M. Z., Zhang, M. Q., & Yuan, Y. C. (2010). Synthesis and characterization of epoxy with improved thermal remendability based on Diels-Alder reaction. *Polymer International, 59*(10), 1339-1345.

Tian, Q., Yuan, Y. C., Rong, M. Z., & Zhang, M. Q. (2009). A thermally remendable epoxy resin. *Journal of Materials Chemistry, 19*(9), 1289-1296.

Tiarks, F., Landfester, K., & Antonietti, M. (2001). Preparation of polymeric nanocapsules by miniemulsion polymerization. *Langmuir, 17*(3), 908-918.

Ting, Z., Min, Z., Xiao-Mei, T., Feng, C., & Jian-Hui, Q. (2010). Optimal preparation and characterization of poly (urea–formaldehyde) microcapsules. *Journal of Applied Polymer Science, 115*(4), 2162-2169.

Tong, X.-M., Zhang, T., Yang, M.-Z., & Zhang, Q. (2010). Preparation and characterization of novel melamine modified poly (urea–formaldehyde) self-repairing microcapsules. *Colloids and Surfaces A: Physicochemical and Engineering Aspects, 371*(1), 91-97.

Toohey, K. S., Hansen, C. J., Lewis, J. A., White, S. R., & Sottos, N. R. (2009). Delivery of two-part self-healing chemistry via microvascular networks. *Advanced Functional Materials, 19*(9), 1399-1405.

Toohey, K. S., Sottos, N. R., Lewis, J. A., Moore, J. S., & White, S. R. (2007). Self-healing materials with microvascular networks. *Nature Materials, 6*(8), 581-585.

Ullah, H., Azizli, K. A. M., Man, Z. B., Ismail, M. C., & Khan, M. I. (2016). The potential of microencapsulated self-healing materials for microcracks recovery in self-healing composite systems: A Review. *Polymer Reviews*, 1-57.

Urban, M. W. (2015). Self-Reparing Polymeric Materials, *Kirk-Othmer Encyclopedia of Chemical Technology*. New Jersey, US: Wiley-Interscience, John Wiley & Sons.

Vahedi, V., Pasbakhsh, P., Piao, C. S., & Seng, C. E. (2015). A facile method for preparation of self-healing epoxy composites: using electrospun nanofibers as microchannels. *Journal of Materials Chemistry A, 3*(31), 16005-16012.

van der Zwaag, S., & Brinkman, E. (2015). *Self Healing Materials: Pioneering Research in the Netherlands*. Amsterdam, Netherlands: IOS Press.

Vijayan, P., & AlMaadeed, M. (2016). 'Containers' for self-healing epoxy composites and coating: Trends and advances. *Express Polymer Letters, 10*(6), 506-524.

Wang, P. P., Lee, S., & Harmon, J. P. (1994). Ethanol-induced crack healing in poly(methyl methacrylate). *Journal of Polymer Science: Part B Polymer Physics, 32*, 1217-1227.

Wang, X., Xing, F., Zhang, M., Han, N., & Qian, Z. (2013). Experimental study on cementitious composites embedded with organic microcapsules. *Materials, 6*(9), 4064-4081.

Warrington, S. B., & Höhne, G. W. (2000). Thermal analysis and calorimetry. *Ullmann's Encyclopedia of Industrial Chemistry*. Weinheim: Wiley-VCH Verlag GmbH & Co. KGaA

White, S. R., Sottos, N. R., Geubelle, P. H., Moore, J. S., Kessler, M. R., Sriram, S. R., . . . Viswanathan, S. (2001). Autonomic healing of polymer composites. *Nature, 409*, 794-797.

Wicks, Z. W. (2002). Alkyd Resins (Vol. 2). *Kirk-Othmer Encyclopedia of Chemical Technology*. New Jersey, US: John Wiley & Sons.

Wiederhorn, S. M., & Townsend, P. R. (1970). Crack healing in glass. *Journal of The American Ceramic Society, 53*(9), 486-489.

Wool, R. P. (1980). Crack healing in semicrystalline polymers, block copolymers and filled elastomers. *Adhesion and Adsorption of Polymers.* New York, US: Plenum Press/ Springer.

Wool, R. P. (2001). A material fix. *Nature, 409*, 773-774.

Xiao, D. S., Rong, M. Z., & Zhang, M. Q. (2007). A novel method for preparing epoxy-containing microcapsules via UV irradiation-induced interfacial copolymerization in emulsions. *Polymer, 48*, 4765-4776.

Xiao, D. S., Yuan, Y. C., Rong, M. Z., & Zhang, M. Q. (2009). Self-healing epoxy based on cationic chain polymerization. *Polymer, 50*(13), 2967-2975.

Yadav, J., Satyanarayana, M., Balanarsaiah, E., & Raghavendra, S. (2006). Phosphomolybdic acid supported on silica gel: a mild, efficient and reusable catalyst for the synthesis of 2,3-unsaturated glycopyranosides by Ferrier rearrangement. *Tetrahedron Letters, 47*(34), 6095-6098.

Yi, H., Yang, Y., Gu, X., Huang, J., & Wang, C. (2015). Multilayer composite microcapsules synthesized by Pickering emulsion templates and their application in self-healing coating. *Journal of Materials Chemistry A, 3*(26), 13749-13757.

Yin, T., Rong, M. Z., Zhang, M. Q., & Yang, G. C. (2007). Self-healing epoxy composites – Preparation and effect of the healant consisting of microencapsulated epoxy and latent curing agent. *Composites Science and Technology, 67*, 201-212.

Yuan, L., Huang, S., Hu, Y., Zhang, Y., Gu, A., Liang, G., . . . Nutt, S. (2014). Poly(phenylene oxide) modified cyanate resin for self-healing. *Polymers for Advanced Technologies, 25*(7), 752-759.

Yuan, L., Liang, G., Xie, J. Q., Li, L., & Guo, J. (2006). Preparation and characterization of poly(urea-formaldehyde) microcapsules filled with epoxy resins. *Polymer, 47*(15), 5338-5349.

Yuan, Y. C., Rong, M. Z., Zhang, M. Q., Chen, J., Yang, G. C., & Li, X. M. (2008). Self-healing polymeric materials using epoxy/mercaptan as the healant. *Macromolecules*, 41(14), 5197-5202.

Yuan, Y. C., Rong, M. Z., Zhang, M. Q., & Yang, G. C. (2009). Study of factors related to performance improvement of self-healing epoxy based on dual encapsulated healant. *Polymer, 50*(24), 5771-5781.

Zako, M., & Takano, N. (1999). Intelligent material systems using epoxy particles to repair microcracks and delamination damage in GFRP. *Journal of Intelligent Material Systems and Structures, 10*(10), 836-841.

Zheludkevich, M. (2009). Self-healing anticorrosion coatings. In S. K. Ghosh (Ed.), *Self-healing Materials: Fundamentals, Design Strategies, and Applications*. Weinheim: Wiley-VCH Verlag GmbH & Co. KGaA.

Zhu, D. Y., Rong, M. Z., & Zhang, M. Q. (2013). Preparation and characterization of multilayered microcapsule-like microreactor for self-healing polymers. *Polymer, 54*(16), 4227-4236.

LIST OF PUBLICATIONS AND PAPERS PRESENTED

Shahabudin, N., Yahya, R., & Gan, S. (2016). Microcapsules filled with a palm oil-based alkyd as healing agent for epoxy matrix. *Polymers*, 8(4), 125. Doi: 10.3390/polym8040125 (ISI).

Shahabudin, N., Yahya, R., & Gan, S. N. (2016). Microcapsules of poly(urea-formaldehyde) (PUF) containing alkyd from palm oil. *Materials Today: Proceedings*, 3, Supplement 1, S88-S95. Doi:10.1016/j.matpr.2016.01.012 (SCOPUS).

Shahabudin, N., Yahya, R., & Gan, S. N. (2015). Microencapsulation of a palm oil-based alkyd by amino resins. *Macromolecular Symposia*, 354(1), 305-313. Doi: 10.1002/masy.201400085 (ISI).

Shahabudin, N., Yahya, R., & Gan, S. (2016). Epoxy/alkyd reactions for self-healing epoxy coating (submitted to *Composites Interfaces*).

Nurshafiza Shahabudin, Rosiyah Yahya and Seng Neon Gan. *Alkyd-loaded microcapsules in epoxy: Mechanical properties and epoxy-alkyd curing reaction*. International Symposium of Advanced Polymeric Materials (IMTCE-ISAPM 2016) under auspices of 10th International Materials and Technology Conference and Exhibition (IMTCE), 16-19th May 2016, PWTC, Kuala Lumpur, Malaysia. – Oral presentation.

Nurshafiza Shahabudin, Rosiyah Yahya and Seng Neon Gan. *Poly(melamine-urea-formaldehyde) microcapsules containing palm oil-based alkyd*. 5th International Conference of Functional Materials and Devices (ICFMD 2015), 4-6th August 2015, New York Hotel, Johor Bharu, Malaysia. – Oral presentation.

Nurshafiza Shahabudin, Rosiyah Yahya and Seng Neon Gan. *Preparation of microcapsules containing alkyd resin as core*. World Polymer Congress MACRO 2014, 6-11th July 2014, Chiangmai, Thailand. – Poster presentation.

Nurshafiza Shahabudin, Rosiyah Yahya and Seng Neon Gan. *Preparation of microcapsules containing alkyd resin as core*. 5th Trilateral Seminar UM-CU-NUS, 11-12th February 2014, Chemistry Department, University of Malaya, Kuala Lumpur, Malaysia. – Poster presentation.

APPENDIX A: Publication (Front Page)

A.1 Paper 1

polymers

MDPI

Article

Microcapsules Filled with a Palm Oil-Based Alkyd as Healing Agent for Epoxy Matrix

Nurshafiza Shahabudin, Rosiyah Yahya and Seng Neon Gan *

Chemistry Department, Faculty of Science, University of Malaya, 50603 Kuala Lumpur, Malaysia; shafizashah@siswa.um.edu.my (N.S.); rosiyah@um.edu.my (R.Y.)
* Correspondence: sngan@um.edu.my; Tel.: +60-3-7967-4241; Fax: +60-3-7967-4193

Academic Editor: Antonio Pizzi
Received: 3 February 2016; Accepted: 28 March 2016; Published: 6 April 2016

Abstract: One of the approaches to prolong the service lifespan of polymeric material is the development of self-healing ability by means of embedded microcapsules containing a healing agent. In this work, poly(melamine-urea-formaldehyde) (PMUF) microcapsules containing a palm oil-based alkyd were produced by polymerization of melamine resin, urea and formaldehyde that encapsulated droplets of the suspended alkyd particles. A series of spherical and free-flowing microcapsules were obtained. The chemical properties of core and shell materials were characterized by Attenuated total reflection-Fourier transform infrared spectroscopy (ATR-FTIR) and proton nuclear magnetic resonance spectroscopy (^{1}H-NMR). Differential scanning calorimetry (DSC) analysis showed a glass transition around −15 °C due to the alkyd, and a melting temperature at around 200 °C due to the shell. Thermogravimetric analysis (TGA) results showed that the core and shell thermally degraded within the temperature range of 200–600 °C. Field emission scanning electron microscope (FESEM) examination of the ruptured microcapsule showed smooth inner and rough outer surfaces of the shell. Flexural strength and microhardness (Vickers) of the cured epoxy compound were not affected with the incorporation of 1%–3% of the microcapsules. The viability of the healing reactions was demonstrated by blending small amounts of alkyd with epoxy and hardener at different ratios. The blends could readily cure to non-sticky hard solids at room temperature and the reactions could be verified by ATR-FTIR.

Keywords: microcapsules; renewable resources; epoxy; flexural strength; microhardness; self-healing

1. Introduction

The failure of a structural polymer begins from cracks within the materials. Continuous efforts are being made to overcome the damages of the cracks by integrating self-healing ability to the material. A recent review article has discussed the various types of self-healing nanocomposite materials [1]. One of the ways to achieve this objective is to store healing agents in microcapsules that are then embedded into the polymer matrix. The healing process is triggered when cracks rupture the microcapsules and release the healing agent to fill the gaps. Subsequently, the healing agent would solidify through reaction such as crosslinking with certain reactive groups of the matrix to repair the crack and prevent further damage, thus extending the lifespan of the material.

There are many recent publications on the usage of microcapsules in self-healing materials, notably in coatings, adhesives and electronic components. Various selected agents have been encapsulated, such as chlorobenzene [2], dimethyl norbornene ester and dicyclopentadiene (DCPD) [3], and norbornene dicarboximide [4]. Microcapsules of linseed oil were used to heal cracks in paint film [5] and epoxy coatings [6,7].

Urea-formaldehyde (UF) resins are widely used in adhesives, particleboard, and molded objects. It has been used in specialized applications such as the fabrication of natural fiber reinforced

A.2 Paper 2

Macromol. Symp. 2015, 354, 309–313 DOI: 10.1002/masy.201400085

Microencapsulation of a Palm Oil-based Alkyd by Amino Resins

Nurshafiza Shahabudin, Rosiyah Yahya, Seng Neon Gan*

Summary: Preparation of microcapsules of poly(urea-formaldehyde) (PUF) and melamine-modified PUF (PUMF) shells that encapsulated a core of palm oil-based alkyd resin was described. Ethylene maleic anhydride (EMA) was used as emulsifier. The effects of core-shell weight ratio on microcapsules size and surface morphology were studied. The microcapsules obtained were inspected using digital microscope and field emission scanning electron microscope (FESEM) to study the formation of microcapsules and their surface morphology. The core and shell content was verified using differential scanning calorimetry (DSC) and attentuated total reflectance fourier-transformed infrared (ATR-FTIR). Thermogravimetric analysis (TGA) shown that the microcapsules have different degradation rates of core and shell thus reconfirmed the formation of microcapsules. The resultant microcapsules appear as white-yellowish and free-flowing spherical particles, having a rough, non-porous shell which was formed by PUF and PUMF nanoparticles. The microcapsules have their diameters ranging from 150–500 microns, and they contain 87–90% of the alkyd as core and 10–13% of shell by weight.

Keywords: alkyd; amino resins; microencapsulation; poly(urea-melamine-formaldehyde); renewable resources

Introduction

Microencapsulation is a process of creating a division between an active material with its surrounding until further needs of it to be released. There are various active materials being encapsulated, including epoxy resins,[1] harderners,[2] solvents,[3] fragrances,[4] oils,[5] etc. The encapsulation was made with objectives for protection of catalyst, drug delivery[6] and also for self-healing materials.[7–9] Another interesting approach for microcapsules' potential usage is as particulate filler to increase mechanical strength of materials, e.g. to increase fracture toughness.[10] Sonication method was employed to produce sub-micron microcapsules that meet the requirements for self-healing materials that have a significant increase in fracture toughness. There are many techniques of micro/nanoencapsulation that includes in-situ polymerization,[11] miniemulsion,[12] coacervation,[13] internal-phase separation,[14] layer-by-layer assembly[15] and radiation.[16] Alkyd resin is a polyfunctional vegetable oil-modified polyester, synthesized by reacting polybasic acids with polyhydric alcohols together with a vegetable oil or its derivatives, via a step-wise polymerization process.[17] It has been widely used for many purposes, mostly for coatings. For instance, Ogunniyi and Odetoye[18] used tobacco seed oil to produce alkyd for white gloss paint application. Ang and Gan[19] used palm stearin alkyd to produce UV curable resin. Drying alkyd contains a certain amount of unsaturation that can be cured by air or by other types of crosslinking reactions initiated by heat or UV irradiation. Alkyd is interesting

Chemistry Department, Faculty of Science, University of Malaya, 50603 Kuala Lumpur, Malaysia
Fax: (+603) 7967 4193;
E-mail: shafizashah@siswa.um.edu.my

A.3 Paper 3

Available online at www.sciencedirect.com
ScienceDirect
materialstoday: PROCEEDINGS
Materials Today: Proceedings 3S (2016) S88 – S95

5th International Conference on Functional Materials & Devices (ICFMD 2015)

Microcapsules of poly(urea-formaldehyde) (PUF) containing alkyd from palm oil

Nurshafiza Shahabudin, Rosiyah Yahya, Seng Neon Gan*

Chemistry Department, Faculty of Science, University of Malaya, 50603 Kuala Lumpur, Malaysia.

Abstract

This paper describes the encapsulation procedure of an alkyd resin derived from palm oil. The palm oil-based alkyd having carboxylic and hydroxyl moieties can be tailor-made to suit the intended application. Microencapsulation process was done using poly(urea-formaldehyde) (PUF) resin as shell material. The microcapsules obtained were free-flowing, with 80 -90 % core encapsulated, and are intended to be used in self-healing material development. The functional groups of alkyd and shell material were observed using ATR-FTIR. DSC analysis shows melting peaks and glass transition of PUF and alkyd in the microcapsules. TGA analysis indicated that the shell of the microcapsules was thermally stable up to 250°C. FESEM examination showed that the microcapsules had rough outer surface.

Selection and Peer-review under responsibility of Conference Committee Members of 5th International Conference on Functional Materials & Devices (ICFMD 2015).

Keywords: Microcapsules; Alkyd; Palm oil; Biorenewable; Poly(urea-formaldehyde)

1. Introduction

Recently, self-healing process utilizing microcapsules as carriers of healing agent has been an interesting topic that has attracted many researchers and the number of related publications has been growing fast. Many healing mechanisms have been studied and the healing agents encapsulated, such as dicyclopentadiene (DCPD), 5-

* Corresponding author. Tel.: +603 7967 4241; fax: +603 7967 4193 .
E-mail address: sngan@um.edu.my

Selection and Peer-review under responsibility of Conference Committee Members of 5th International Conference on Functional Materials & Devices (ICFMD 2015).
doi: 10.1016/j.matpr.2016.01.012

APPENDIX B: Microencapsulation procedure of Method 3

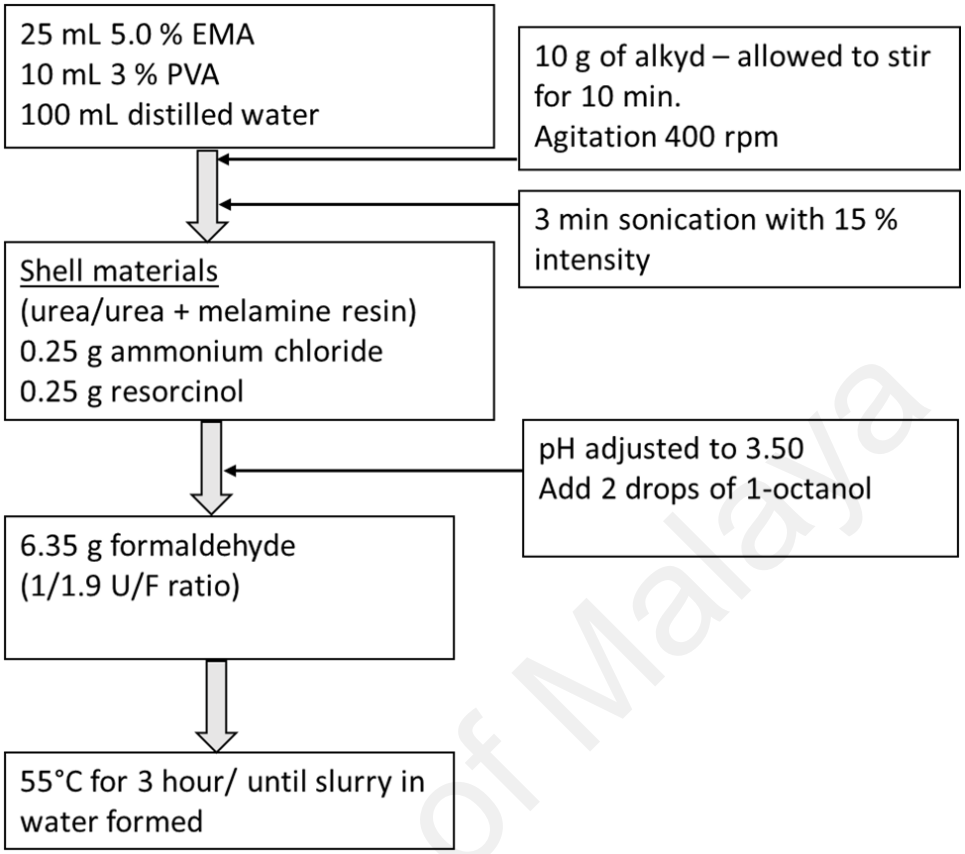

APPENDIX C: ATR-FTIR spectra

C.1 ATR-FTIR spectra of AlkydFA35 and extracted core of D1 microcapsules

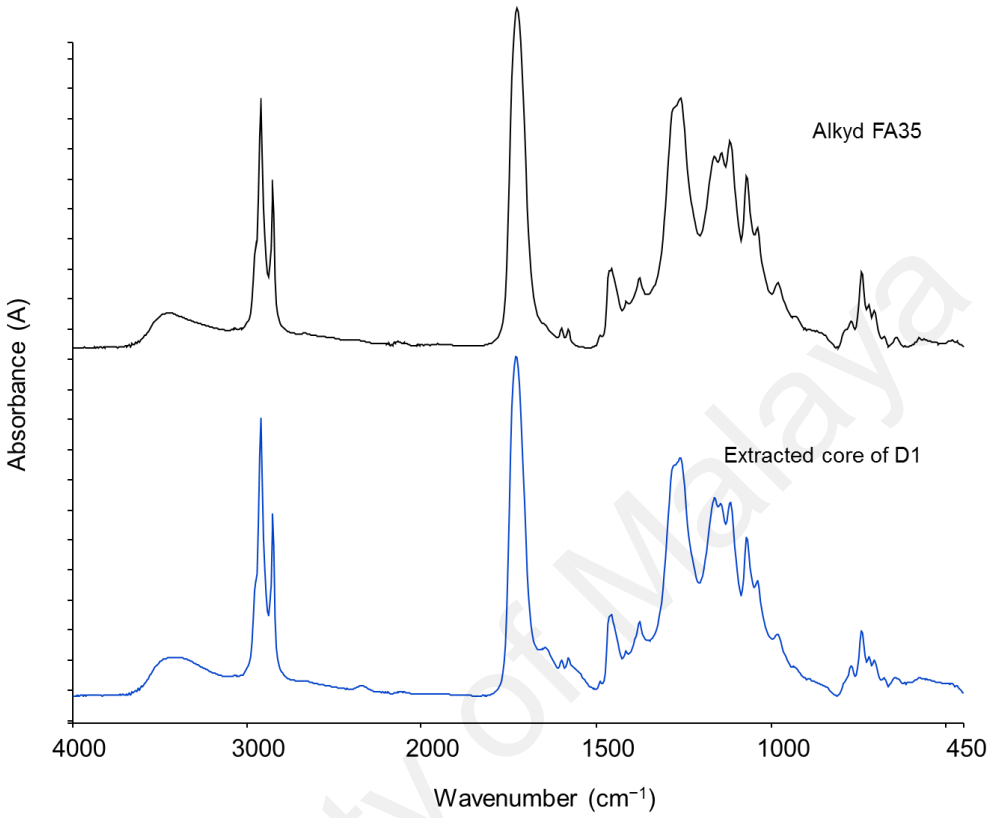

C.2 ATR-FTIR spectra of microcapsules of B series

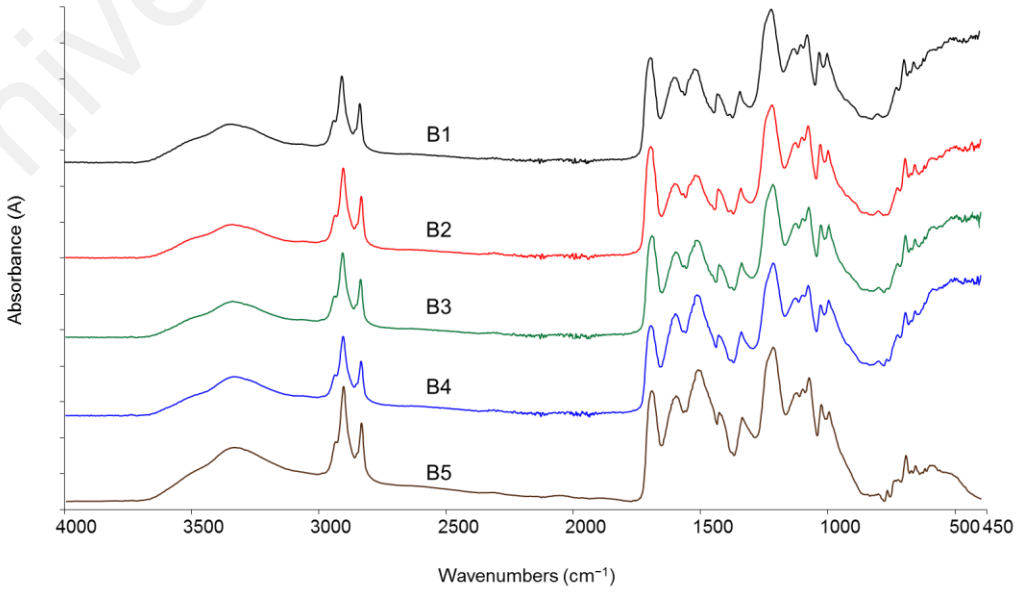

C.3 ATR-FTIR spectra of neat alkyd, epoxy resin and cured epoxy, EA1, EA2 and EA3 samples cured at 100°C for 2 h.

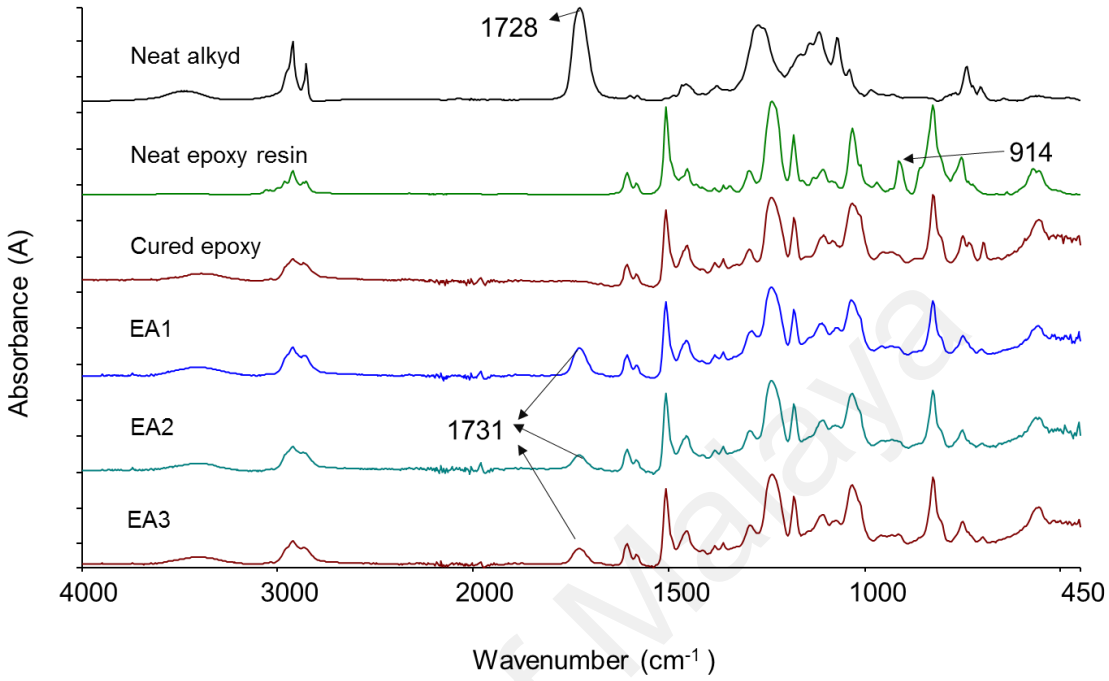

APPENDIX D: ^{1}H-NMR spectra of AlkydFA35 and the extracted core of D1 microcapsules

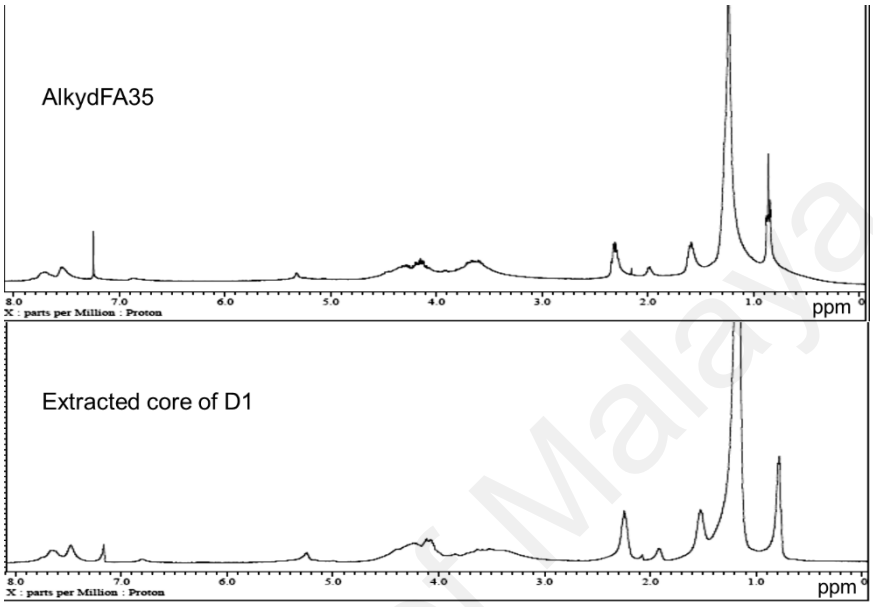

APPENDIX E: DSC thermograms and characterization data

E.1 DSC thermograms of microcapsules of Series A, the alkyd core and PUF shell.

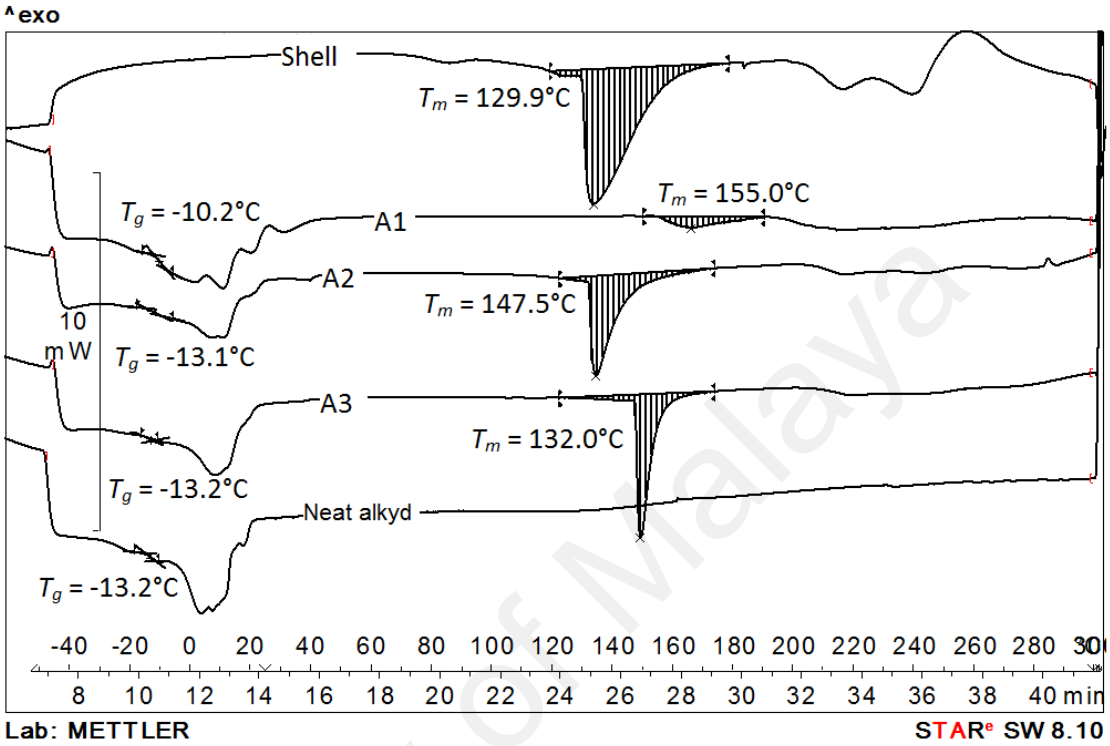

E.2 DSC thermograms of microcapsules of Series B, the alkyd and PMUF shell

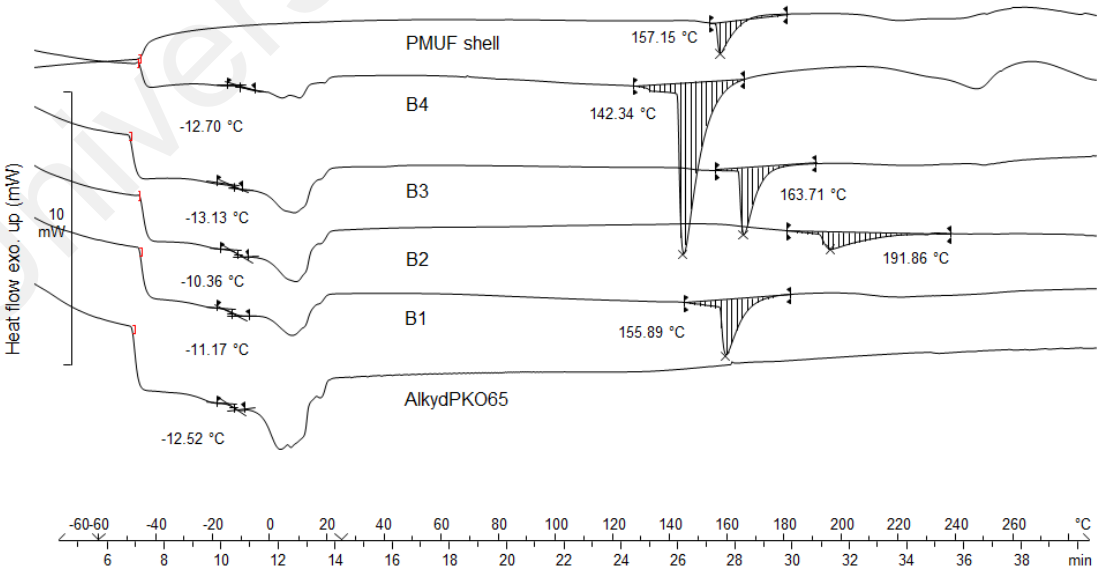

E.3 DSC thermograms of D1 microcapsules and AlkydFA35

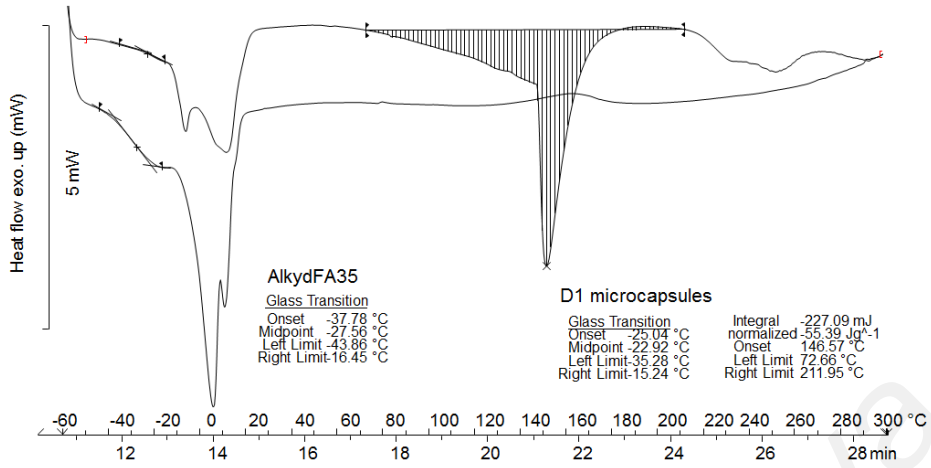

E.4 DSC characterization data of PUF and PMUF microcapsules

Sample	T_g of alkyd (°C)	T_m of alkyd (°C)	T_m of shell (°C)	T_d onset (°C)	T_d peak (°C)
AlkydPKO65	−13.2	−15−15	–	n.d.	n.d.
Extracted PUF	–	–	130	204	219, 241
Extracted PMUF	–	–	156	204	225
A1	−10.2	0−15	155	200	218
A2	−13.1	0−15	148	205	220
A3	−13.2	0−15	132	208	220, 245
B1	−11.2	0−15	156	205	220
B2	−10.4	0−15	192	n.d.	n.d.
B3	−13.1	0−15	164	208	228
B4	−12.7	0−15	142	215	250
D1	−22.9	−15−20	147	220	230, 255
AlkydFA35	−22.9	−15−20	–	n.d.	n.d.

*n.d. = not detected.

E.5 DSC thermograms of C1-C3 microcapsules

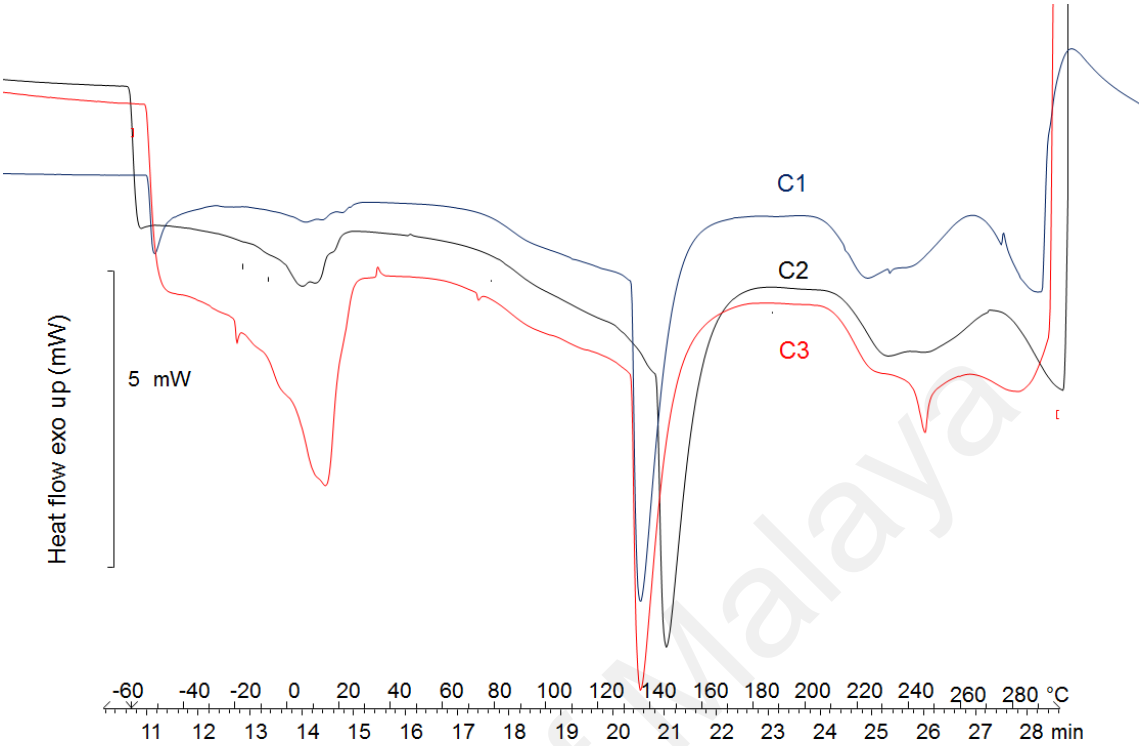

E.6 Enlarged T_g area of C1 microcapsules

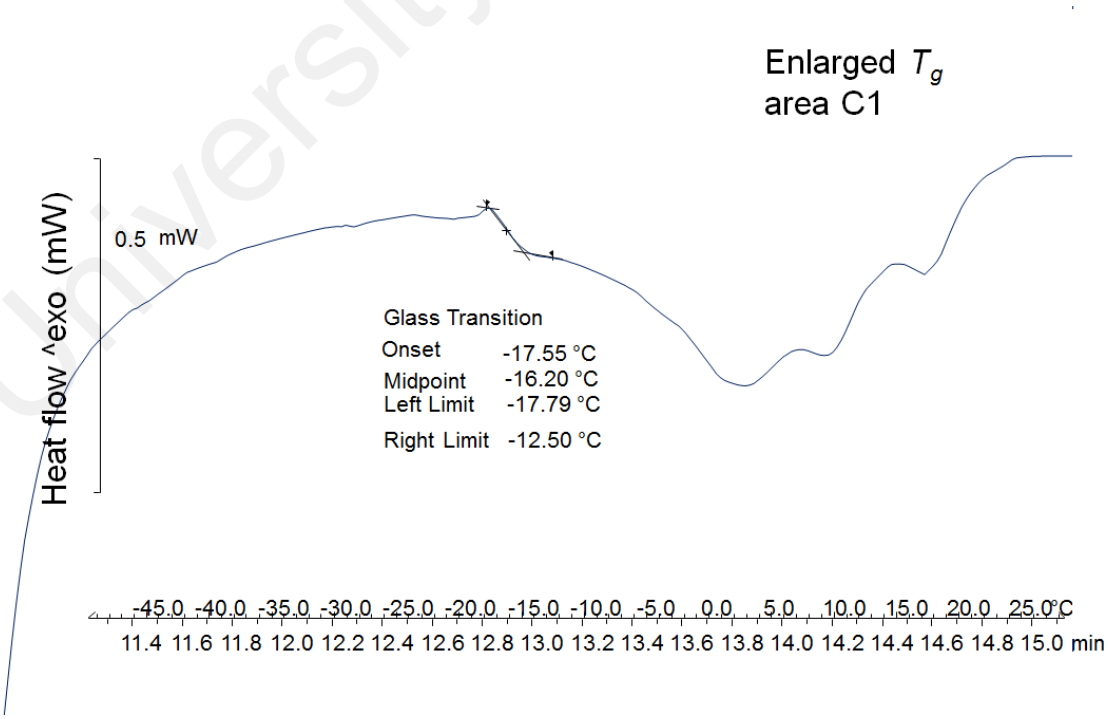

E.7 DSC thermogram of C4 microcapsules

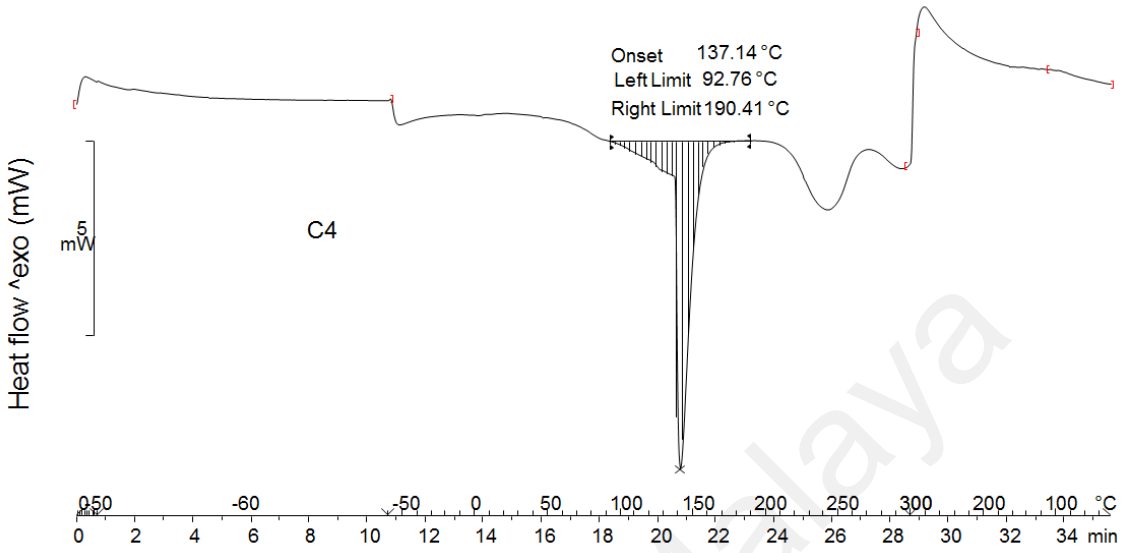

E.8 DSC characterization data of C series microcapsules

Sample	T_g of alkyd (°C)	T_m of shell (°C)
C1	-16.2	133.3
C2	-11.0	141.2
C3	-9.4	132.7
C4	n.d.	137.1

APPENDIX F: TGA thermograms

F.1 TGA thermogram of A2 microcapsules, PUF shell and AlkydPKO65

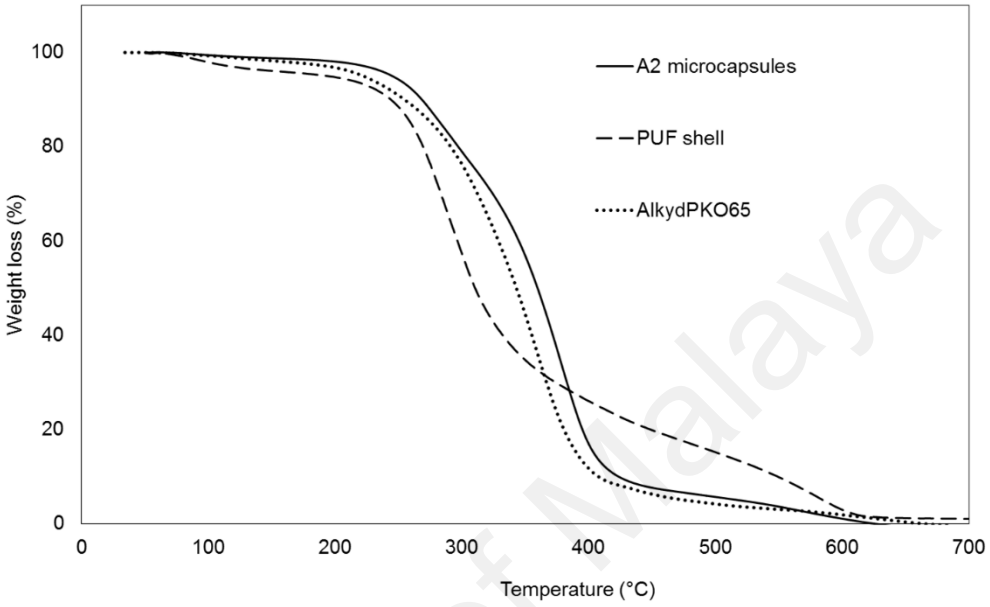

F.2 TG and dTG of A1 microcapsules

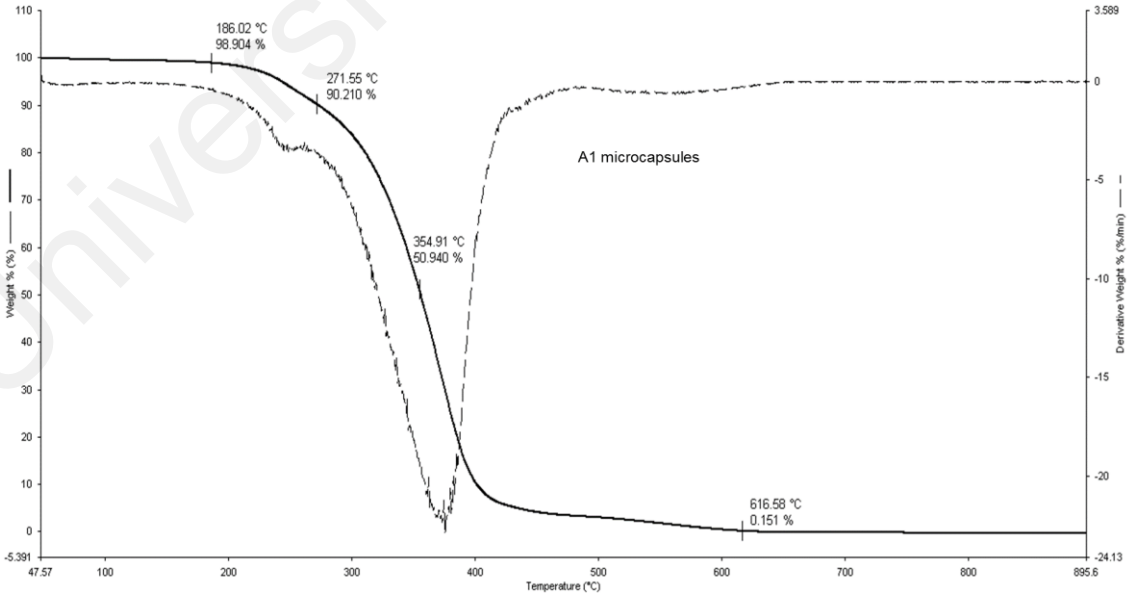

F.3 TG and dTG of A2 microcapsules

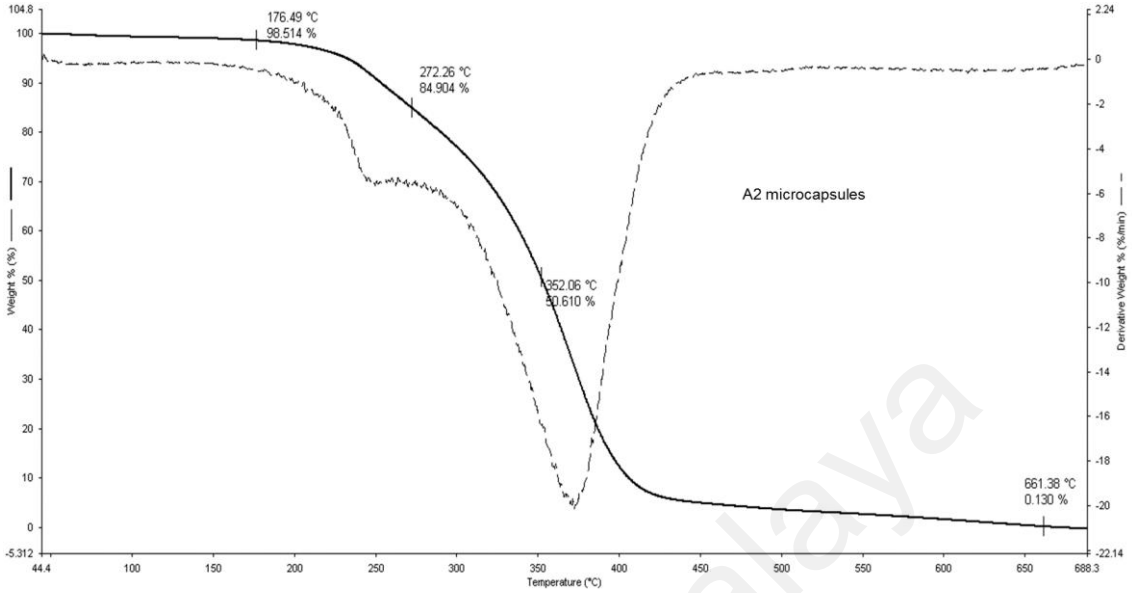

F.4 TG and dTG of A3 microcapsules

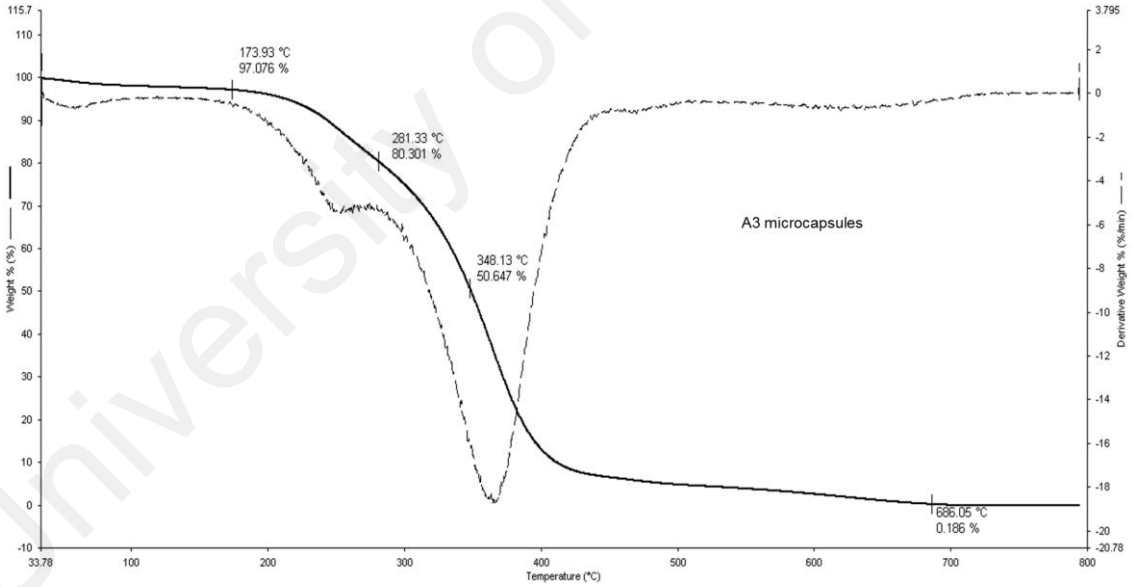

F.5 TG of microcapsules from Series B, AlkydPKO65 and PMUF shell

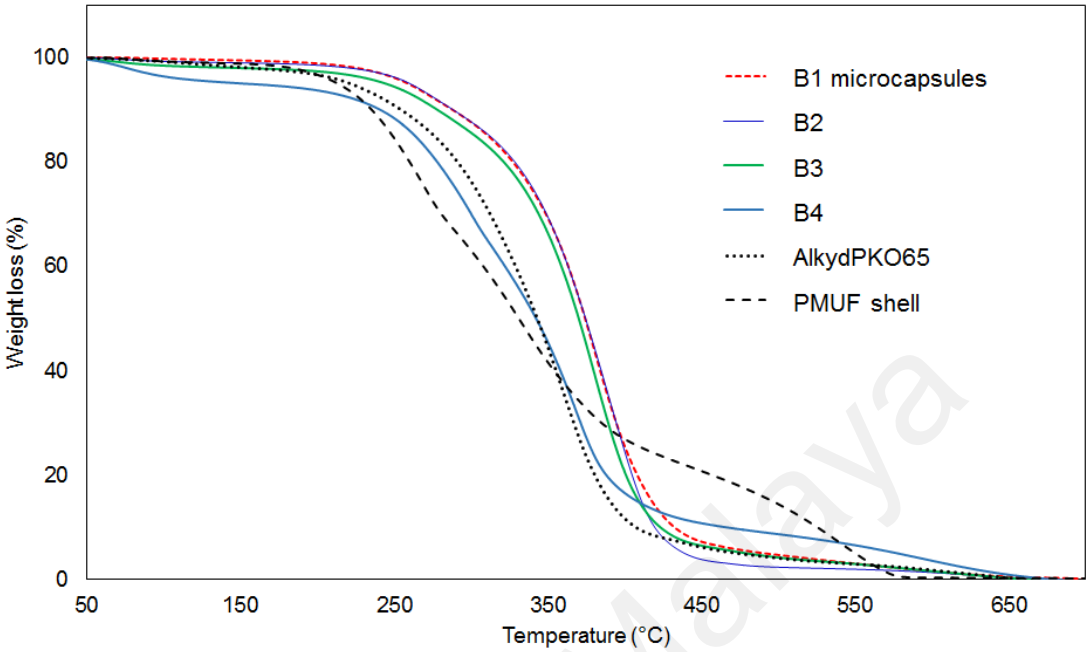

APPENDIX G: STA thermograms

G.1 STA thermogram of C2 microcapsules

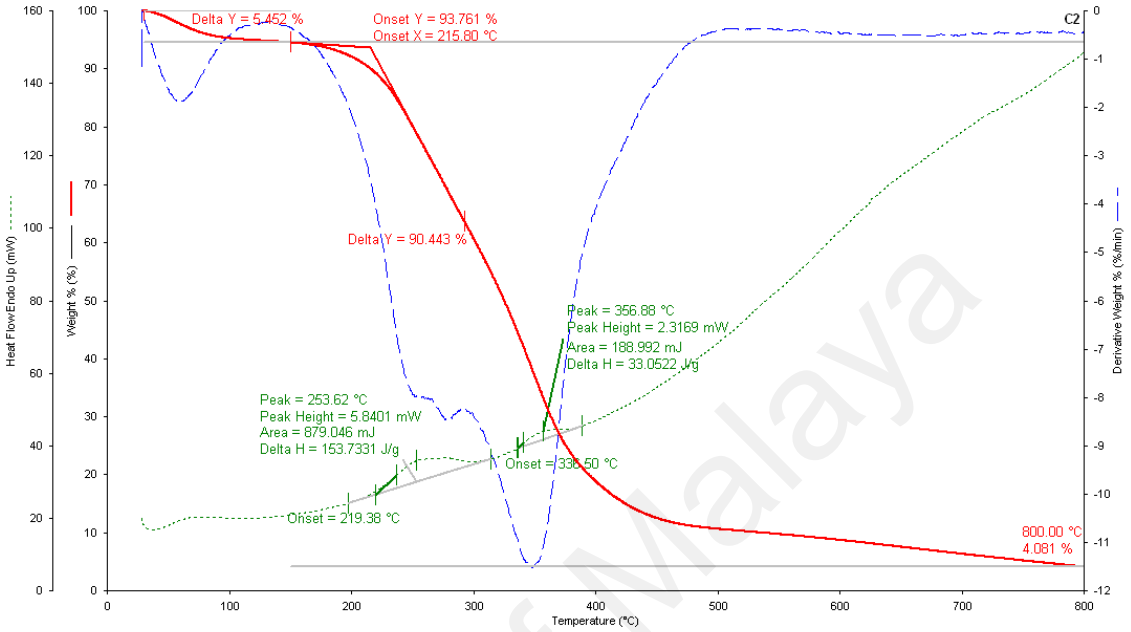

G.2 STA thermogram of D1 microcapsules

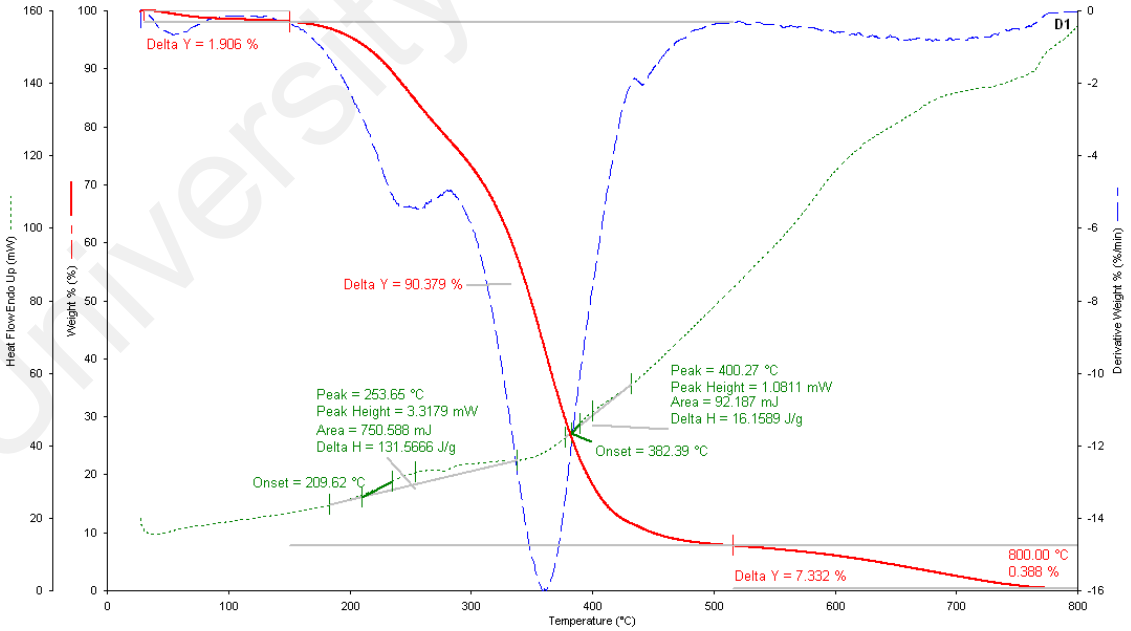

G.3 STA characterizations data of C2 and D1 microcapsules

Sample	T_d onset (from wt. %)	$T_{50\%}$ (from wt. %)	T_d onset (from heat flow)	T_d peak (from heat flow)
C2	216	325	219	254
D1	207	350	210	254

T_d onset= onset temperature of degradation; $T_{50\%}$ = temperature at 50 % weight loss.

APPENDIX H: FESEM micrographs

H.1 FESEM micrographs of A2 microcapsule at magnification: (a) 800×; (b) 2500x (c) 12 000×

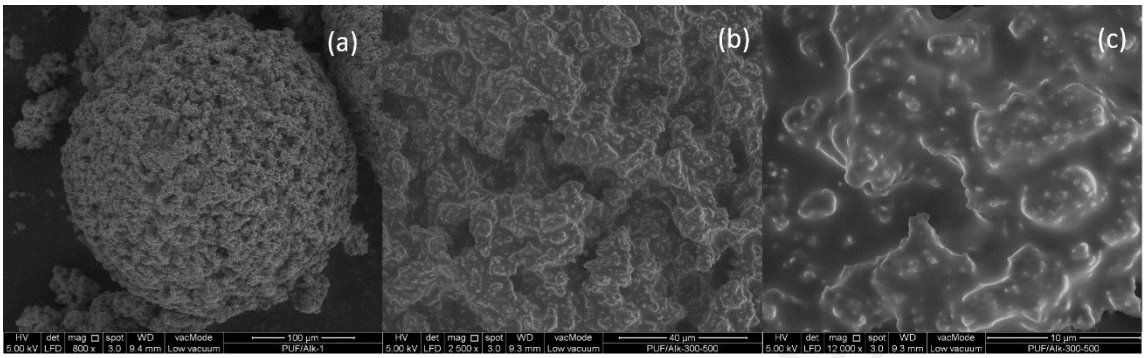

H.2 FESEM micrographs of rupture A2 microcapsules at magnification: (a) 600× (b) 5000×

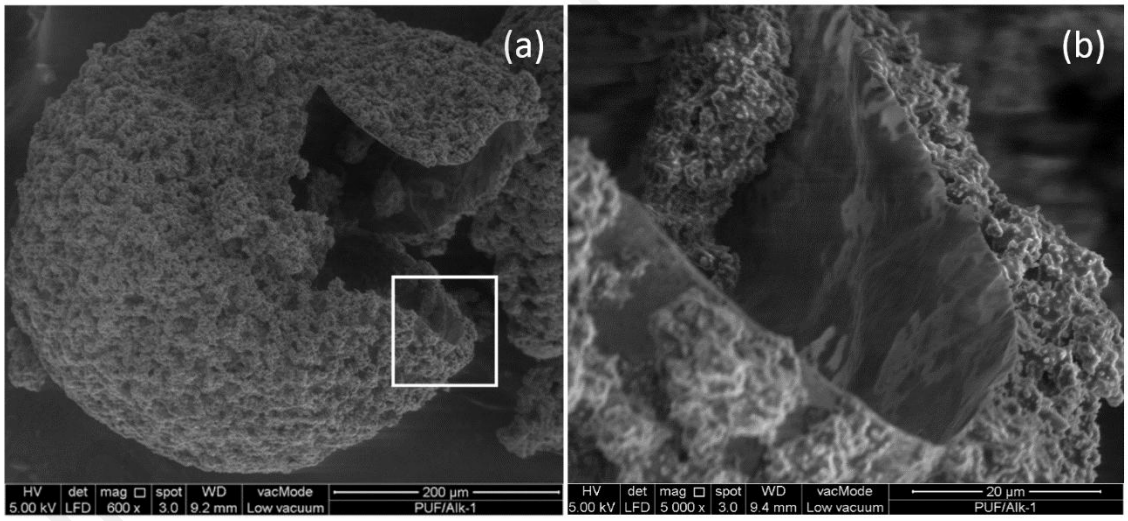

APPENDIX I: MECHANICAL TEST DATA

I.1 Flexural strength (MPa) of epoxy samples filled with microcapsules B2

Instrument: Shimadzu AG-X high precision universal testing machine Software: TrapeziumX Test Mode: Single Test Type: 3 Point Bend Speed: 1 mm/min Shape: Plate Qty/Batch: 4 Test result: Max Stress in [MPa] Load cell: 5 kN Test date: 29/9/2015				
Microcapsules loading (wt. %)	0/ Neat epoxy	1	3	6
Reading 1	40.2358	50.0845	44.5174	30.6440
Reading 2	43.5061	42.9353	42.2094	34.0377
Reading 3	45.4667	50.7838	42.4937	32.4460
Reading 4	43.4370	49.2310	40.2658	33.1200
Average	43.16	48.26	42.37	32.56
Std. Deviation (SD)	1.9	3.1	1.5	1.2
% SD	4.3	6.5	3.6	3.8

1.2 Vickers micro-indentation hardness (HV) of epoxy samples filled with microcapsules B2

Instrument: Shimadzu Micro Hardness Tester HMV-2 Series Software: EasyTest V1.1.0.0, Shimadzu AD Test force: HV 0.01 = 98.07 mN Measurement mode: Simple test Duration time: 5 sec Indenter type: Vickers Test result: Vickers Hardness Test date: 28/10/2015						
Microcapsules loading (wt. %)	Micro-indentation hardness (HV)					
	Indent 1	Indent 2	Indent 3	Mean	SD	% SD
0/ Neat epoxy	9.75	9.56	9.52	9.6	0.1	1
1	9.29	9.6	9.52	9.5	0.1	1
3	9.36	9.17	9.48	9.3	0.1	1
6	9.4	9.36	9.51	9.4	0.1	1

APPENDIX J: FORMULATION OF THE EPOXY/ALKYD BLENDS & CORE CONTENT DATA

- Eq. wt. of epoxy = 191 g (from manufacturer)
- Eq. wt. of amine = 111 g (from manufacturer)
- Eq. wt. of AlkydPKO65 (based on OH)
  = 56100 / 151 mg KOH/ g alkyd (calculated OHV)
  = 372 g.

- Eq. wt. of AlkydPKO65 (based on COOH)
  = 56100 / 15 mg KOH/ g alkyd (experimental acid number)
  = 3740 g.
- Therefore, 191 g epoxy eq. to 111 g amine **OR** 1 g epoxy eq. to 0.58 g amine
- Therefore, 191 g of epoxy eq. to 372 g of OH alkyd **OR** 191 g of epoxy eq. to 3740 g of COOH alkyd

1 g epoxy eq. to **1.95 g OH alkyd** OR **1 g epoxy** eq. to **19.6 g COOH alkyd**

Code	M/U wt. ratio	Rep.	W_s	$W_{empty\ filter\ paper}$	$W_{dried\ shell\ and\ filter\ paper}$	W_m	E_{core}	$E_{core\ (mean)}$	S.D.
A1	0	1	0.3272	0.9077	0.9318	0.0241	92.6	93.9	1.3
		2	0.3055	0.9025	0.9173	0.0148	95.2		
A3	0	1	0.3115	0.9030	0.9405	0.0375	88.0	88.0	0.0
		2	0.3292	0.8797	0.9191	0.0394	88.0		
A2	0	1	0.3070	0.8801	0.9128	0.0327	89.3	89.9	0.5
		2	0.3080	0.9081	0.9376	0.0295	90.4		
B1	0.03	1	0.3031	0.8889	0.9056	0.0167	94.5	94.8	0.3
		2	0.3367	0.8905	0.9068	0.0163	95.2		
B2	0.06	1	0.3107	0.8844	0.9052	0.0208	93.3	92.0	1.3
		2	0.3022	0.8884	0.9164	0.0280	90.7		
B3	0.12	1	0.3100	0.8832	0.9096	0.0264	91.5	91.9	0.4
		2	0.3079	0.9109	0.9347	0.0238	92.3		
B4	0.29	1	0.3135	0.9070	1.0239	0.1169	62.7	63.1	0.4
		2	0.3071	0.9004	1.0124	0.1120	63.5		
C2	0.03	1	0.3073	0.7959	0.9459	0.1500	51.2	54.3	3.1
		2	0.3032	0.8592	0.9888	0.1296	57.3		

W_s - Weight of sample; W_m - weight of the shell.

APPENDIX K: Publications of smart materials in Malaysia

Field	Institution/ collaborator	Author/year	Type of publication/ Journal	Tier/Index/ Publisher
Self-healing polymers and polymer composites	UM	Then et al., 2011	Research paper/ Sains Malaysiana	Q3/ Penerbit UKM
		Then et al., 2011	Research paper/ J. App. Polym. Sc.	Q2/ Wiley
		Sonja Then, 2011	Thesis	UM
	Monash University, Malaysia	Vahedi et al., 2015	Research paper/ J. Mater. Chem. A	Q1/ RSC
		Hia et al., 2016	Review/ Polymer Rev.	Q1/ Taylors & Francis
	UTM	Kam & Kueh, 2015.	Review/J. Teknol.	Scopus/ Penerbit UTM Press.
	UTP	Ullah, H. et al., 2016	Review/ Polymer Rev.	Q1/ Taylors & Francis
Intrinsic self-healing epoxy	UKM	Jamil and Jones, 2012	Proceeding paper	Scopus/ AACM
		Muhamad et al., 2014	Research paper/MJAS	Scopus/ ANALIS
		Makenan et al., 2014	Research paper/MJAS	Scopus/ ANALIS
		Jamil et al., 2015	Research paper/ Sains Malaysiana	Q3/ Penerbit UKM
		Jamil et al., 2015	Research paper/MJAS	Scopus/ ANALIS
		Muhamad et al., 2015	Research paper/MJAS	Scopus/ ANALIS
		Sirajudin et al., 2015	Research paper/MJAS	Scopus/ ANALIS
Intrinsic self-healing hydrogel	UKM	Sirajudin et al., 2015	Research paper/ e-Polymers	Q3/ De Gruyter
		Sirajudin et al., 2015	Research paper/MJAS	Scopus/ ANALIS
		Sirajudin et al., 2015	Research paper/ Sains Malaysiana	Q3/ Penerbit UKM
	USM	Ullah, F. et al., 2015	Review/Mat. Sc. Eng. C	Q1/ Elsevier

Self-healing concrete	UKM	Alebrahim et al., 2015	Research paper/Comp. Struct.	Q1/ Elsevier
	UTM	Taleikhozani, Keyvanfar et al., 2013	Research paper/ Desaline Water Treat.	Q2/ Taylor & Francis
		Keyvanfar et al., 2014	Research paper/ Desaline Water Treat.	Q2/ Taylor & Francis
		Taleikhozani et al., 2014	Review/ JETT	Non-ISI/ non-Scopus
		Arifin et al., 2015	Research paper/Const. Building. Mater.	Q1/ Elsevier
		Arifin et al., 2015	Research paper/J. Teknol.	Scopus/ Penerbit UTM Press.
		Huseien et al., 2015	Research paper/J. Teknol.	Scopus/ Penerbit UTM Press.
		Sam et al., 2015	Research paper/J. Teknol.	Scopus/ Penerbit UTM Press.
		Muhammad et al., 2016	Review/ Construc. Building Mater.	Q1/ Elsevier
	UMP	Shahid et al., 2014	Research paper/JMES	Scopus/ UMP Publisher
	UMS	Lim & Pickering, 2014	Research paper/ J. App. Sc.	Q3/ Asian Network for Sc. Information
	UiTM-Delft TU	Yunus et al., 2015/ Proceeding	Extended abstract	ICSHM 2015
Supramolecular photo rheological fluids	UiTM-Cambridge	Tan et al., 2015	Research paper/ Polym. Chem.	Q1/ RSC
Self-healing adhesives	UMS-Australia	Ghazali et al., 2016.		
Self-healing anti corrosion coating	UTM	Hamzah et al., 2016	Proceeding	10th IMTCE 2016
Shape-memory alloy	UNIKL-RMIT Australia	Jani et al., 2014	Review/ Mater. Design	Q1/ Elsevier

ANALIS: Malaysian Analytical Sciences Society; UM: University of Malaya; UKM: Universiti Kebangsaan Malaysia; UTM: Universiti Teknologi Malaysia; USM: Universiti Sains Malaysia; UTP: Universiti Teknologi Malaysia; UNIKL: Universiti Kuala Lumpur; UMP: Universiti Malaysia Perlis; UMS: Universiti Malaysia Sabah; UiTM: Universiti Teknologi Mara; RSC: Royal Science Society; ICSHM: International Conference on Self-healing Materials; AACM: Asian-Australasian Conference on Composite Materials; JETT: Journal of Environmental Treatment Technique; JMES: Journal of Mechanical Engineering and Sciences; Delft TU: Delft Technology University, Netherland; IMTCE: International Materials and Technology Conference and Exhibitions.